THÈSE

En vue de l'obtention du

DOCTORAT DE L'UNIVERSITÉ DE TOULOUSE

Délivré par l'Université Toulouse 3 – Paul Sabatier

Présentée et soutenue par

Mateusz SZCZEPANSKI

Le 29 mars 2019

Development of methods allowing the test and the comparison of low-voltage motors insulation systems running under partial discharges (fed by inverter)

École doctorale : **GEET - Génie Electrique Electronique et Télécommunications du système au nanosystème**

Spécialité : **Génie Electrique**

Unité de recherche :
LAPLACE - Laboratoire PLAsma et Conversion d'Énergie - CNRS-UPS-INPT

Thèse dirigée par
David MALEC et Pascal MAUSSION

Jury

M. Ian COTTON	Professor at The University of Manchester, UK	Rapporteur
M. Farid MEIBODY-TABAR	Professor at Université de Lorraine, France	Rapporteur
M. Thierry LEBEY	Director of research at CNRS – LAPLACE, France	Examinateur
Mme Sonia AIT-AMAR	Associate Professor at Université d'Artois, France	Examinateur
M. Mats ALAKÜLA	Professor at Lund University, Sweden	Examinateur
M. David MALEC	Professor at Université Paul Sabatier, France	Directeur
M. Pascal MAUSSION	Professor at INP de Toulouse, France	Co-directeur
Mme. Anne GIMENEZ	Laboratory Manager at Nidec Leroy-Somer, France	Invitée
M. Philippe MANFÉ	Technical Director at Nidec Leroy-Somer, France	Invité

ABSTRACT

Title: Development of methods allowing the test and the comparison of low-voltage motors insulation systems running under partial discharges (fed by inverter).

Key words: partial discharges, electrical insulation system, low-voltage motor, inverter, PWM, design of experiments.

Since the development of power electronic components, which allowed the manufacturing of reliable and efficient inverters, variable speed drives using inductive motors have become more and more popular. The PWM technique has proven to be a very effective method of rotational speed control. However, the fast changing voltage pulses, with very steep slopes (in the order of a few kV/μs), has brought new hazards for the electrical insulation system of such motors. Very high frequency harmonic components of PWM voltage will result in significant overvoltage due to an impedance mismatch between the cable and the motor. As an effect, the voltage seen by some parts of the insulation system may exceed the Partial Discharge Inception Voltage (PDIV) stating localized partial discharges activity.

The insulation system in low-voltage machines (called type I) is based almost entirely on polymer materials, which are not able to support partial discharge activity throughout their lives. Due to the use of frequency inverters especially the primary insulation of the magnet wire is endangered in comparison with system-powered machines. As a result this is often the weakest link of the insulation system leading to a premature breakdown of the machine.

The aim of this thesis is to investigate and analyze the aging process of the enameled wire exposed to different factors and to propose a method allowing to predict their lifespans in given conditions. This study introduces a prediction based on the Design of Experiments method and the statistical Weibull distribution. Thanks to the model obtained with short multi-stress (temperature, voltage, frequency) aging tests, it is possible to predict the results of significantly longer ones. Moreover, the adapted methodology is proposed that allows to predict the scatter of the long tests basing on the short-time results dispersion. The predictions are compared with the experimental data in order to prove the model accuracy.

_____

RESUME

Titre: Mise au point de méthodes permettant le test et la comparaison de systèmes d'isolation des moteurs basse tension fonctionnant en régime de décharges partielles (alimentation par onduleur).

Mots clé: décharges partielles, système d'isolation électrique, moteur basse tension, onduleur, MLI, plan d'expériences

Depuis le développement des composants d'électronique de puissance qui ont permis la fabrication d'onduleurs fiables et efficaces, les entraînements à vitesse variable utilisant des moteurs asynchrones sont devenus de plus en plus populaires. La technique MLI s'est avérée être une méthode très efficace de contrôle de la vitesse de rotation. Cependant, les impulsions de tension, avec des pentes très raides (de l'ordre de quelques kV/μs), ont apporté de nouveaux risques pour le système d'isolation électrique des moteurs. La richesse harmonique de la tension MLI entraînera une surtension significative due à une différence d'impédance entre le câble et le moteur. En effet, la tension observée par certaines parties du système d'isolation peut dépasser la tension d'apparition des décharges partielles (*ang.* PDIV); ce qui amorcera une activité de décharges partielles localisée.

Le système d'isolation des machines basse tension (appelé type I) est basé presque entièrement sur des matériaux polymères qui ne sont pas conçus pour supporter des décharges partielles tout au long de leur vie. En raison de l'utilisation de variateurs de fréquence, l'isolation primaire du fil émaillée est en danger par rapport aux machines alimentées par réseau. En conséquence, c'est souvent le point le plus faible du système d'isolation qui conduira à la panne prématurée d'une machine.

Le but de cette thèse est d'étudier et d'analyser le processus de vieillissement du fil émaillé exposé aux différents facteurs et de proposer une méthode permettant de prédire les durées de vie dans des conditions fixées. Cette étude introduit une prédiction basée sur la méthode des plans d'expériences et la distribution statistique de Weibull. Grâce au modèle obtenu avec des tests de vieillissement courts multicontraintes (température, tension, fréquence) il est possible de prédire les résultats de tests significativement plus longs. De plus, la méthodologie proposée permet de prédire la dispersion des essais longs en se basant sur la dispersion des résultats à court terme. Les

_____

prédictions sont comparées avec les données expérimentales afin de prouver la précision du modèle.

_____

TABLE OF CONTENT

_____

_____

_____

GENERAL INTRODUCTION

The electric insulation system (EIS) consist of all the insulating materials altogether allowing the correct functioning of electric machine. Although it is not directly influencing the machine's efficiency, its design is crucial. For years, it has been optimized in order to reduce its costs and increase its performance. The insulation electrical systems can be divided into 2 main categories. Type I is generally used in low-voltage machines as it is based almost entirely on polymer materials. Type II uses more robust inorganic materials, but due to its significantly higher cost, it is reserved almost uniquely for high voltage machines (>700 V_{RMS}).

The development of power electronic components allowed the manufacturing of reliable and efficient inverters. As a result, variable speed drives using inductive motors have become more and more popular. They use mostly PWM technique, which has proven to be a very effective method for rotational speed control. Nevertheless, the fast changing voltage pulses generated in PWM, with very high dV/dt (in the order of a few kV/µs), has brought new hazards for the electrical insulation system. New components based on wide band gap semiconductors, such as SiC or GaN, will on one the hand enable to limit the commutation losses in the inverter, but on the other hand will even further increase the dV/dt. Very high frequency harmonic components of the PWM voltage will result in significant overvoltage due to an impedance mismatch between the cable and the motor. As an effect, the voltage seen by some parts of the insulation systems can be significantly higher than the rated value. This is particularly the case for turn-to-turn voltage in random wound machines (majority of low voltage machines). If high enough, the voltage can exceed the Partial Discharge Inception Voltage (PDIV), leading to a localized partial discharges activity in the machine. Partial discharges (PDs) are electrical discharges that partially short-circuit the insulation. Although the short-circuit is just partial and does not immediately lead to the machine's failure, the PDs induce a phenomenon of erosion due to the bombardment of charged particles, chemical deterioration and local thermal stress. Type II insulation system is designed to withstand the PDs during his lifespan. However type I, i.e.: low-voltage insulation system, can be quickly degraded by PDs, leading inevitably to machine's premature breakdown. The defects in the insulation system are, beside the problems with bearings, one of the most common causes of machines breakdown. Due to the use of frequency inverters,

_____

especially both primary and secondary insulations of the magnet wires are endangered in comparison with system-powered machines. If all the winding is not correctly impregnated by the varnish (secondary insulation), the weakest part of the insulation system will be the primary insulation (enamel).

The aim of this thesis is to investigate and analyze the aging process of enameled wires exposed to different aging factors and to propose a method allowing to predict their lifespans in given conditions. The main aging factors studied in this work are voltage amplitude, switching frequency and temperature. However, the influence of other secondary factors, such as ozone concentration, has also been studied. This work introduces a lifespan prediction based on the Design of Experiments (DoE) method and the Weibull distribution. This methodology is very flexible, which means that it is not limited by the number or nature of aging factors as well as it automatically includes the interactions between factors. Thanks to the model obtained with short multi-stress accelerated aging tests in the order of few hours, it is possible to predict the results of significantly longer ones. Moreover, an original adapted methodology is proposed that allows to predict the scatter of the long tests based only on the short-time results dispersion. The predictions are compared with the experimental data and show a good correlation, even for lifespans 100 times longer than short-time test points. Finally, we have shown that the same technique can be used as a quick and reliable comparison method between samples of different insulating materials.

This thesis is the result of a collaboration between the Laboratory on Plasma and Conversion of Energy (LAPLACE) in Toulouse and Leroy-Somer (part of Nidec group) in the framework of a CIFRE thesis. The works in LAPLACE laboratory were conducted in collaboration between the two research teams: Dielectrics Materials in the Energy Conversion (MDCE) and Control and Diagnostic of Electrical Systems (CODIASE). This cooperation gave to the company the scientific support for manufacturing better quality products, while the laboratory could profit from technical experience of Leroy-Somer.

_____

This PhD dissertation is divided into four chapters. A brief description of the content of those chapters is given below.

Chapter I: Partial discharges in low voltage machines

This chapter explains in detail how partial discharges can appear in low voltage machines. First it gives some basic information concerning electric machines and some insulating materials, typically used in those machines, as well as some key parameters used to characterize those materials. It is followed by a detailed description of electrical insulation system. In the next subchapter the information concerning the physics of partial discharges are given. Finally, the chapter is concluded by the problem of partial discharges in inverter-fed machines.

Chapter II: Accelerated aging tests on insulating materials

This chapter gives general information about accelerated aging tests through a comprehensive literature review. After some general introduction concerning the types of such tests, it describes the test bench constructed for the purpose of those tests. In this chapter also partial discharges measurements are discussed in details, as a PD activity is the key factor determining the aging mechanism in this study. Finally, the chapter covers life data analysis, especially Weibull's distribution.

Chapter III: Factors influencing the lifespan of insulating materials

Chapter III describes the factors influencing the lifespan of insulating materials in electrical machines. First, the choice of a typical sample for accelerated aging tests is discussed. Other subchapters describe the influence of temperature, voltage amplitude and frequency on the lifespan. Lastly, the influence of environmental factors, such as ozone concentration, and surface state are discussed. All those preliminary tests enabled the correct lifespan model construction, as presented in the last chapter.

Chapter IV: Lifespan modeling

The last chapter focuses on the lifespan modeling using the design of experiments (DoE) method. Firstly, it presents the brief overview of different techniques of lifespan modeling. Then, it gives a detailed theoretical description of the DoE method, followed by the construction of 2- and 3-factors lifespan models. Next, the technique used for lifespan prediction with scatter prediction is explained. Finally,

_____

the model is confronted with experimental results for the lifespans up to 100 times longer than the ones of the model tests. Lastly, the chapter shows how this approach can be applied as a comparison method, providing a quick while reliable rank of original solutions.

Finally, a conclusion of this work is presented as well as future works are proposed.

CHAPTER 1

State of the art

_____

Table of content

_____

1. CHAPTER 1: STATE OF THE ART

1.1. Introduction

This aim of this chapter is to present to the reader the context of this thesis. The first part presents a brief description of AC machine stators, concerning mostly on the parameters that can influence the lifespan of a final product. This part gives also some information concerning the materials typically used in low-voltage machines as well as their characteristics.

The second part describes in details the electrical insulation system of low voltage AC machine stators. It gives examples of all the insulating materials as well as their properties in order to better understand how they can influence the lifespan of the insulation system of such machines.

The third part explains the phenomenon of partial discharges, describing in details its physical principles. It introduces as well the terminology used later throughout the whole thesis.

The last part of this chapter is dedicated to inverter fed machines. It shows how the different parameters of drive and cable can influence the voltage amplitude at the motors terminals. Higher electrical stress seen by the electrical insulation of inverter fed machines may lead to their premature failure.

1.2. General information

1.2.1. Electric machines

Electric machine is defined as an energy transducer that can transform electric energy into mechanical energy (electric motor) or vice versa (generator). Depending on the waveform of the power supply, machines can be divided into 2 categories: direct current (DC) machines and alternative current (AC) machines.

The **DC machines** are very versatile. Different combinations of field windings (separate excitation, shunt, series or compound) results in a wide variety of final characteristics while assuring the relative simplicity. Thanks to the ease of control, DC machines have been frequently used in application requiring a wide range of rotating speeds or precise control of motor output. Unfortunately, these machines are quite expensive, taking into consideration both high initial cost as well as increased maintenance and operation costs due to the presence of commutator and brush gear. So-called "brushless DC machines", using permanents magnets to create excitation field, although allow to eliminate the problematical commutator, are often too expensive due to elevated price of the magnets. Since the development of power electronics, the technology of AC drive systems has flourished. As a result these system replace DC machines in applications previously associated almost exclusively with the latter, for instance in robots and railway application [1] [2].

The **AC machines** can be subdivided into 2 categories: synchronous and asynchronous (also called inductive). For the former, the rotating speed is directly proportional to the frequency of the stator voltages. This is not the case for the latter ones – asynchronous machines (see 1.2.1.1). In synchronous machines in most cases (except for e.g. reluctance machines, which will not be discussed in this work) currents in rotor windings are supplied through a rotating contact from the stationary frame by means of carbon brushes, which contact rotating corrector or slip ring. On the contrary, in asynchronous machines these currents are inducted by the motion of the rotor in the rotating magnetic field created by the alternating currents in stator windings.

1.2.1.1. Asynchronous machines

Asynchronous machines can be divided into 2 categories, depending on the type of the rotor. **Wound rotor** machines have rotor with the polyphase winding similar to

the one on the stator. In order to make rotor terminals accessible, insulated slip rings mounted on the shaft and carbon brushes bearing are used. These machines, due to quite complicated construction and thus higher price and maintenance cost, are relatively rarely used, only in a limited number of specialized applications.

On the contrary, squirrel-cage rotor machines, where the rotor winding consists of metal bars embedded in the slots and short-circuited at each end, have much simpler construction and thus are cheap, very rugged and require minimal maintenance costs. Thanks to all those advantages these machines are by far the most commonly used type of motor, available in wide range of sizes and powers [3] [2].

1.2.1.2. Random-wound machines

The windings of the machines can be divided into two groups: form-wound or random-wound [4].

Form windings use rectangular or square magnet wires. The position of each individual turn inside the slot is well controlled. As a result a turn-to-turn voltage stress as well as temperature distribution is more uniform compared to random-wound machines. Also the end windings are shaped to optimize the material consumption, promote cooling or reduce coil contamination by allowing better air circulation. The coils are very rigid with almost no possibility of movement thus limiting the probability of mechanical damages. Due to much higher cost, both of materials and labor, this type of winding is used almost only for high voltage or high power (typically more than hundreds of kW) low voltage machines.
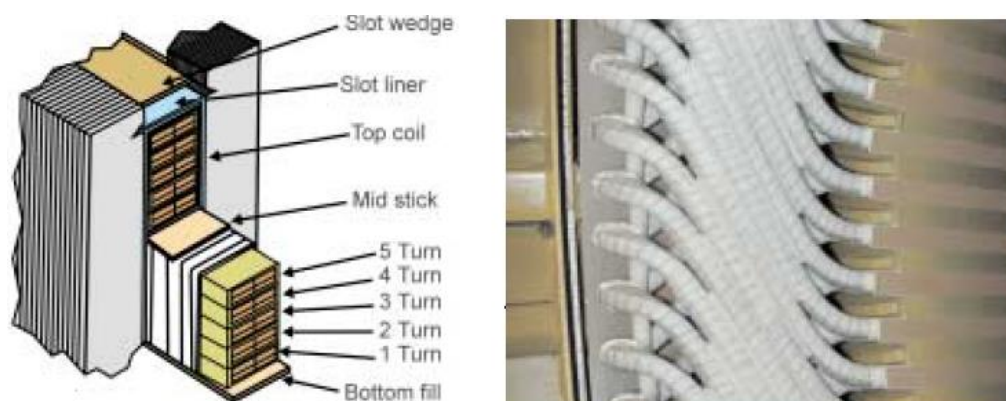
Figure 1.1. Form winding: scheme of the slot (left) and picture of end winding (right) [4].

_____

Low voltage and/or low power machines are almost exclusively random-wound. The windings are made with insulated round copper conductors, called magnet wire. As their arrangement in the coil during skeining or insertion cannot be controlled, the winding is called random. As a result wires from one turn can touch any other turn and therefore the maximum turn-to-turn voltage can be significantly higher than for form-wound machines. In the worst-case scenario the beginning and the end of the winding can be adjacent. According to some studies [5] the probability of such a situation can be higher than 90%. Moreover, this type of winding is much more vulnerable to mechanical damages due to vibrations or loose wire. Further problems can be caused by uneven resin build-up, non-uniform temperature distribution or higher accumulation of moisture and contaminates due to unsteady air circulation.
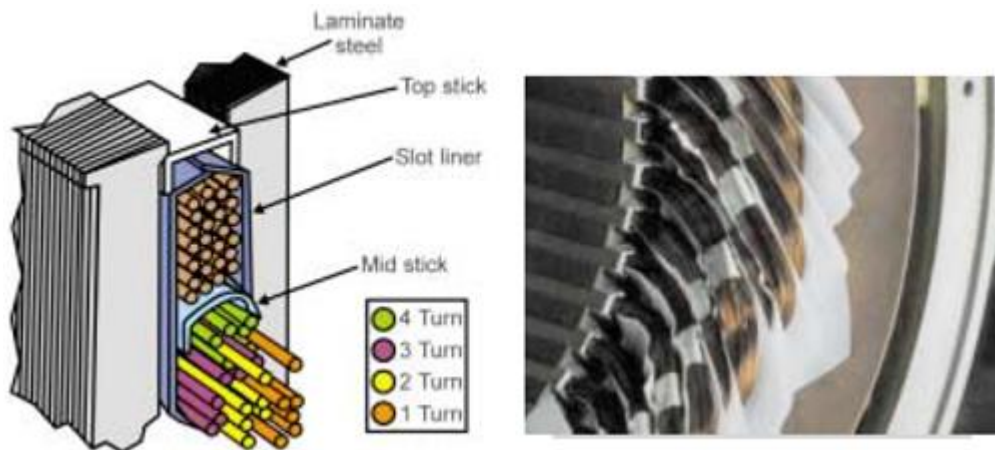
Figure 1.2. Random winding: scheme of the slot (left) and picture of end winding (right) [4].

1.2.1.3. *Manufacturing process*

Machine manufacturing is a complex, multistage process. It varies significantly depending on the type of the machine, its size, rated power and voltage and many other factors. The processes range from unitary production, manual or semi-automated, of special machines to fully automated massive production of most popular models. This section concentrates mostly on stator manufacturing process of low-voltage machines, as it can strongly influence the final properties of the electrical insulation system.

Stator magnetic core is made with laminated steel sheets welded together. The lamination allows to significantly limit the eddy currents induced in the core thus keeping related losses to the minimum [6].

_____

The winding of the stator starts with lining each slot of the machine with a slot liner providing phase-to-ground insulation (see section 1.3.1). This stage can be done manually or automatically. Some grease can be added so that the slot liner can be smoothly inserted or to facilitate the coils insertion [6].

Figure 1.3. Stator core with slot liners in each slot [7]

The next step consists in the preparation of the coils. As most of the low voltage motors are random-wound (see section 1.2.1.2), the winding is made with round copper magnet wire. In semi-automated winding systems, the coils are first spooled, manually or automatically, on the coil former. Then the coils are inserted inside the slots manually. In fully automated winding systems the coils are spooled on the special forks. The magnet wire can be lubricated to assure smooth coil insertion. Once all coils are spooled they are simultaneously pulled inside the stator slots. If the winding design requires the coils of 2 different phases inside the same slot, the slot separators are added in-between the coils prior to insertion in order to provide the phase-to-phase insulation (see section 1.3.2) [6].

Once the winding is finished, each slot is closed with a wedge separator. At end winding, different phases are separated with phase separators (see section 1.3.2) and coil outhangs are reshaped and immobilized using tie cords. At this stage the leads, in adapted sleeving, are connected and all other insulation reinforcements are added (see Figure 1.10).

The next step is an impregnation. There are three major techniques of impregnation depending upon the type and size of winding or production rate.

First, called dip impregnation, it consists in slowly dipping the preheated winding inside the varnish tank. After a certain time, the winding is removed to allow the excess varnish to drip. Afterwards, the varnish is cured, usually in a continuous

_____

furnace. In a slight variation of this simple process, called flood impregnation, the pre-dried winding is kept in a tank. The varnish is slowly pumped until the winding is completely submerged. This method is cheap and best adapted to mass production. Unfortunately, the varnish does not always penetrates properly inside the slot, due to high fill factor, as well as it can accumulate on unwanted parts of the winding [8] [9] [10].
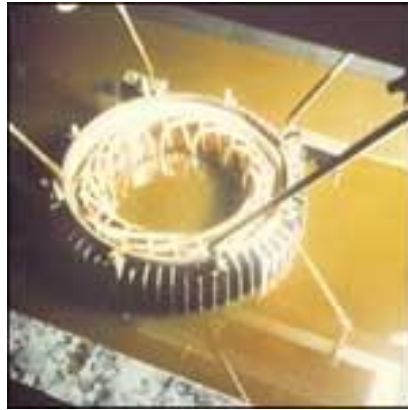
Figure 1.4. Dip impregnation of a stator winding [8]

In order to better control the impregnation process the Vacuum-Pressure Impregnation (VPI) method was developed. First, the winding placed in a chamber is subjected to low vacuum. The varnish is fed in until the winding is completely submerged. Then, to provide better penetration of varnish, dry compressed air or pressurized nitrogen is applied. In comparison to dip impregnation this method is far more expensive and time-consuming, thus is not commonly used for the low-voltage machines [8] [9] [6] [10].

Figure 1.5. Tank used for Vacuum-Pressure Impregnation (VPI) [9]

_____

The last technique, used mostly for smaller machines, is trickle impregnation. In this method, the resin is applied by a thin jet on preheated rotating winding. The used resin polymerizes shortly after it penetrated through the winding. The method offers several advantages such as: short processing time, high retention and consistent quality of impregnation [8] [9] [10].

Figure 1.6. Trickle impregnation of a stator winding [8]

An increasing number of machines is impregnated using the technique called "potting". It combines the advantages of VPI method and trickle impregnation. It uses the fast polymerizing resins injected inside the mold enclosing the winding, including the coil outhangs. As a result, the secondary insulation is a casting with significantly reduced gas voids number. On the other hand, the use of this method does not allow the rewinding of the machine in case of breakdown [10].

Figure 1.7. Potted stator winding

_____

As stated before, the chosen assembly technique as well as impregnation method and its parameters have a fundamental impact on the final properties of the machine insulation system. Thus, the study of the insulating materials only in their "unprocessed" form cannot be representative in every aspect for the assembled machines.

The quality of the stator winding is verified by many tests, most of them conducted prior and after the impregnation process. The winding continuity and phase equilibrium is verified by measuring the coils resistance. The quality of insulation system is tested for example by a surge test or a partial discharges test. An exhaustive list of tests conducted on the insulation system is presented in [11] or in [6].

1.2.2. Electrical insulating materials

Insulating materials can be divided into 3 groups taking into consideration their state of aggregation in the working conditions. Although gaseous materials are widely used in high voltage insulation systems, their use in electric machines, especially in the low-voltage ones, is reduced to air. Its insulating properties are discussed in chapter 1.4. Liquid materials, still commonly used in e.g. transformers or high voltage cable lines, are not used in low-voltage rotating machines [12] [13].

Solid insulating materials are widely used in all types of electric machines. Depending on their origin they can be classified as:

- Natural organic substances, such as: paper, cotton, silk, wool, flax, natural plant resins;
- Inorganic natural materials, like mica;
- Synthetic products, like different plastics: elastomers, thermoplastics and thermosetting polymers;

The first insulation systems were almost entirely reliant on naturally occurring materials. The fast development of synthetic products since the beginning of the 20th century allowed to gradually replace the natural material by cheaper and more resistant polymers. Inorganic natural materials are still in use nowadays thanks to their outstanding electrical properties.

_____

1.2.2.1.   Typically used materials

The International Electrotechnical Commission (IEC) divides the electrical insulation systems used in electrical machines into 2 main categories. The first group, called type I [14], consists in those which are not expected to experience a partial discharges activity within specified conditions in their service lives. Systems which are expected to withstand a partial discharges activity in any part of the insulation system throughout their service lives, are classified as type II [15].

The type I systems are used in low voltage machines, generally having rated voltage of 700 V_{RMS} or less. These machines are typically random-wound (see 1.2.1.2) and use almost uniquely organic polymer materials (see section 1.2.2.1.1).

The type II systems are used in high voltage machines, generally having rated voltage higher than 700 V_{RMS}. These machines are typically form-wound (see 1.2.1.2) and use both the organic polymer materials and inorganic materials (see section 1.2.2.1.2).

1.2.2.1.1.   Organic polymer materials

Organic polymer materials are widely used in insulation systems, both for low- and high-voltage machines. The existing gamut of these materials is extremely diverse. Their choice depends upon the severity of electrical, thermal and mechanical stresses they would face in their applications. Usually, the thermal stresses are given primary consideration, inasmuch as even small changes of the temperature may induce considerable damage to insulators due to chemical degradation, cracking, melting etc., thus reducing the lifespan. The thermal class (see section 1.2.2.2.3 for definition and examples) is most commonly used to thermally characterize the materials [6] [13].

Generally speaking the polymer materials are appreciated for their low price and low processing costs thanks to easy machinability. They are chemically resistant and age slower than natural organic substances. Although the polymers in general present a high breakdown strength (see section 1.2.2.2.4), high bulk resistivity and low dielectric loss tangent (see section 1.2.2.2.2), they are quite liable to tracking and do not resist a partial discharges activity. This is why, according to the standard [14] definition, the type I systems should be exempted from a partial discharges activity. This standard deals also with approval of such a systems powered by voltage converters [6] [13].

_____

1.2.2.1.2.   Inorganic materials

Inorganic materials are widely used in electrical engineering thanks to their excellent insulating properties. They have high breakdown strength and support temperatures significantly higher than any synthetic polymers. These materials are very resistant to chemical reagents and age much slower.

The main disadvantage of inorganic materials is their poor mechanical properties. They are very brittle and fragile in comparison to synthetic polymers, thus their low machinability. As a result their processing costs are significantly higher.

Especially one inorganic material has gained its place in the insulation system of electric machines: mica. It is a mineral, complex silicate, mined in chunks or books. In order to improve mica's poor mechanical properties, it is processed and used as a mica paper. By adding different binders and mica splitting one can achieve built-up mica, which properties can be modified according to needs by the choice of a binding agent.

Mica, beside its excellent breakdown and thermal strength, is highly resistant to erosion caused by a partial discharges activity. Thus it is widely used in type II insulation systems that are expected to withstand a PD activity in any part of the system throughout their service lives. Due to elevated price and high processing costs it is almost never used in low voltage machines' insulation system [16].

1.2.2.2.   Characteristic parameters

The general characteristics of the insulating materials can be divided into 5 categories [13] [17]:

- Mechanical properties: tensile, compressive, shearing and bending strength, elastic modulus, hardness, impact and tearing strength, viscosity, extensibility, flexibility, machinability, fatigue, resistance to abrasion, stress crazing;
- Electrical properties: electric breakdown strength (bulk medium), surface breakdown strength, liability to track, volume and surface resistivity, dielectric permittivity, dielectric loss tangent, insulation resistance (bulk and surface), frequency dependency of electrical properties;
- Thermal properties: thermal conductivity, thermal expansion, primary creep, plastic flow, thermal decomposition, spark, arc and flame

_____

resistance, temperature coefficients of other parameters, melting point, pour point, vapor pressure, low smoke generation;

- Chemical properties: resistance to chemical reagents, effects upon adjacent materials, electrochemical stability, stability against aging and oxidation, solubility, solvent crazing;

- Miscellaneous properties: specific gravity, refractive index, transparency, color, porosity, permeability to gases and vapors, moisture adsorption, surface adsorption of moisture, resistance to fungus, resistance to aging by light, degassing.

Taking into consideration a very large number of parameters, only few, the most important ones from the point of view of electric machine insulation system, will be discussed in the following paragraphs.

1.2.2.2.1. *Relative permittivity*

Relative permittivity can be defined as a quotient of the capacitance C_x of a condenser where a studied material constitutes as the dielectric to capacitance C_0 of the same condenser when this material is replaced by vacuum [18] [19]:

$$\varepsilon_r = \frac{C_x}{C_0} \tag{1.1}$$

The absolute permittivity ε of insulating material is a product of vacuum permittivity ε_0 and relative permittivity ε_r:

$$\varepsilon = \varepsilon_0 \varepsilon_r \tag{1.2}$$

where:

$$\varepsilon_0 = 8.854 \cdot 10^{-12} \left[\frac{F}{m} \right]$$

Table 1.1 present values of ε_r for some solid insulating materials.

Real dielectric materials get polarized once the external electric field is applied. This phenomenon has multiple levels: displacement polarization (displacement of electron cloud (induced dipole) or atoms in the molecule (induced dipole moment)), orientation polarization (arrangement of the permanent dipoles to the field lines) and boundary surface polarization or space charge (accumulation of electric charges at the

_____

interface of different phases). As each of these phenomena has certain inertia, once the alternating field is applied the polarization current, out of phase of capacitive charging current, will appear (see Figure 1.8).

Thus the need of introducing the complex relative permittivity $\overline{\varepsilon_r}$. According to [19] [20] it can be defined as in (1.3):

$$\overline{\varepsilon_r} = \varepsilon_r' - j\varepsilon_r" \tag{1.3}$$

where:

ε_r' – real part of the complex permittivity; it is related to the stored energy, thus can be call the AC capacitivity

$\varepsilon_r"$ – imaginary part of the complex permittivity; it is related to the dissipation (loss) of energy within the medium; also known as dielectric loss factor or loss index

The relation between the complex current and voltage at the capacitor terminals can be expressed as:

$$\underline{I} = j\omega\overline{\varepsilon_r}C_0\underline{U} \tag{1.4}$$

1.2.2.2.2. *Dielectric dissipation factor*

Dielectric dissipation factor, called also the dielectric loss tangent, $\tan\delta$, is defined [19] as the quotient of active to reactive power loss in a capacitor or in the volume of dielectric (see Figure 1.8):

$$\tan\delta = \frac{active\ power}{reactive\ power} = \frac{u \cdot i_{ins} \cdot cos\varphi}{u \cdot i_{ins} \cdot sin\varphi} = \frac{|i_R(Total)|}{|i_c(Total)|} \tag{1.5}$$

$$\delta = \frac{\pi}{2} - \varphi \tag{1.6}$$
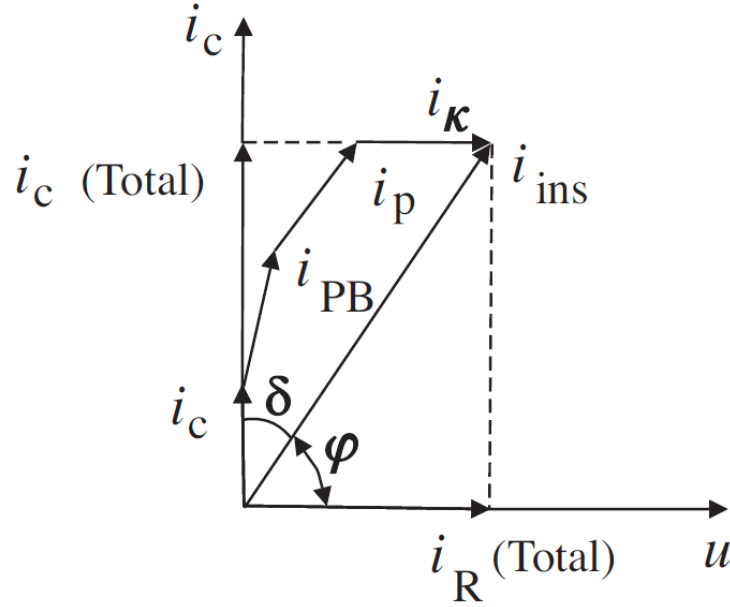
Figure 1.8. Phasor diagram of a real capacitor (i_c – capacitive charging current, i_{PB} – partial discharge impulse current, i_p – polarization current, i_κ – conductive current) [19]

If the currents associated with partial discharges impulses and conductive current can be neglected, the tanδ can be expressed as:

$$\tan\delta = \frac{\varepsilon_r{''}}{\varepsilon_r'} \tag{1.7}$$

Table 1.1 present values of tanδ for some solid insulating materials.

Table 1.1. Standard values of electrical properties of some solid insulating materials (at 20ºC) [21] [22] [12] [23] [18]

Insulating material	tanδ			ε_r		
	50 or 60 Hz	1 kHz	1 MHz	50 or 60 Hz	1 kHz	1 MHz
Polyurethane (PUR)	0.015	0.03 – 0.10		2.9 – 4.3	2.9 – 4.3	2.9 – 4.3
Polyamide (PA)	0.006 – 0.016	0.010 – 0.025	0.01 – 0.03	3.7 – 4.5	3.4 – 4.1	3.6 – 4.2
Poliamideimide (PAI)	0.03	0.03	0.03	4.3	4.1	3.9
Polyimide (PI)	0.002 – 0.007	0.003 – 0.01	0.005	3.5 – 4.0	3.5 – 4.0	3.5
Epoxyde	0.005 – 0.04	0.01 – 0.02	0.01-0.04	3.5 – 5.0	3.5 – 5.0	3.5 – 5.0
Mica	0.0002 – 0.0025	0.001 – 0.005	0.0005- 0.01	5.0 – 8.0	5.0 – 8.0	5.0 – 8.0

_____

1.2.2.2.3.   Thermal class

According to the IEC definition [24], the thermal class is a designation of an insulating material or system by a number that is equal to the numerical value of the maximum temperature, expressed in degrees Celsius, for which the material or system is appropriate in normal use.

The same material or insulation system might be assigned to different thermal class if used in different service conditions. Also the thermal class of an insulation system does not imply that all the materials used are of the same thermal capability.

For most chemical reaction its rate *r*, for example describing aging process, can be described by the equation (1.8):

$$r = -\frac{dC}{dt} = k(T) \cdot C_1{}^n \cdot C_2{}^m \cdot C_3{}^p \cdot \ldots \tag{1.8}$$

where:

C_i – concentration of the reacting material

t – time

$k(T)$ – rate constant, as a function of the temperature T

$n+m+p+\ldots$ – rank of the reaction

By assuming that the aging process is a first order reaction, which means that the reaction rate depends only on the concentration of one reagent (a unimolecular reaction), the equation (1.8) can be simplified to (1.9):

$$r = -\frac{dC}{dt} = k(T) \cdot C \tag{1.9}$$

By solving the equation (1.9) we get:

$$\ln(C) = -k(T) \cdot t + \ln(C_0) \tag{1.10}$$

where:

C_0 – initial concentration of the reagent (at $t = 0$)

The rate constant k can be expressed using the Arrhenius law as:

$$k = A \cdot e^{\frac{-E_a}{R \cdot T}}$$

(1.11)

where:

A – constant characteristic for each chemical reaction

T – absolute temperature

E_a – activation energy

R – universal gas constant

By rearranging (1.10) using (1.11) we obtain:

$$t = \frac{\ln(C_0) - \ln(C)}{A \cdot e^{\frac{-E_a}{R \cdot T}}}$$

(1.12)

$$\ln(t) = \ln\left(\frac{1}{A} \cdot \ln\left(\frac{C_0}{C}\right)\right) + \frac{E_a}{R \cdot T}$$

(1.13)

As a first summand is constant, the equation (1.13) shows that, according to the theory of T. W. Dakin [25], the logarithm of lifespan is proportional to the reciprocal of the absolute temperature.

By conducting the accelerated aging tests for at least 3 or 4 temperatures (higher than the maximum allowed temperature) and plotting the corresponding lifespans on $\log(t) = f\left(\frac{1}{T}\right)$ graph, we can evaluate the thermal class by extrapolating the life line to lower temperatures and reading the cross-point with $t = 20\,000$ [h] (see Figure 1.9). The thermal class is obtained by rounding down the temperature T (expressed in degree Celsius) to the closes value given by the standard [26] (see Table 1.2). The detailed test procedures, defining e.g. the choice of test temperatures or sample type, can be found in standards [27] [28].

_____
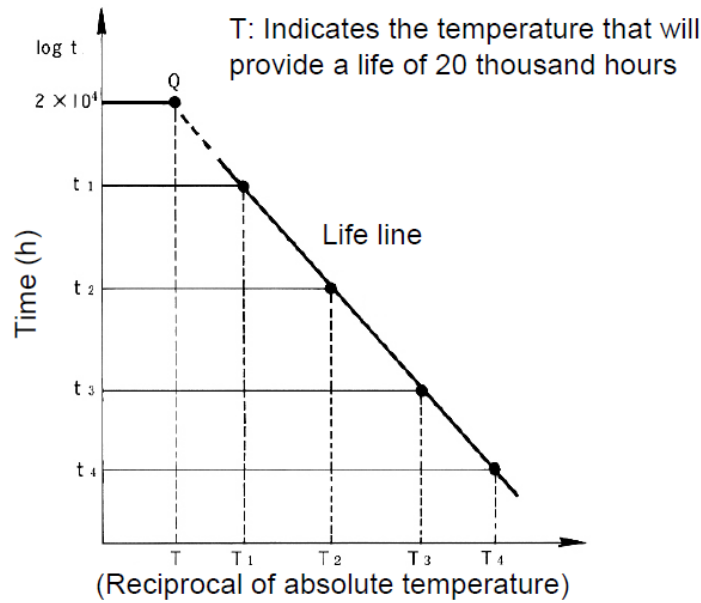
Figure 1.9. The $\log(t) = f\left(\frac{1}{T}\right)$ plot used for calculating the thermal class T.

Table 1.2 presents thermal classes defined in [26] with examples of materials.

Table 1.2. Thermal classes with examples of materials [29] [12]

IEC 60085 Thermal class	IEC 60085 Previous nomenclature	Maximum hot spot temperature allowed	Examples of materials
90	Y	90ºC	Paper, polyethylene (PE)
105	A	105ºC	Polychloropropylene
120	E	120ºC	Polyethylene terephthalate (PET)
130	B	130ºC	Melamine
155	F	155ºC	Polyurethane (PU)
180	H	180ºC	Polyester (PES)
200	200	200ºC	Polyesterimide (PEI) /polyamidimide (PAI)
220	220	220ºC	Polyamidimide (PAI)
Not present in IEC60085, but exists in NEMA standard MG-1 Motors and Generators (class S)		240ºC	Polyimide (PI)
250	250	250ºC	Inorganic components (ceramics)

_____

1.2.2.2.4.   Breakdown strength

The breakdown strength, called also (di-)electric strength, is defined [24] as a quotient of the maximum voltage applied without breakdown *U*, by the distance *d* between conducting parts under prescribed test conditions:

$$E_b = \frac{U}{d}$$
(1.14)

The breakdown strength depends on multiple conditions, such as [12] [19]:

- Type of dielectric material, its purity and presence of imperfections,
- Voltage waveform (DC, sine wave, square wave, surge, etc.),
- Voltage frequency,
- Rate of voltage amplitude increase (usually around 1kV/s),
- Settings of maximum leakage current,
- Electric field configuration (shape of electrodes, their size),
- Experimental conditions (temperature, humidity, pressure etc.),
- Sample thickness and surface (generally speaking the thicker the sample or the larger the sample surface the lower the breakdown strength due to higher probability of finding structure imperfections).

Table 1.3 presents some examples of breakdown strengths for insulating materials.

Table 1.3. Breakdown strength

Material	Breakdown strength [V/µm]	
	Bulk [21] [22] [12] [23]	**Thin film** (~ tens of µm) [21] [22] [12] [23] [30]
Polyurethane (PUR)	2-25	180
Polyester (PES)	21	180
Polyesterimide (PEI)	19	175-250
Polyamidimide (PAI)	23	180
Polyimide (PI)	20-25	180-430
Epoxy	20	130-320
Mica	80-130	120-250

1.3. Electrical insulation system of low voltage motors

The insulation system plays a very important role and its presence is absolutely substantial to assure the correct functioning of any electric machine. The properties of materials used in the insulation system are the key factor determining the machine rated voltage, life expectancy or thermal class.

The role of the insulation system is threefold [6] [31]:

- Electrical short circuits preventions

This is a primary function of the insulation system. Any short circuits due to dysfunction of the insulation system leads, usually very soon, to a complete breakdown of the machine. The choice of the insulating materials and their thickness is dictated by the machines rated voltage. In low voltage machines, almost solely the type I insulating materials are used (see section 1.2.2.1.1), due to their low cost and easy manufacturing. The thickness of any insulating material must be adapted in such a way that its breakdown voltage is significantly higher than the applied voltage. The lifespan of the weakest part insulating system will define the life expectancy of the whole machine.

- Dissipation of heat loses

According to Joule's first law, the current I circulating inside the conductor having the electrical resistance R produces the energy proportional to I^2R. Thus the current circulation inside the winding creates the heat, which is often referred as copper losses (or more generally speaking winding losses). This heat needs to be dissipated in order not to increase too much the temperature of the winding. Unless, the high temperature will decrease the machine efficiency as well as greatly accelerate the insulation aging process. The heat must be transferred to the heat sink (stator frame) via some parts of the insulation system. As most of the insulating materials are very bad heat conductors, their thickness must be elaborately chosen not to worsen the heat transport yet still assuring their primary function.

- Winding movement prevention

Winding is subjected to many forces that may displace its parts. Such movement might occur due to transport, mechanical vibrations as a result of machine working or Lorentz forces acting on conductors in the magnetic field of the machine. One of the functions of the impregnating varnish (see section 1.3.4) is to prevent any movement of

_____

any parts of the winding and to glue the wires together. Additionally, in order to keep the winding inside the slots, wedges or top sticks are used.

The design of the insulation system is a complex process. Generally speaking, the thicker insulation is, the higher its breakdown voltage and the longer the lifespan. On the other hand, thicker insulation usually means worse heat dissipation and thus lower overall efficiency of the machine as well as smaller specific output (power-to-mass ratio) due to, inter alia, smaller slot fill factor.

The insulating components in low voltage machines can be divided according to their function into the following groups [6]:

- Phase-to-ground insulation (see section 1.3.1)
- Phase-to-phase insulation (see section 1.3.2)
- Turn-to-turn insulation (see section 1.3.3)
- Impregnating varnish or resin (see section 1.3.4)

The first three components are often called primary or major insulation, as opposed to impregnating liquid, which is a secondary insulation. Figure 1.10 shows the overview of the components of a low-voltage insulation system.
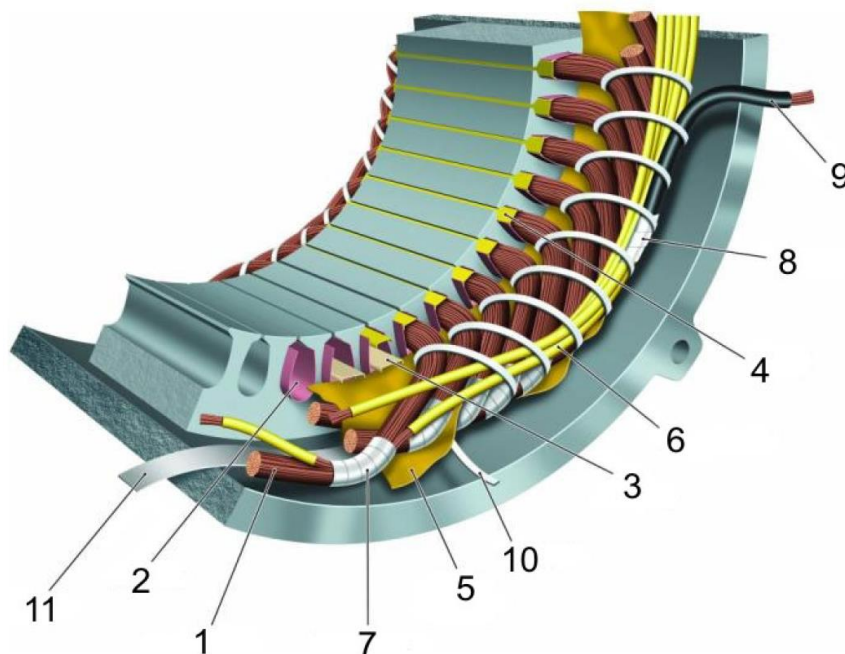

Figure 1.10. Overview of materials in a low-voltage insulation system: 1 turn insulation, 2 slot liner, 3 slot separator, 4 wedge, 5 phase separator, 6 lead sleeving, 7 coil-nose tape, 8 connection tape, 9 cable, 10 tie cord, and 11 bracing [31].

_____

1.3.1. Phase-to-ground insulation

The phase-to-ground insulation prevents the winding coils from touching the stator core. Each slot of the stator is lined with a slot liner (see Figure 1.10 – 2). Slot liner is made most commonly of so-called insulating "paper", although it is a synthetic material, such as aramid paper (well-known under its DuPont trade name Nomex™), polyester film (known as Mylar™) or polyester fleece (known as Dacron™). Generally, they present high breakdown strength, good mechanical properties, such as tear resistance and they resist well to chemical attack. The choice of the insulating material is often defined by the thermal class of the machine. The slot liners are available in wide range of thicknesses, depending of their voltage class [6] [31].

In order to further improve the properties of these discrete materials they can be piled together into flexible laminates. These laminates are best known under their trade names, e.g. NMN (Nomex™/Mylar™/Nomex™) or DMD (Dacron™/Mylar™/Dacron™).

1.3.2. Phase-to-phase insulation

The phase-to-phase insulation prevents the any two coils of different phases from touching one-another. At the end winding the coils are separated by the phase separators (see Figure 1.10 – 5). For those winding configurations with two different phases in the slots, their coil must be separated by the slop separators (see Figure 1.10 – 3).

For phase-to-phase insulation, the same materials are used as for the phase-to-ground insulation (see section 1.3.1). The insulators are typically slightly thicker due to higher voltage that they need to support. For specific machines, usually type II, Dacron™ tapes are used as enwinding phase separators, as they retain the varnish during impregnation thus improving their insulating properties. This effect is undesired for the slot separators because it would limit the slot fill factor [6] [31].

1.3.3. Turn-to-turn insulation

The role of turn-to-turn insulation is to electrically separate the turns of the same coil from each other. In low voltage machines this insulation consists in the thin enamel layer on the copper wire. For each diameter of a magnet wire there are 2 main enamel

_____

thicknesses available: grade 1 (thinner enamel) and grade 2 (thicker enamel). Some producers offer also grade 3 with a thicker enamel layer. All the wire dimensions are standardized in European standard IEC 60317-0-1 [32] or American standard NEMA MW1000. Table 1.4 shows the wire dimensions for few diameters used in this thesis.

Table 1.4. Standard magnet wire dimensions and tolerances (some examples) [32]

Nominal conduction diameter [mm]	Conductor diameter tolerance (±) [mm]	Min. increase [mm]		Max. overall diameter [mm]	
		Grade 1	Grade 2	Grade 1	Grade 2
0.500	0.005	0.024	0.045	0.544	0.566
0.800	0.008	0.030	0.056	0.855	0.884
1.000	0.010	0.034	0.063	1.062	1.094
1.120	0.011	0.034	0.065	1.184	1.217

The higher enamel grade allows higher breakdown strength and longer lifespan of the insulation [32]. On the other hand it limits the slot fill factor and thus lower power-to-mass ratio. Figure 1.11 shows the maximum slot fill factor as a function of insulation grading and nominal conductor diameter.
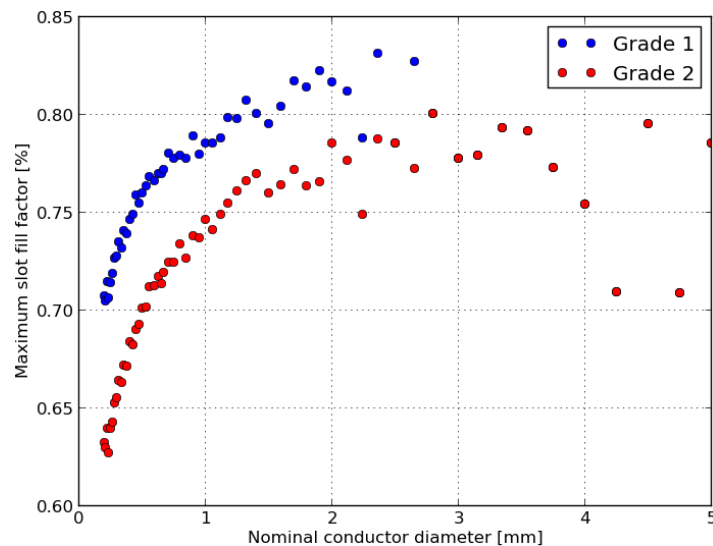

Figure 1.11. Maximum slot fill factor as a function of insulation grading and nominal conductor diameter according to IEC 60317-0-1 [32].

___

1.3.3.1.   Magnet wire manufacturing process

Figure 1.12 presents the manufacturing process of enameled wire.
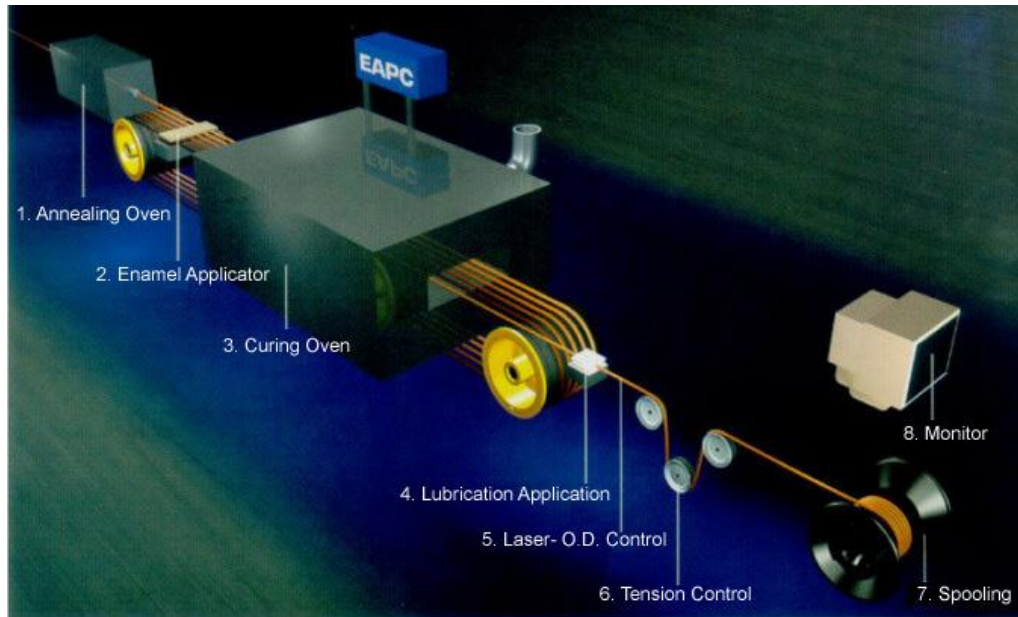
Figure 1.12. Winding Wire Production Flow. Description in the text below. [33]

First the bare wire of an appropriate diameter is annealed in the oven (1) in order to soften the copper. Then the very thin layer (about 1 μm thick) of the enamel is applied (2) on the copper surface to guarantee good adhesion and ensure good insulating properties. In the oven (3) the enamel is cured to evaporate the solvent from the enamel. The process of application and curing is repeated up to 30 times in order to achieve the desired enamel thickness. Once all the layers of enamel are cured, the lubricant is applied (4) to achieve a good slidability of the magnet wire. During the whole manufacturing process the outer diameter (5) and winding tension (6) are continuously controlled. Finally the product is reeled on a supply spool (7) [33] [30].

Due to the complicated manufacturing process, the properties of each layer of the enamel are slightly different. The one closest to the copper core undergoes multiple curing processes, while the external layer just one. As the standard [32] allows some dispersion the enamel thickness may vary, especially from one lot to another. It may change also along the wire of the same spool, especially due to centricity problems (copper core might not be centered). All these factors increase significantly the dispersion of any tests conducted on magnet wires.

_____

1.3.3.2.   Enamel materials

Magnet wires are covered with different enamels. They can be divided into 2 main categories: conventional wires (see section 1.3.3.2.1), covered with polymer enamel, and so-called corona resistant wires (see section 1.3.3.2.2) where the polymer matrix is charged with the nanoparticles of inorganic oxides.

1.3.3.2.1.   Conventional wires

There are several polymer materials widely used as enamel in conventional magnet wires. They present different thermal properties, thus are classified in different thermal class. Table 1.5 presents the list of polymer enamels with their properties.

Table 1.5. Typically used conventional enamel materials for magnet wires [33] [30] [34]

Polymer name	Abbr.	Thermal Class	Properties
Polyurethane	PUR	155 180	• Good solderability • Not for high current nor for high temperature applications
Polyester	PES	180	• Not solderable • Not suitable for high moisture applications
Polyesterimide	PEI	180	• Solderable (at high temperatures) • Good thermal properties • Good chemical resistance
Polyesterimide /polyamidimide	PEI/PAI	200	• PEI basecoat with PAI topcoat • Not solderable • PAI topcoat guarantees better resistance to chemicals and moisture
Polyamidimide	PAI	220	• Not solderable • Very good thermal properties • Good chemical resistance • Suitable for high moisture applications • Low coefficient of friction
Polyimide	PI	240	• Not solderable • Very good properties even at very high temperatures (highest thermal index) • Excellent chemical resistance • High radiation resistance

1.3.3.2.2.   Corona resistant wires

As mentioned before (see section 1.2.2.1) synthetic polymer materials are easily eroded by a partial discharges activity. The enamel of conventional wires is also highly vulnerable to PDs. On the other hand, inorganic materials can withstand a partial

discharges activity for a long time, but are hard to process and thus expensive (see section 1.2.2.1.2).

Magnet wire manufacturer desired to combine the advantages of those two groups of materials. As a result, composite materials were developed, where the micro- or nano- inorganic particles, such as TiO_2, SiO_2 or Al_2O_3, are dispersed in the polymer matrix. The wires enameled with such composites are often referred to as "corona resistant". Although they are not completely resistant to a PD activity, they have significantly higher breakdown strength and lifespan in a partial discharges regime than the conventional wires.

The properties of such composites depend naturally on 2 factors: the properties of the polymer matrix (will influence for example the thermal class) and of the inorganic filler. For the filler, the key factor defining the final properties of the magnet wire is the size of the particles, or rather of the possible aggregates in the final composite. The smaller the particles are, the bigger the surface contact is. This zone of contact, called interface, has recently gained increased attention in order to better understand its influence on the properties of the final product. Nevertheless, these composite materials, although having only few weight percent of inorganic particles, exhibits very interesting properties. They have higher breakdown strength but especially significantly longer lifespan than the conventional wires while exposed to partial discharges activity [35].

1.3.4. Impregnating varnish or resin

As mentioned before, the impregnation liquid serves in the machines as a secondary insulation. Naturally it strengthens the primary insulation, but also improves heat transfer (better thermal conductor than the air) as well as mechanically blocks the winding and protects it toward vibrations and environmental conditions.

The difference between the varnish and resin is in the solvent. In order to lower the viscosity of the resin to facilitate the application process an important quantity of organic solvents is added to achieve varnish. These solvents evaporate during curing and later on during drying, allowing the toughening of the coating. As during this process large quantities of potentially toxic volatile organic compounds (VOC) are emitted, the solventless resins are become more and more popular.

_____

The polymers most commonly used as the impregnating varnishes or resins are [6] [31]:

- Polyester-based liquids: easy to use, but brittle and dielectrically weak at high temperatures

- Epoxy-based liquids: mechanically and chemically more resistant, but quite viscous; better proprieties in high temperatures that the polyester-based ones

- Polyesterimide-based liquids: similar to polyester-based, but with better thermal properties

One has to remember that the solvent properties as well as many additives may change significantly the proprieties of the impregnating liquids. As the detailed data is often kept secret by the producers, it is difficult to compare products based only on their principle chemistries.

1.4. Partial discharges

According to the standard definition [24], a partial discharge (PD) (sometimes referred to as a partial breakdown (PB) [19]), is an electric discharge that only partially bridges the insulation between two conductors.

Papers [36] [37] define partial discharges (called corona) as a type of localized discharges resulting from transient gaseous ionization in an insulation system when the voltage stress exceeds a critical value. This ionization process is localized over only a portion of the distance between the electrodes of the system.

Partial discharges can be classified into 3 categories depending on their nature [19]:

- Corona discharges: when stable partial discharges occurs at a free electrode in gaseous dielectrics;
- Internal partial discharges: when discharges occur in gas voids imprisoned inside solid or liquid dielectrics;
- Surface discharge (also commonly known as tracking discharges): when discharges occur on the surface of solids or liquid dielectrics but in gas.

This study is mainly concentrated on internal partial discharges. In the next sections of this chapter we will concentrate on breakdown in gases (mainly air).

Partial discharges give rise to multiples secondary effects, such as [36]:

- Generation of ultraviolet radiation and light;
- Nascent oxygen (strong oxidizing agent) that can produce ozone and in the presence of moisture, nitric acids (see chapter 3);
- Absorption or generation of different substances, also gaseous, within enclosed voids;
- Heat generation in the discharge channel and power losses in the power supply;
- Mechanical erosion of surfaces by ion bombardment;
- Interference with radio communication within the broadcast band frequency spectrum;
- Audible noise and ultrasounds.

_____

These phenomena are the basis of different techniques used to detect the partial discharges activity. Those methods are described in chapter 2.

1.4.1. Discharge mechanism

The breakdown of a gas is possible only by forming a highly conductive channel between the electrodes. It means the necessity of vigorous ionization processes in order to produce a large number of charge carriers. The phenomenon strongly depends on multiple conditions, such as parameters of electric field (its uniformity, electrodes shapes, gap distances), gas type and experimental conditions (pressure, temperature, humidity, etc.).

There are two basic mechanisms of breakdown in gases: Townsend mechanism [38] and Streamer mechanism [39] [40]. They will be discussed in the following sections.

1.4.1.1. Townsend mechanism

The multiplication of charge carries in gas takes place mainly by impact of electrons with neutral molecules, which is known as α or primary ionization. The secondary or β process, occurs when ions make a contribution to ionization by ejecting electrons from the electrodes surface after impact.

In order to begin a discharge process, some charge carries, called germs, need to be present in the gas before applying the electric field. When an electron accelerated by the electric field gains sufficient energy to ionize, i.e. ejecting another electron from the neutral molecule leaving behind a positive ion (α process), the new electron, along with the primary electron, continue the process of ionization. The process continues, releasing further electrons, thus creating an electron avalanche [19] [36].

By neglecting the processes of recombination and diffusion, the number of electrons dn_x produced by collisions in element dx at distance x from the electrode can be calculated as:

$$dn_x = n_x \alpha dx \qquad (1.15)$$

where:

α – Townsend's first ionization coefficient $\left[\dfrac{1}{\text{cm}}\right]$

n_x – number of electrons at distance x from electrode

By solving the equation (1.15) for a case of very small gap length d, the number of electrons striking the anode per second is:

$$n_d = n_0 e^{\alpha d} \qquad (1.16)$$

Thus each from n_0 germ electrons leaving the cathode produces $\left(e^{\alpha d} - 1\right)$ new electrons and the same number of positive ions while traversing the distance d.

The Townsend's first ionization coefficient α for electropositive gases is defined as the mean number of ionizing collision made by a single electron while its drift across the gap in a uniform field [19]. In air, this coefficient at a constant temperature can be approximated by [41]:

$$\alpha \approx 1.11 \times 10^{-4} \left(\frac{E}{p} - 25.1\right)^2 \cdot p \qquad (1.17)$$

where:

E – electric field strength $\left[\dfrac{\text{V}}{\text{cm}}\right]$

p – air pressure [Torr]

During an electrical breakdown, a conducting channel bridges the electrodes through the insulating gas. The electrons required to build this channel are not only produced within the gas across the gap (α process), but are also released from the electrode surface (γ process). These γ ionization processes are a consequence of the transfer of energy gained by the electrons in an avalanche:

_____

- effect of positive ions (they have sufficient energy to eject the electrons upon striking the cathode);

- photon effect (the cathode radiation from excited molecules returning to their ground state energy level);

- metastable effect (molecules in this condition may diffuse back to the cathode thus causing electrons emission on striking) [19] [42].

The Townsend's secondary ionization coefficient γ is defined as the number of secondary electrons on an average produced at the cathode per electron generated by the α process [19]. It strongly depends upon the cathode material, field intensity and gas pressure. As a result the mean number of secondary electrons μ is:

$$\mu = \gamma\left(e^{\alpha d} - 1\right) \tag{1.18}$$

In order for the process to be self-sustaining, the μ must meet so-called Townsend criterion:

$$\mu = \gamma\left(e^{\alpha d} - 1\right) = 1 \tag{1.19}$$

_____

Figure 1.13 presents the schematic of Townsend breakdown mechanism.

(a) Ejection of electron
from cathode.

(b) Generation of series
of avalanches.

(c) Building of +ve space
charge near anode
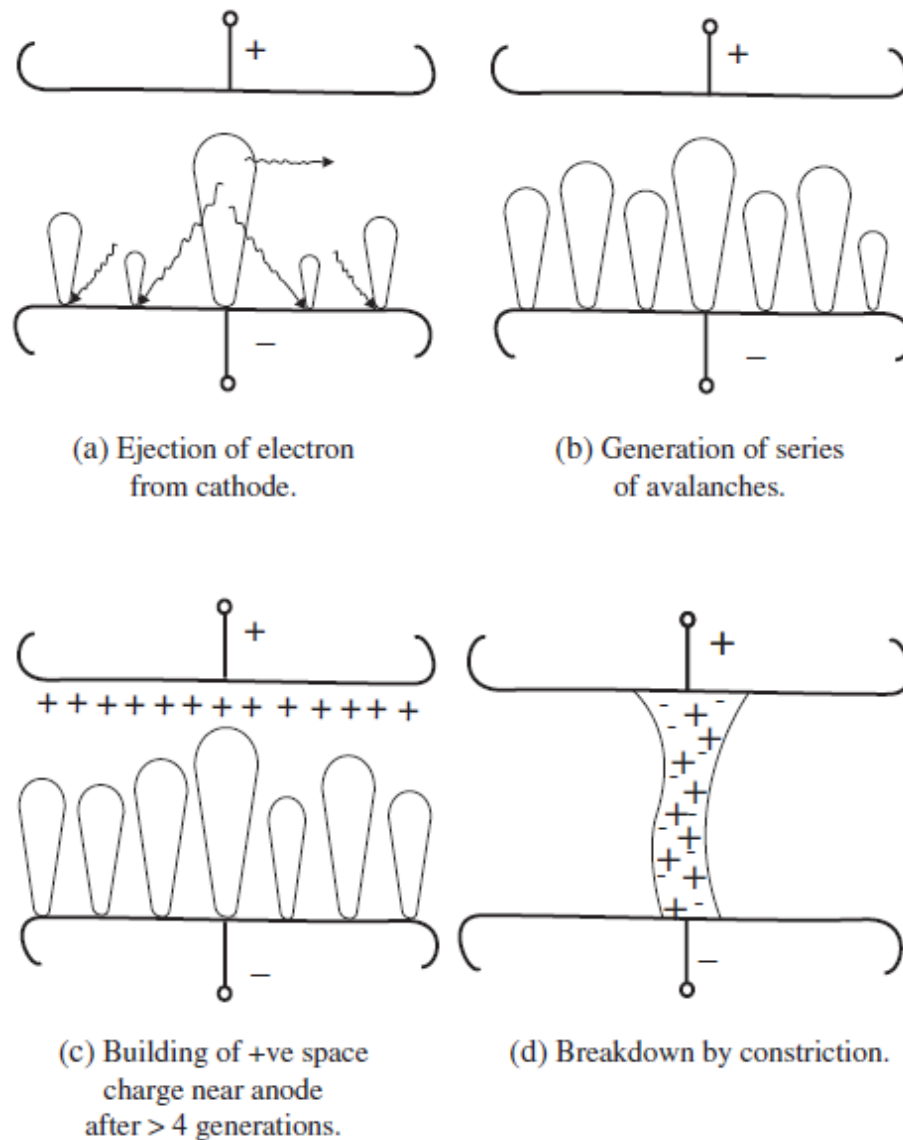after > 4 generations.

(d) Breakdown by constriction.

Figure 1.13. Schematic of Townsend breakdown mechanism [19]

1.4.1.2.   *Streamer mechanism*

The avalanche exponential growth, being the base of Townsend's mechanism, requires uniform field. However, this hypothesis is no longer valid if the electrical field modification due to space charges (electrons and ions) cannot be neglected. Once the number of charge carriers in an avalanche exceeds $\sim 10^7$ to 10^8, the head of the avalanche (consisting mostly of electrons) and its tail (mostly ions) are in a state of an enhanced field. Thus the ionization has a higher rate at the avalanche extremities (head and tail) than at the center. The avalanche can proceeds faster toward the anode by generating fresh or secondary avalanches thank to the enhanced field intensity in the

upper region. New electrons, being at the origin of these new avalanches, can be produced by photo ionization caused by the primary avalanche. This process, known as anode-directed streamer, is shown in Figure 1.14 [19].
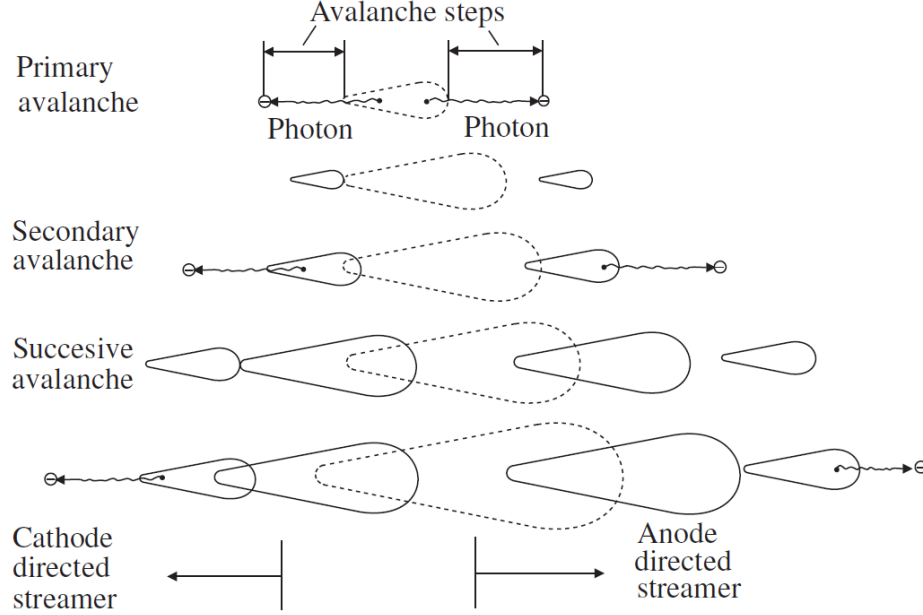

Figure 1.14. Development of anode and cathode directed streamers [19]

Some studies [36] have shown that the streamer mechanism can be predominant in small gas voids inside dielectrics. It is due to the resulting field distortions arising from deposited surface charges on the dielectric electrodes, following the previous discharges. This is possible when the surface resistance of the dielectric is high enough. For lower surface resistances the surface charge can be sufficiently quickly redistributed over the entire surface. As a result a system will return to uniform field conditions and a proceeding discharge will be governed by the Townsend's mechanism [36].

1.4.2. Paschen's law

In uniform fields the criterion for breakdown in electropositive gases was given by Townsend (see equation (1.19)). As both coefficients α and γ are the functions or applied electric field E and gas pressure p, they can be expressed as:

$$\alpha = pf_1\left(\frac{E}{p}\right) \tag{1.20}$$

$$\gamma = f_2\left(\frac{E}{p}\right) \tag{1.21}$$

In a uniform field the electric field strength E can be replaced as a quotient of breakdown voltage U_b and gap distance d (see equation (1.14)). Thus a Townsend criterion can be expressed as:

$$f_2\left(\frac{U_b}{pd}\right)\left\{\exp\left[pdf_1\left(\frac{U_b}{pd}\right)\right]-1\right\}=1 \tag{1.22}$$

By solving this equation one gets breakdown voltage U_b as a function of product of the gas pressure p and the electrode gap separation d:

$$U_b = f(pd) \tag{1.23}$$

This relationship is well known as a Paschen's law. It was established by German physicist Friendrich Paschen in 1889 [43]. Figure 1.15 presents Paschen's curves for various gases.
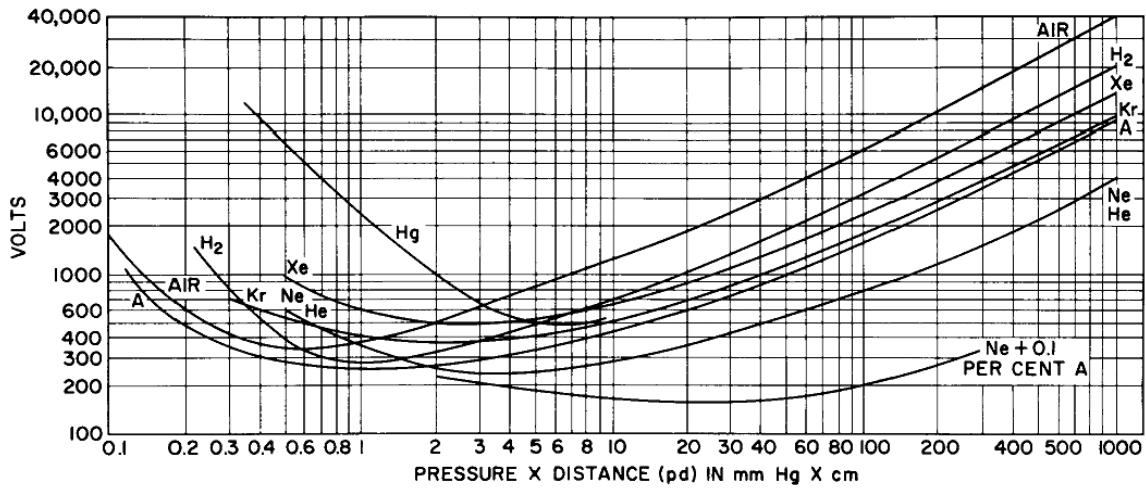
Figure 1.15. Paschen's curves for various gases [44]

The curves present a minimum for certain product of *pd*. For example the minimum for air is for a breakdown voltage $U_{bmin}=352$ [V] and for $(pd)_{min}=0.55$ [Torr·cm] which means the gap distance of $d_{min}=7.2$ [μm] for standard pressure (760 [Torr]). The behavior of dielectric gases has been found to be very similar in uniform as well as in weakly non-uniform (Schweiger factor $\eta \in \langle 0.25;1\rangle$) field configuration [19].

The coordinates of the minimum varies slightly depending on the experimental conditions, such as temperature or humidity. [45] presents the study of different correcting factors present in the literature with their verification.

_____

Although the Paschen's law is widely used for breakdown in gases, its use for discharges in gas voids inside the solid dielectrics is limited. One need to take into consideration that Paschen's law was determined for both metal electrodes and uniform field, which conditions are usually not met in voids. Also it is hard to evaluate the exact composition of gases inside the void as well as their partial pressures, hence the exact value of breakdown voltage is difficult to predict.

1.4.3. Partial discharge inception voltage (PDIV)

As stated before (see section 1.4) partial discharges in solid dielectrics may take place at the weak points, such as gas voids, cavities, cuts, foreign particles or protrusions. Figure 1.16 is showing the example circuit of a dielectric with a gas void inside. The voltage applied to the dielectric is divided between the capacities C_1 (describing the capacitance of void) and C_2 (describing the capacitance of the rest of the dielectric). The weak points usually (the case for e.g. air) have lover electric strength and their relative permittivity ε_{r1} is lower than that of the dielectric ε_{r2}, which makes the electric stress at the weak point increase proportionally. If the electric field across the void exceeds gas dielectric strength (which can be approximated by the Paschen's law), the breakdown inside the void occurs, which is a partial discharge. The voltage applied to the dielectric terminal is a partial discharge inception voltage (PDIV).
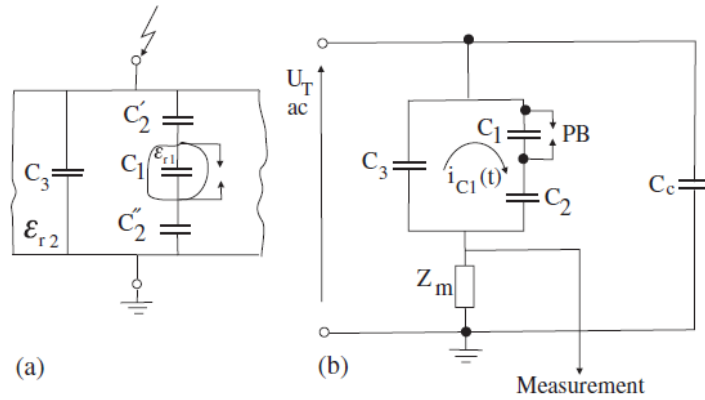
Figure 1.16. Internal partial discharge (a) schematic showing a PD inside a void
(b) equivalent circuit diagram for measurement
(C_1 – capacitance of void, $C_2 = C_2'+C_2''$ – capacitance between voids and electrodes,
C_3 – test object capacitance, C_c – coupling capacitor, Z_m – measuring impedance) [19]

PDIV is defined ([24] [46]) as the lowest peak value of the test voltage at which the apparent charge becomes greater than the specified discharge magnitude when the test voltage is increased above a low value for which no discharge occurs.

_____

For tests using AC voltage the PDIV is usually given as a rms value. The apparent charge, measured in pC, is an electric charge which can be measured at the terminals of the specimen under test [46]. It is the charge which, if instantaneously injected between the terminals of the test object, would momentarily change the voltage between its terminals by the same amount as by the partial discharge itself and its absolute value is often referred to as the discharge magnitude. The apparent charge notion was introduced as neither the actual inception voltage at the void nor the magnitude of the charge transposed to the void can be calculated or measured [19].

The standards [47] [14] [48] [49] define the PDIV slightly different, as a lowest voltage at which partial discharges are initiated in the test arrangement when the voltage applied to the test object is gradually increased from a lower value at which no such discharges are observed. The apparent charge notion is no longer used for tests under short rise time and repetitive voltage impulses.

Analogically the partial discharge extinction voltage (PDEV) is defined as the highest voltage at which partial discharges are extinguished when the voltage applied is gradually decreased from a higher value at which such discharges are observed ([47] [24]). The PDEV is usually slightly smaller than the PDIV.

For the PD tests under short rise time and repetitive voltage impulses the standard [48] introduced also the term of RPDIV (repetitive partial discharge inception voltage) defined as a minimum peak-to-peak impulse voltage at which more than five PD pulses occur on ten voltage impulses of the same polarity. This is a mean value for the specified test time and a test arrangement where the voltage applied to the test object is gradually increased from a value at which no partial discharges can be detected.

_____

1.5. Inverter fed machines

1.5.1. Variable-speed drive

A very wide range of applications requires a possibility of changing the rotating speed. There are numerous non-electrical methods allowing to adjust the speed using different types of mechanical or hydraulic transmission gears connected to a fixed-speed drive. Unfortunately these solutions, called continuously variable transmissions (CVT), have many disadvantages, such as higher losses, significant noise level or elevated maintenance cost. They will not be further discussed in this work.

Considering purely electrical variable-speed drives, for many years DC machines were the natural choice thanks to their characteristics (see section 1.2.1). Since the development of power electronics, the technology of AC drive systems has been significantly developed.

The AC motors are, by default, a fixed-speed machines. The rotating speed is a function of, among others, the powering voltage frequency and pole number. For asynchronous machines the speed varies slightly with the load, while for synchronous machines is independent from this variations. The change of pole numbers allows only step changes of rotational speed, thanks to specially designed winding.

1.5.1.1.   The principle of frequency converter

Smooth change of speed is AC drives requires smooth change of the powering frequency. A device allowing such a change is called frequency converter. It is a variable frequency drive, a type of AC/AC converter using a rectifier and inverter connected via a DC link (see Figure 1.17).
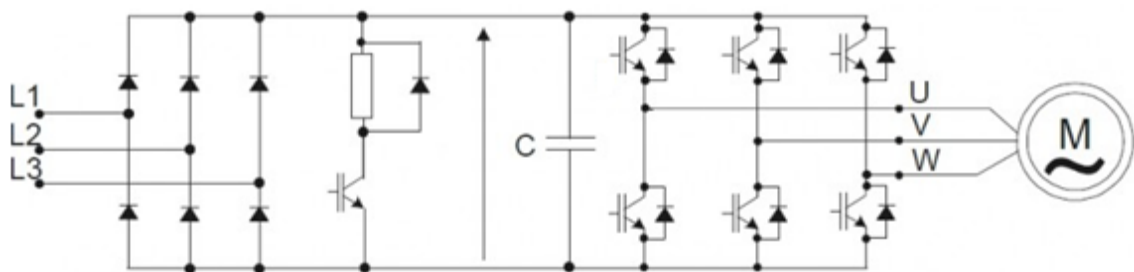

Figure 1.17. Topology of a frequency converter [50]

_____

The rectifier is usually a 3-phase diode bridge. The role of a capacitor in the DC link is to filter the voltage from rippling. The DC chopper is used in parallel to enable the energy dissipation in case of motor braking. The inverter is a DC/AC converter that allows to generate at motor terminals the waveform of a desired frequency (fundamental harmonic). It requires the electronic elements supporting quite high voltages and enabling to switch high currents. At the same time they need to have sufficiently high switching frequency to limit the losses. Such properties are mainly assured by IGBT transistors (see section 1.5.1.2) [50] [51].

The principles of transistor command in order to obtain a variable frequency voltage are detailed in section 1.5.1.3.

1.5.1.2. *IGBT*

The insulated-gate bipolar transistors (IGBT), introduced in early 1980s, are nowadays widely used in power electronics application thanks to their excellent characteristics. IGBT can be considered as a hybrid between the MOSFET and bipolar transistor. The former has much simpler gate-drive requirements and exhibits very high switching speeds, but can support neither high voltages nor high current densities. The latter has good on-state characteristics but much longer switching times, especially at turn-off. As it is a current-controlled device, it requires complex base-drive circuit to provide the base current during on-state, thus increasing the power loss in the control electrode.

The IGBT combines the insulated gate technology of the MOSFET transistor with the output performance characteristics of the bipolar one. As a result, they are easy to control and maintain high switching frequencies. IGBT can support voltages higher than 1 kV and conduct the current of hundreds of Amperes while allowing the switching frequency of tens of kHz (naturally these values vary, depending on the model).

With the introductions of wide-bandgap (> 3 eV) semiconductors, based on silicon carbide (SiC), gallium nitride (GaN) or diamond, the switching frequencies will increase and turn-on and turn-off times will be significantly smaller. This will enable to minimize the switching losses, but at the same time will significantly increase the stress on the insulation system of the electric machines (see section 1.5.2) [51] [52].

_____

1.5.1.3.   Pulse width modulation (PWM)

Pulse width modulation (PWM) is technique used for signal modulation where the duty cycle of the impulse is variable while its amplitude and frequency stays constant in order to produce a certain output waveform.

By changing the duty cycle of the rectangular pulse one can change its mean value over the period. The mean value for each period for this high frequency rectangular signal, called the carrier, is calculated to best follow the instantaneous value of the much slower changing signal that needs to be generated.

The carrier frequency in inverter usually ranges between few kHz (used for big, high-power machines of hundreds of kW) and some tens of kHz (smaller machines, up to tens of kW) and in case of some devices can be modified by the user. As the signal that is modulated is of low frequency (depending on the desired rotational speed of the motor), it can be quite effectively filtrated from the rest of the harmonics using low-pass filters. They are rarely used, as the motor's stator winding acts as a low-pass. As a result, although the voltage harmonic spectrum is quite rich (see Figure 1.18) the THD for corresponding current is reasonably low.
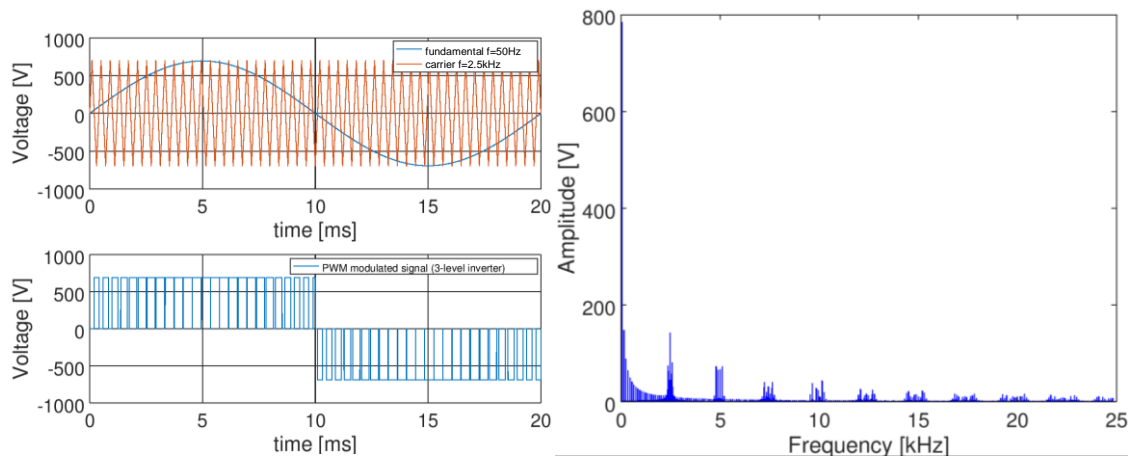

Figure 1.18. PWM signal for fundamental frequency at 50Hz and carrier frequency at 2.5 kHz (left), and its FFT spectrum (right)

The harmonic spectrum of the PWM modulated voltage has a very strong fundamental harmonic of 50 Hz (the frequency of sinusoidal referential signal) and groups of harmonics around the switching frequency (2.5 kHz) and its multiples.

1.5.2. Partial discharges in inverter-fed machines

In low-voltage machines powered directly from the grid, the voltage seen by any part of the insulation system is lower than the minimum required in order to start a partial discharges activity. Thus the problem of partial discharges was associated only with high voltage machines.

Since the introduction of power electronic inverters the stress seen by the insulation system has raised significantly. Very short surges produced by such sources creates voltage transients having very short rise times (as short as a fraction of μs), which can result in a partial discharges activity.

1.5.2.1.   Theory of transmission line

The parameters, such as inductance or resistance, of each real conductor, e.g. a cable between a motor and an inverter, depend on its length. In most cases, it is enough to analyze the lumped element circuits, i.e. to model the conductor as a few elements circuit that characterizes its whole length (depending on the complexity on can use a simple serial model or inductance and resistance or more complex ones, such as "Γ" or "Π" including also the capacitance and/or conductance of a cable line). However, if the length of the cable line is in the same order of magnitude as the wavelength of the voltage signal we have to use a distributed parameter system and the theory of transmission line. This is the case for e.g. very long power lines (> 400 km), but especially high frequency circuits. It can be used also for high frequency harmonics associated with very short rise or decay time of the signal at the output of inverter (up to tens of MHz; see section 1.5.1.3).

A transmission line is defined as a one-dimensionally distributed two-terminal-pair circuit element characterized by lineic inductance L, lineic capacitance C, lineic resistance R and lineic conductance G [53]. Figure 1.19 shows a schematic representation of the elementary components of a transmission line. [54] [55]
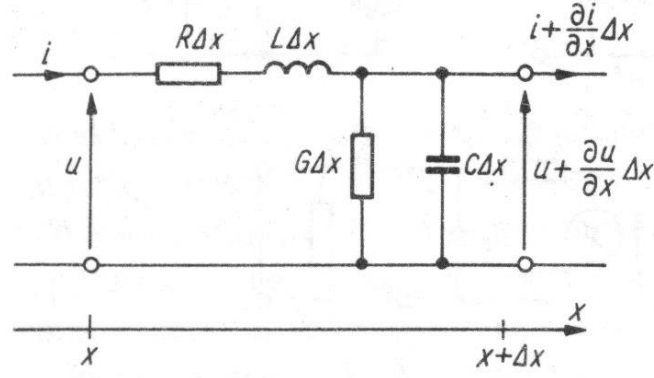
_____

Figure 1.19. Schematic representation of the elementary component of a transmission line [54]

The transmission line is described using a Telegrapher's equations:

$$\frac{\partial}{\partial x}U(x,t) = -L\frac{\partial}{\partial t}I(x,t) - RI(x,t)$$

$$\frac{\partial}{\partial x}I(x,t) = -C\frac{\partial}{\partial t}U(x,t) - GU(x,t)$$

(1.24)

In many cases the losses in the line are negligible ($R = 0$, $G = 0$).

1.5.2.2.   *Voltage reflection and overvoltage at machine terminals*

The characteristic impedance of a transmission line, for example a cable, is defined as:

$$Z = \sqrt{\frac{R + j\omega L}{G + j\omega C}}$$

(1.25)

When the incident wave *e* travelling through the cable of characteristic impedance *Z* arrives at the closing impedance R_0, a reflection will take place. The reflected wave *e'* will add up to the incident wave *e* resulting in total voltage at the end of the cable $e_0 = e + e'$ [55] [56]:

$$e' = \frac{R_0 - Z}{R_0 - Z} \cdot e$$

$$e_0 = \frac{2R_0}{R_0 - Z} \cdot e$$

(1.26)

Depending on the impedance of the load at the end of the line, the voltage wave can be reflected and significantly increase the peak voltage at the load terminals. Figure 1.20 shows the voltage at the terminals of closing impedance R_0 as a result of step wave traveling in the cable.
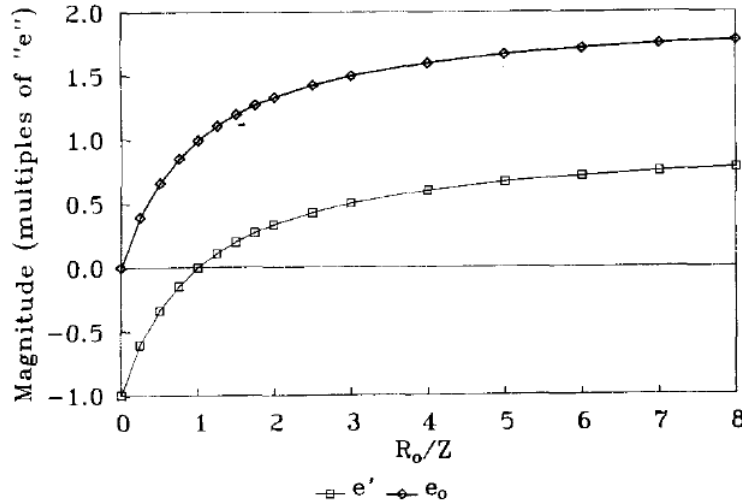

Figure 1.20. The reflected (e') and total (e_0) voltage at the closing impedance R_0 the cable of characteristic impedance Z [56]

The input impedance of the machine is usually significantly larger than the characteristic impedance of the cable connecting the inverter and the motor, especially for smaller machines. This impedance mismatch, completely negligible for low frequency harmonics (associated with fundamental frequency and its harmonics), is the reason for a significant increase of the peak voltage at the motor terminals. This voltage can exceed the partial discharge inception voltage (see section 1.4.3) and result in the activity of partial discharges causing accelerated aging. One of the first to identify this problem in inverter-fed machines was E. Persson in his paper from 1992 [56].

Figure 1.21 presents the example if such overvoltage measured at the machine terminals with a 13 m cable between the inverter and the motor. In comparison to voltage at the inverter output V_H, the maximum voltage at the machine terminals E is twice as high.
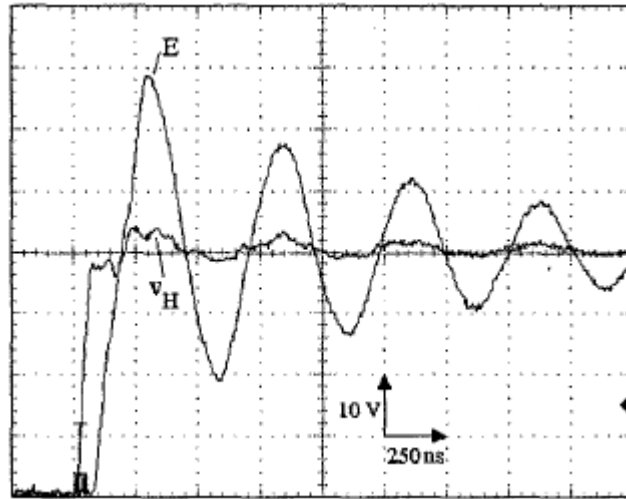
_____

Figure 1.21. The voltage at the motor terminals (E) in comparison with voltage at the inverter output (V_H) with a 13 m cable. [57]

1.5.2.3.   Influence of both cable length and voltage rise time

There are many parameters of the electromagnetic chain that will influence the final voltage amplitude at the motor terminals. They can be divided into the following categories:

- inverter output characteristics (rise time, possible overvoltage),
- cable characteristics (length, characteristic impedance),
- motor characteristics (its design including material properties and special arrangement of winding.

Figure 1.22 shows, by means of circuit simulations, how the overvoltage at the machine terminals is influenced by the impulse rise time and the length of the cable between the inverter and the motor. Generally speaking the longer the cable and the smaller the rise time, the higher the overvoltage factor (defined as the ratio between the peak voltage at motor terminals and at the inverter output). Thus the introduction of new wide-bandgap semiconductors (see section 1.5.1.2), which will allow to further reduce the rise time, will result in even higher stress applied to machines insulation system.
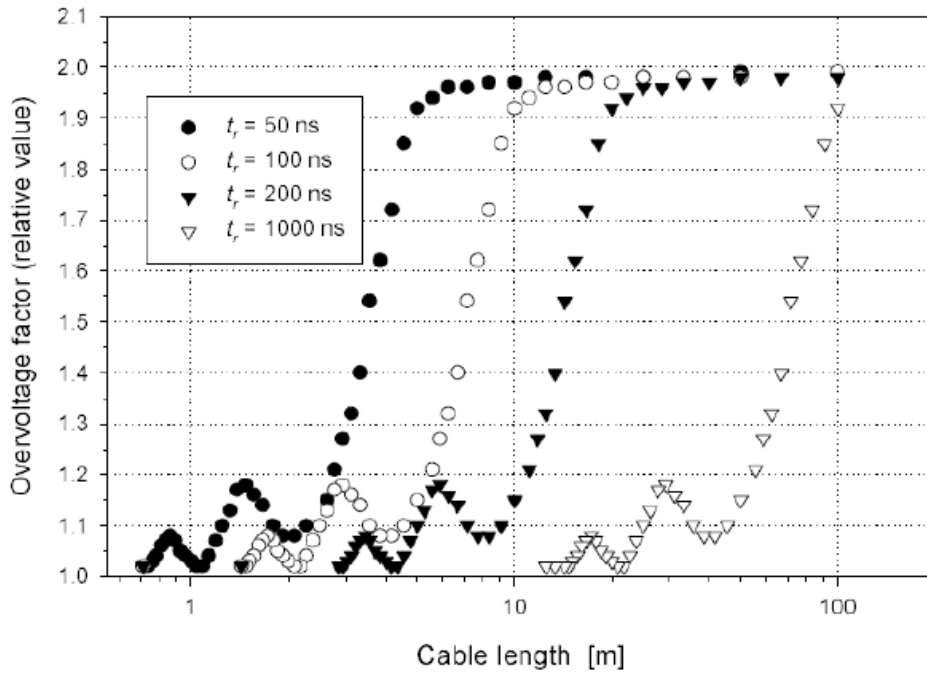
Figure 1.22. Overvoltage at the motor terminals as a function of cable length for different risetimes [58]

More recent studies [59] show that the overvoltage factor can exceed 2 in case of unfavorable superposition of overvoltages at the inverter output or the resonance for certain harmonics components of PWM signal.

1.5.2.4. *Turn-to-turn voltage in inverter-fed motors*

When a very steep impulse voltage is applied to a stator winding, the voltage distribution is nonlinear, contrary to equal distribution at power frequency (i.e. 50 or 60 Hz). As a result, a much greater percentage of the voltage appears across the first turns. This non-uniformity occurs because the pulse voltage goes through the winding not instantaneously but at the speed given by $v = \frac{1}{\sqrt{LC}}$, where L is the lineic inductance and C the lineic capacitance. Consequently first turns are energized; but not the others. As a consequence, a very high voltage appears across the turn insulation in the first few turns of the winding [6].

Figure 1.23 shows the voltage waveform for 6 different parts of the coil of the same phase. E is a voltage at the phase terminal, V_1 after the first ⅙ of the turns in this coil, V_2 after the following ⅙, etc. The resulting turn-to-turn voltages confirm that the electric stress across the first few turns is significantly higher than for the rest of the coil.
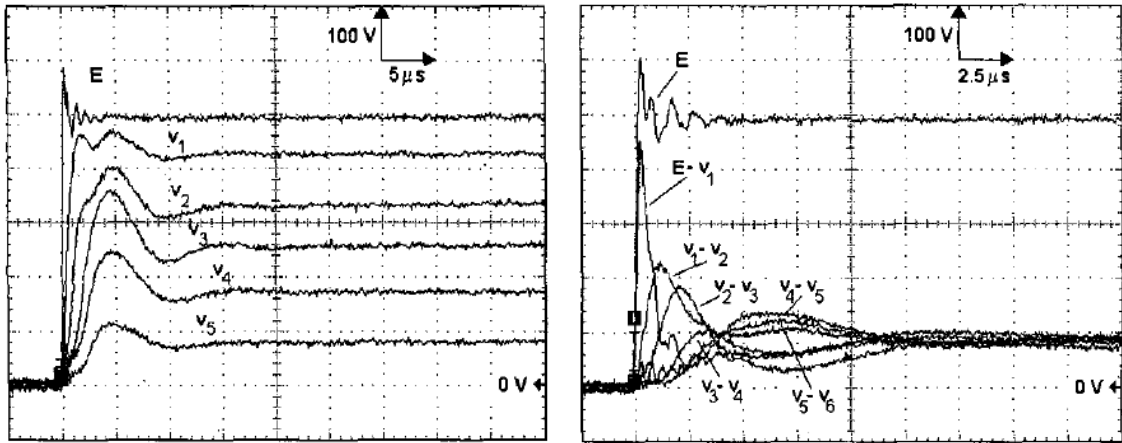
Figure 1.23. Transient voltage waveforms at the different parts of the coils (left) and the resulting turn-to-turn voltage calculated between these parts [60]

As stated in the previous paragraphs, the electric stress seen by the insulation system of the inverter-fed machine is significantly higher than the one seen by the motor powered directly from the grid. Even if only few of the impulses result in the partial discharges activity, the very high repetition rate (tens of thousands of surges per second) might create enough cumulative damage to cause failure. As a result of the premature breakdowns the lifespan of inverter-fed machines is still unsatisfactory. This problem is the core of this study.

1.6. Conclusion

As presented in this chapter, using the inverter to power the machine can significantly increase the stress to be withstood by its electrical insulation system. Due to the transmission line phenomena, the voltage at the machine terminals can be significantly higher than the one at the inverter output. The voltage amplitude can exceed the partial discharge inception voltage (PDIV) in various parts of the motor insulation system, starting thus an activity of partial discharges. Especially the turn-to-turn insulation is exposed to much higher stress that in grid-power machine.

Insulating materials used in low voltage machines (type I insulation system) are easily and quickly degraded by a PD activity; this can lead to a premature breakdown of the machine. The understanding of their aging process in this regime seems crucial to estimate the influence of PDs on the machine lifespan.

In order to be able to quantify the influence of some aging factors on the insulation system special accelerated aging tests were designed (see chapter 3). The methodology proposed in the following chapter enables to model the lifespan of the components of the insulation system and their comparison, which will enable to design more reliable machines with much longer lifespans.

CHAPTER 2

Accelerated aging tests on insulating materials

Table of content

2. CHAPTER 2: ACCELERATED AGING TESTS ON INSULATING MATERIALS

2.1.Introduction

This chapter is subdivided into 4 sections:

The first part gives some general information concerning types of accelerated aging tests as well as lists most well-known stress factors that can influence the lifespan of insulating materials.

The second section provides detail description of the test bench designed during this thesis to perform accelerated aging tests.

The third part is dedicated to partial discharges measurements, both on simplified samples and on the low-voltage machine. It explains in details the test protocol used and gives some example of results.

Finally, the last section explains in details the statistical analysis of lifespan data, especially the Weibull distribution used throughout this thesis.

2.2. Introduction to accelerated aging tests

Each manufacturer of electrical machines needs to assure the reliability of its products. For most applications, the lifespan of 20 – 30 years should be achieved [61].

For years, the design of the electrical insulation system was done by trial and error method. Usually the extra safety margins were added to protect the electrical machines from premature breakdowns. The insulation thickness was higher and copper cross section was greater than needed to limit the electric stress and operating temperature. As a result such machines often greatly outperformed the designed life and some of these first machines are still operating.

On the other hand, such an excessive design is not reasonable from the point of view of power-to-mass ratio, not to mention the economic aspect. By eliminating these unnecessary safety margins, according to [61] [62], it is possible to reduce the weight of the stator steel by 13-33%, copper weight by 5–64% and as a result the total mass of the machine by 12–57%, depending on the motor's parameters. As a price of machine strongly depends on material cost, these significant reductions of mass result in lower price, invaluable on very competitive global market. Moreover, the environmental footprint will be consequently reduced [63].

This need to reduce the material consumption while still assuring the high quality of a final product led to development of life data analysis methods. Naturally the most representative life data would be obtained under normal operating conditions. But obtaining such data may be very problematic, as they are very time- and energy-consuming. As stated before, the lifespan of machine is usually in the order of tens of years. Such a delay is inacceptable from the marketing point of view. Taking into consideration all these difficulties, yet still the need to lead to product breakdown to better understand its failure mode, the technique of accelerated aging tests was developed. The basic concept is to subject the model of insulation system to higher than normal stresses and thus accelerate the deterioration rate.

2.2.1. Qualitative and quantitative accelerated life tests

Accelerated tests can be divided into 2 categories: qualitative and quantitative accelerated life test (respectively see sections: 2.2.1.1 and 2.2.1.2).

_____

2.2.1.1. *Qualitative accelerated life tests*

Qualitative accelerated life tests are used if one is interested in identifying 'weakest links' of the product and in studying failure modes without attempting to make any predictions of the product's life under normal conditions. They are used to reveal the probable failure mode, often providing a necessary feedback for designing correct quantitative tests.

There are different types of qualitative accelerated life tests [64] [65] [66], e. g.:

- HALT (Highly Accelerated Life Testing);
- HASS (Highly Accelerated Stress Screening);
- ESS (Environmental Stress Screening).

Properly designed qualitative test can quickly reveal possible failure modes. However, if the stress level is too high, the product may fail due to modes that would never have been encountered in real life.

2.2.1.2. *Quantitative accelerated life tests*

Contrary to qualitative tests, the main aim of quantitative accelerated life tests (QALT) is to predict the life of the product at nominal use conditions from data obtained in an accelerated aging test.

There are 2 principle methods of accelerating the test:

- Usage Rate Acceleration
  - This method is used for products which do not operate continuously under normal conditions. In such case, failures are encountered earlier by continues operating. It is particularly effective for products used occasionally, thus unfortunately this method is not adapted for most of electric machines.
- Overstress Acceleration
  - The test can be accelerated by increasing the stress level above the nominal conditions. Generally speaking the higher the stress, the shorter the lifespan. This method is widely used for insulation system of electrical machines.

_____

The choice of the stress levels is of crucial importance. They should be chosen so that they accelerate the failure mode under consideration but do not introduce failure modes that would never occur under normal conditions.

2.2.2. Aging factors and stress types

2.2.2.1. Aging factors

We can distinguish four different aging factors of stress that influence the lifespan of insulation system: **t**hermal, **e**lectrical, **a**mbient and **m**echanical (so-called **TEAM** stresses [67]). They are briefly described below [61]:

- Thermal
    - The influence of temperature as an aging factor is discussed in chapter 3
- Electrical
    - The influence of voltage (waveform and level) and switching frequency as an aging factors is discussed in chapter 3
- Ambient
    - Humidity
        - Low humidity reduces breakdown voltage of air
        - High humidity can lead to moisture condensation (see below)
    - Moisture condensation
        - Conductive water drops on the winding surface alter the electric field distribution and can locally significantly increase the electric stress
        - In machines designed for working in humid climate, the special heating resistance is installed to preheat and dry the air inside the machine before its start to avoid any moisture condensation effect
    - Air pressure
        - As shown before by Paschen (see chapter 1), the electric strength of air varies with changing air pressure for a given inter-electrode distance. This factor is especially important for electric machines used in aeronautics

- o Radiation
  - ▪ This stress applies only to machines operating in very specific locations, such as nuclear plants, nuclear powered vessels or in space (cosmic radiation). Radiation leads to chemical bond scissions, similarly to thermal aging, causing insulation embrittlement
- o Aggressive chemicals, e. g.: ozone
  - ▪ The influence of ozone as an aging factor is discussed in chapter 3
- o Mechanical impurities
  - ▪ This includes all dirt and debris brought into the machine from the environment (insects, dust, etc.) as well as those generated within the machine (brake shoe wear, carbon brush wear)
  - ▪ The influence of some mechanical impurities as an aging factor is discussed in chapter 3
- Mechanical
  - o Due to ill balanced rotor
    - ▪ Although highest care is paid to properly balance the rotor, it is always a source of vibration, that increases as the bearings wear out
  - o Due to centrifugal force
    - ▪ This stress allies to rotor winding and is a non-vibrating stress, directly proportional to square of rotating speed
  - o Due to magnetic force oscillations
    - ▪ As magnetic force charges its direction twice during the power period, the winding is under repetitive mechanical stress
  - o Due to switching on
    - ▪ As the starting current can be significantly higher, the magnetically induced mechanical force, proportional to the square of current, stress the insulation system much stronger than in normal service;

_____

- Applies also to out-of-phase synchronization of synchronous machines
- Does not apply to machines with soft-start system as well as to inverter fed machines

2.2.2.2.   Stress types

Taking into consideration how stress level changes in time, one can distinguish the following types of stress [66] [68]:

- Constant stress
  - This is the simplest and most widely used stress type. Test protocol is simple to apply and stress type is coherent with working at nominal conditions. Such data are relatively easy to use and extrapolate. On the other hand, the test can be time consuming and it is not possible to take into consideration any stress variation during machine functioning

- Step stress
  - Stress level is gradually increased, thus reducing the test duration. As the stress changes, the aging mode may change as well, thus the results are difficult to be extrapolated

- Ramp stress
  - Stress level is constantly increased, which considerably reduces the test duration. Same as for step stress, the aging achieved is different at the beginning and at the end of the test

- Cyclic stress
  - This type of stress is the closest to normal functioning of electric machines, but the frequency of this cycling becomes another aging factor

- Random stress
  - This type of stress is usually used to describe environmental constraints

_____

2.3. Accelerated aging test bench

2.3.1. General information and requirements for accelerated aging test bench

Accelerated aging tests usually demand a special test bench adapted to their special requirements. The most critical parameter is a long duration of test: in case of insulating materials for electrical machines those tests can last weeks, months or even years. We need to assure that all devices can function for such a long time without any stops or failures. The other, but equally important challenge, is to assure that the applied stress parameters will not change during the aging process.

Assuring these two key factors may be particularly difficult as the aging processes, naturally far less rapid, will apply to all the components of a test bench: power supplies, cables, connectors, probes, detectors, heaters, fans, etc. This aging is truly troublesome, especially for tests with partial discharges activity. Partial discharges in air can create ozone, a particularly noxious gas, that attacks not only the sample under test but also all the exposed components of the test bench. For more information concerning the influence of ozone as an aging factor, see chapter 3.

Taking into consideration the cost of the test equipment, such as climate chambers or high voltage power supplies, it is often impossible to provide an individual test bench for each sample. In order to provide statistically significant data we need to test at least few specimens in the same conditions. Samples are usually connected in parallel in the same climate chamber. Naturally this can reasonably reduce the experimental costs, but we need to assure that all samples have the same aging conditions and they do not interact with each other.

In order to recreate the real-life stress submitted to the insulation of an inverter-fed machine, a special test bench was constructed in LAPLACE. It allows to deliver square waves of the desired amplitude, frequency and duty cycle, thus simulating the PWM waveform withstood by the insulation. To better control the experimental conditions, all the test were conducted inside a climate chamber to assure controlled ambient temperature during all tests. The description of those key components can be found in paragraph 2.3.2.

2.3.2. Components and their roles

2.3.2.1. High voltage power supply

Figure 2.24. Technix High Voltage Power Supply SR6-X-600 [69]

High voltage power supply is naturally the key component of our test bench. For all the stations we used different Technix High Voltage Power Supplies: both of positive and negative polarities. They can deliver DC voltage of maximum 6 kV and current of maximum 170 mA (mean value).

The voltage amplitude can be regulated with the precision of ±10V. All sources are working in the current limiting mode, which means that in case of short-circuit the voltage is decreased to the level, where current drawn from the source does not exceed the limit (here set by user to an allowed maximum of 170 mA).

According to numerous preliminary tests, the protection of voltage source is much slower than the one of the high voltage pulse generator (see section 2.3.2.2). It can be therefore neglected in the analysis of detection process.

2.3.2.2. High voltage pulse generator

In order to recreate the inverter-like signal we used a high voltage pulse generator provided by Directed Energy (DEI). It is a solid state pulser designed to drive capacitive loads, such as twisted pairs. It produces very flat voltage pulses with steep ramps (high dV/dt in the order of tens of kV/μs). It uses input signals from two high voltage sources: one positive and one negative. The output signal is alternating between those 2 voltage levels according to the signal from the driver frequency generator.

_____

Figure 2.25. High voltage pulse generator (here: PVX-4140) [70]

For different switching frequencies and depending on the needed peak-to-peak voltage there are different models of pulse generators. Table 2.6 shows all the most important parameters for all 3 models of pulse generators used during my thesis.

Table 2.6. Output characteristics of high voltage pulse generators [70]

Model	Unipolar voltage	Bipolar voltage	Maximum frequency	Rise/Fall time (10%-90%)	Pulse width
PVX-4130	0 to 6 kV 0 to -6 kV	max. 6 kV (peak-to-peak)	10 kHz	< 60 ns (typically <52 ns)	< 150ns to DC
PVX-4140	0 to 3.5 kV 0 to -3.5 kV	max. 1.75 kV (peak-to-peak)	30 kHz	< 25 ns	< 60ns to DC
PVX-4150	0 to 1.5 kV 0 to -1.5 kV	max. 0.75 kV (peak-to-peak)	240 kHz	< 25 ns (typically <20ns)	< 60ns to DC

The short-circuit protection in those pulse generators will automatically disconnect the load if the instantaneous current exceeds 10 A or the average current exceeds 100 mA. As the pulse generator delivers signal of very steep slopes (high dV/dt), an instantaneous current drawn by a capacitive sample can be significant $\left(i_C = C \frac{dV}{dt} \right)$. If a sample has a high capacity or if too many samples in parallel are connected to the pulse generator, the instantaneous current can exceed 10 A and as a result the test cannot start. If a sample (or one of the samples connected in parallel) is broken down, a resulting short-circuit will increase the average current well above the

_____

100 mA thus disconnecting the pulse generator. This protection is, according to multiple preliminary tests, faster than the one of the voltage source.

2.3.2.3.   Function generator

Function generators are used to provide a switching signal for the high voltage pulse generator (see section 2.3.2.2). In all the test benches we used a function generator by Française d'Instrumentation (model FI 5004). In order to assure a correct functioning of the pulse generator, the amplitude of the gate signal must have the amplitude of at least 5 V and a rise time of less than 20 ns.

2.3.2.4.   Climate chamber

In order to apply a thermal stress to the sample we used a climate chamber VT7011 by Vötsch. Thanks to strong ventilation inside the chamber it was possible to assure the homogeneity of the ambient temperature for all the samples. This is especially important for the tests at very high electric stress level, where the partial discharges activity can significantly increase the temperature of the samples. As a result, the measured lifespan would have been shorter due to local overheating of the enamel. Strong ventilation was also needed to limit the detrimental influence of ozone being produced during the partial discharges activity, both on the lifespan of the samples as well as the test bench components, e.g. connectors.

Figure 2.26. Climate chamber Vötsch VT7011

_____

Table 2.7 shows some technical parameters of the climate chamber.

Table 2.7. Technical data of climate chamber Vötsch VT7011 [70]

Parameter	Value
Temperature range	-70ºC to 180ºC
Temperature regulation precision	± 0.1ºC
Chamber volume	110 L
Temperature range of change (in accordance with IEC 60068-3-5)	3.5ºC (heating) 3.2ºC (cooling)

2.3.3. Measurement automation

In order to provide statistically reliable results, each test should be performed on at least few *a priori* identical samples. As aging tests are usually time consuming, the parallels tests on those samples are preferred to sequential tests. Due to the elevated price of a high voltage sources, pulse generators and climate chambers, it is often not reasonable to test each sample individually. When connecting samples in parallel we need to assure that each of them will be subjected to exactly the same stress levels and that the breakdown of one sample will not affect the aging process or the lifetime of the others.

Naturally the first technical problem to overcome is the breakdown detection: broken down sample must be quickly and unequivocally detected. Current monitoring, using high frequency current transformers, was experimentally proven to be expensive and ineffective, as it requires complicated and rapid signal analysis which has to be slightly reconfigured for each sample to provide reliable information. What is more, due to close proximity of samples in the same test bench as well as benches from one another, the signal was very noisy which led to many false positive and false negative results. This approach was abandoned in favor of other simpler and more robust solution.

As stated before the pulse generator protection can be used for the breakdown detection. If average current drawn from the source exceeds 100 mA, the output is automatically disconnected in few ms. This 'protection' signal can be easily detected even in the environment with high electromagnetic noise, as in our case. If such signal

is detected all sample are disconnected thanks to relays and the pulse generator should automatically return to its 'working' state. Once the relay is disconnected, the aging time counter is automatically stopped. Than samples are sequentially tested, one at a time, to detect which sample gave rise to overcurrent. The broken down sample is then retracted, its lifetime is stored and the test continues for remaining samples until the next breakdown appears ('protection' signal turns on). When it happens the whole procedure is repeated.
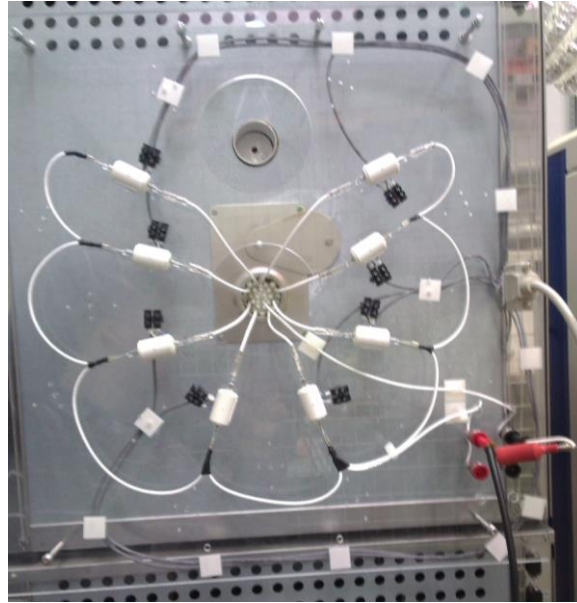
Figure 2.27. High voltage relays used to automatically disconnect the broken down samples

The described procedure allows to measure the lifespan of samples with a precision of 1 s. They are measured using counters that are able to measure time with 1 s precision up to 1000 h.

Figure 2.28. Test bench operating panel with 8 lifespan counters

_____

The test bench enables to measure the lifespan of 8 samples connected in parallel at the same time. This number was a good compromise between a good statistical representation and an elevated equipment cost. The power of the voltage supplies was high enough to power those 8 samples for a wide range of test voltages and switching frequencies. Only for tests with the highest voltage and frequency the number of samples had to be reduced but for such tests the measured lifespans were short so it was not a problem to repeat it 2 times for 2 groups of 4 samples.

Figure 2.29. Rack with powering sources and lifespan counter for accelerated testbench

2.4. Partial discharges measurements

Partial discharges activity is one of the main factors influencing the aging rate. As stated in chapter 1 partial discharges may appear if the voltage submitted to any part of the insulation system exceeds its partial discharge inception voltage (PDIV; see chapter 1). PDIV value naturally divides the voltage range into 2 zones with completely different aging modes. It is thus absolutely necessary to be able to measure the PDIV level to assure in which aging mode the accelerated aging tests are performed.

2.4.1. On-line and off-line PD measurements

Partial discharges measurements on electric machines can be divided into different categories.

PD measurement are divided into on-line and off-line categories depending whether the measurements are performed on the working rotating machine connected to its power source (on-line measurements) or on a stopped machine (or rather machine parts, for example only a stator) using the external high voltage source (off-line measurements). On-line measurements allow to monitor partial discharges activity (or to assure there are no PDs) in the real-life working conditions, while off-line measurements are designed for insulation system quality control, usually to find the partial discharge inception voltage (PDIV) and partial discharge extinction voltage (PDEV). This chapter is focused on off-line measurements.

Depending on the waveform of voltage applied during the test (off-line measurements) or used to power the machine (on-line measurements), one can distinguish power frequency measurements (50/60 Hz sine waveform) or measurements under short rise time repetitive voltage impulses.

2.4.2. Overview of partial discharges detection methods

Partial discharges activity is accompanied by several phenomena, such as: electrical pulses generation, electromagnetic waves emission (radiofrequencies, visible and UV light), changes in power absorption (power factor tip-up, charge transfer), acoustical or ultrasonic noise and various chemical reactions within cooling gases (either air or hydrogen). The measurements of these manifestations allow to detect and quantify partial discharges activity [71]:

- **Electrical pulse sensors:** Partial discharge involves a flow of electric charges inside insulators: electrons and ions. One can measure this current flow by using high-frequency current or voltage external probes. Current probes are often used as the external measuring circuit, which is classically composed of a high voltage capacitor and a measuring impedance allowing a current flow. This method can be applied both for on-line and off-line measurements. Thanks to its high sensitivity this method is widely used for PD measurements [72] [48].

- **Radio Frequency (RF) sensors:** Each partial discharge generates also radio frequency electromagnetic waves ranging from 100 kHz to several hundreds of MHz. The use of directional antenna may enable to locate the sites of PD activity. On the other hand, electromagnetic waves are attenuated by metal elements of the machine (e.g. housing) thus making their detection much more difficult [73].

- **Energy-based methods:** Each PD event absorbs a certain amount of energy, so it must be supplied from the source. The significant difference between the power-factor for low voltage (below PDIV, so without the PD activity) and for high voltage (above PDIV), called power-factor tip-up, may be indicative of severe PD activity [74] [36]. The modified version of this method, called Loop Trace Method, consists in measuring of the energy and integrated charge transfer resulting from PD activity using high voltage capacitance bridge [75]. Unfortunately both of these methods are less sensitive than electrical pulse sensing of RF methods and can only be applied to motors or generators out of service.

- **Ozone detection**: Ozone, or trioxygen (O_3) is a highly noxious gas generated in air-cooled machines in case of a partial discharges activity. If there is considerable surface PD activity, ozone concentration increases significantly above normal levels (0.003-0.01 ppm). Internal partial discharges cannot be detected using this method. Different ozone detection methods range from inexpensive chemical tubes to more accurate electronic sensors. Unfortunately the concentration of ozone is affected by the temperature, humidity and air flow fate [76].

_____

- **Acoustic and ultrasonic detection**: Rapid temperature increase in the vicinity of the partial discharges creates a small shock wave. As a result the acoustical noise, described sometimes as sizzling, occurs with frequencies ranging from several hundred Hz to over 150 kHz, but most of the acoustical energy occurs in ultrasonic range, around 40 kHz. Using directional microphones allows to measure partial discharges and localize them. But this method is reserved almost only to surface PDs and of sufficiently high activity [77].

- **Visible and UV light detection:** Partial discharges activity generates also electromagnetic waves in visible and UV region. It means that using a photomultiplier or even with naked eye, usually in a dark room (so called back-out test) one can detect and localize PDs. Obviously, this method is reserved only to surface PDs.

2.4.3. PDIV measurements on twisted pairs

2.4.3.1. Measurement equipment

2.4.3.1.1. Measurement equipment for tests using sinusoidal voltage

PD measurement equipment in LAPLACE Laboratory is based on the measuring device provided by Power Diagnostix Systems GmbH. It is designed only for off-line PD detection, i.e. to measure the PDIV, PDEV or PD activity at given voltage level. The test equipment for is fully compliant with the relevant standard [78].

Test bench uses a function generator in order to generate a low THD sine waveform. This voltage, of the amplitude of few V, is then amplified – first by an amplifier and then by a corona-free high voltage transformer. All this aims to assure that voltage source is completely PD free and that any measured PDs originate from the object under test. The transformer as well as the object under test are placed in a well-grounded Faraday cage to prevent the measurements from any external noise.

Figure 2.30. Partial discharges testbench by Power Diagnostix Systems GmbH

2.4.3.1.2. *Measurement equipment for tests using inverter-type voltage*

PDIV level can change depending on the voltage frequency or waveform. In order to be able to measure the PDIV level in the conditions used later in the accelerated aging tests, the sample is directly connected to the output of high voltage pulse generator (see section 2.3.2.2). To detect the partial discharges activity, a high frequency current transformer with high-pass filter was used. The voltage at the sample terminals is measured using high voltage wide bandwidth probe (Tektronix P6015A). This method can be used also for high temperatures, as the sample is placed inside the climate chamber.

The partial discharges detection was verified using an ozone detector (Oldham CTX 300 O_3; sensibility of 0.01 ppm) placed as closed to the sample as possible. Once

_____

the partial discharges activity was detected using a high frequency current transformer the ozone level has rapidly increased.

Figure 2.31. Ozone detector Oldham CTX 300 O_3 [79]

2.4.3.2. Test protocol

2.4.3.2.1. Test protocol for tests using sinusoidal voltage

The sample under test is connected to the high voltage output of the source. The voltage at sample terminals is measured using high voltage probe (Tektronix P6015A) and constantly controlled on the oscilloscope screen. On the other channel the signal from PD detector is presented. Once the gates of Faraday cage are closed, the amplifier is turned on and the operator can begin to gradually increase the output voltage of the function generator. The rate of change should be very small, in the order of few volts per second. If a repetitive partial discharges activity is observed (the voltage is high enough to maintain the partial discharges activity) the test is stopped and the corresponding measured voltage level (RMS value) is registered as the PDIV.

2.4.3.2.2. Test protocol for tests using inverter-type voltage

The test protocol for tests using inverter-type (square) voltage is almost the same as for the sinusoidal waveform. The voltage from the high voltage sources, both positive and negative, is slowly, gradually and simultaneously increased. If PDs are detected, the voltage level (expressed as peak-to-peak voltage) is noted as PDIV level.

_____

2.4.3.3. Example of results

Table 2.8 shows the measured PDIV values for 8 twisted pairs (conductor diameter: 1.12 mm; enamel material: PAI (ε_r = 4.3); enamel grade: 2). All the measurement were performed according to the test protocol described above. By comparing peak-to-peak values we can see that the PDIV levels for sine and inverter-type voltage are very similar, as already found in [80].

Table 2.8. PDIV values (Weibull α parameter of 10 measurements for each sample; 27ºC, HR 47 %) for twisted pairs (conductor diameter: 1.12 mm; enamel material: PAI (ε_r = 4.3); enamel grade: 2)

Sample number	PDIV for sine voltage [V]		PDIV for inverter-type voltage [V]
	RMS value	Peak-to-peak value ($PDIV_{RMS} \cdot 2\sqrt{2}$)	Peak-to-peak value (square voltage)
1	753	2130	2102
2	749	2118	2086
3	768	2172	2184
4	745	2107	2134
5	750	2121	2098
6	771	2181	2204
7	764	2161	2154
8	759	2147	2140

2.4.4. Determination of the PDIV of a twisted pair using finite element method simulation

For the geometries as simple as the one of a twisted pair, the PDIV level can be predicted using finite element method.

Taking magnet wire dimensions (see Table 1.4) and relative permittivity of enamel (see Table 1.1) it is possible to calculate the maximum field strength for a given voltage applied to one of the wires in a twisted pair (the other is grounded). By using the coordinates of Paschen minimum (see chapter 1): 352 V for the distance of 7.2 μm, we can predict the PDIV level. One needs to define the distance between the external diameters of the wires as equal to 7.2 μm and find the voltage (peak value) that when applied to one wire results in a voltage drop across the air gap equal to 352 V.

_____

Figure 2.32 shows the electric field distribution for a cross-section of a twisted pair (conductor diameter: 1.12 mm; enamel material: PAI (ε_r = 4.3); enamel grade: 2). The enamel thickness was a minimum allowed by the standard [32]. In order to obtain the voltage drop of 352 V across the air gap we need to apply to the wire (in our case the left one) the voltage of 1075.9 V (760.8 V_{RMS}), which is a simulated PDIV value.
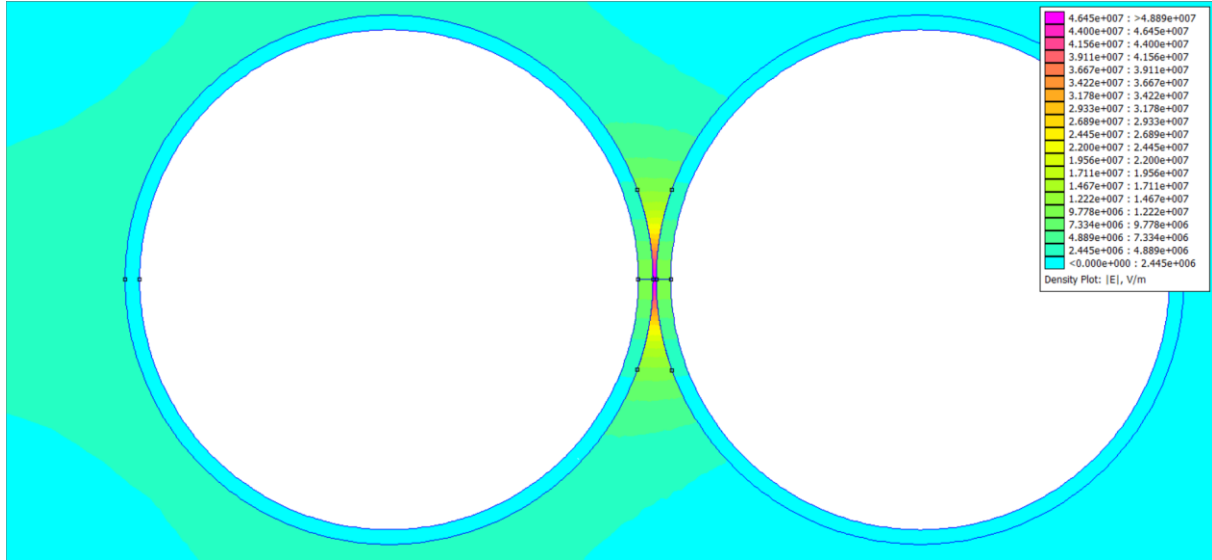

Figure 2.32. Electric field distribution for a cross-section of a twisted pair (conductor diameter: 1.12 mm; enamel material: PAI (ε_r = 4.3); enamel grade: 2)

As it can be seen the simulated PDIV value (760.8 V_{RMS}) is close to the one measured on the real twister pairs (see Table 2.8). The differences can be explained by:

- Differences in the enamel thickness, conductor diameter and conductors eccentricity;

- Differences in the enamel relative permittivity (as shown in chapter 1 the enamel consists on multiple thin layer that have seen different curing cycles, thus the relative permittivity of each layer may slightly vary);

- Conductor core and magnet wire surface roughness (may locally vary the enamel thickness);

- Paschen's theory (see Chapter 1) may "normally" be applied in a uniform field and with metallic electrodes, having their own secondary electrons emission coefficient.

_____

2.4.5. PDIV measurements on a low-voltage motor

2.4.5.1. Measurement equipment

2.4.5.1.1. Measurement equipment for tests in sine mode

The industrial PD measurement equipment available for measurements operated in Leroy-Somer was a test bench constructed utterly by Solfas Technologie GmbH. The test bench is adapted for measurements on different types of samples: both capacitive, such as twisted pairs, and inductive, such as motorettes or complete stator windings. It is designed only for off-line PD detection.

Figure 2.33. Partial discharges testbench by Solfas Technologie GmbH

The test bench consists of a high voltage 50Hz sine power source with adjustable amplitude, a high voltage switch matrix (allows to perform consecutive tests of each phase of the machine without the need of manually changing the terminal connections),

a PD detector using a high-frequency current transformer and a computer allowing to automate the measurement process. The test equipment for test in sine mode is fully compliant with the standard [78].

2.4.5.1.2.   Measurement equipment for tests in pulse mode

For the tests in pulse mode, almost the same test equipment is used as for sine mode. Only instead of using the sinusoidal voltage source, the pulse source is used generating repetitive short rise time voltage impulses. The PD detector (high frequency current transformer) used in both modes stays the same. The test equipment for test in pulse mode is fully compatible with the standards [48].

The IEC 60034-18-41 standard from 2014 [14] introduces more severe characteristics concerning the waveform of the voltage impulse than [48]. The impulse rise time is defined as 0.3 µs with a tolerance of ±0.2 µs. The impulse width and shape are specified in this standard using the "forbidden zone". The examples of correct and incorrect waveforms are presented in Figure 2.34.
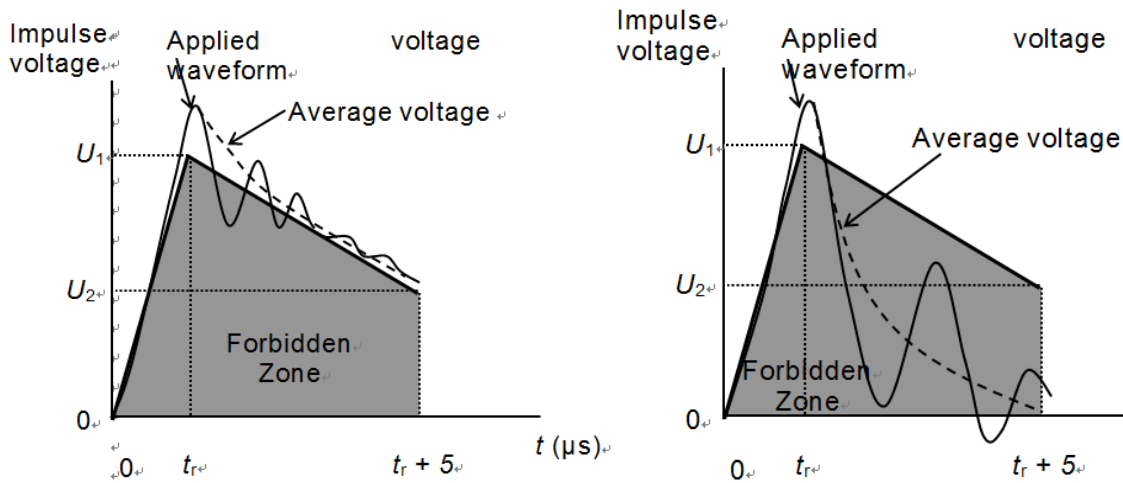

Figure 2.34. Deformation of unipolar impulse voltage with oscillation superposition due to test sample impedance and pass criteria of forbidden zone: correct waveform (left), incorrect waveform (right) [14]

The pulse source used here is compliant also with the standard [14]. It generates 2 square pulses, each lasting 8 µs, of the same adjustable amplitude 15 µs from each other (see Figure 2.35). The source generates such pulses every 20 ms. Measured risetime is also compliant with the standard requirements: around 0.3 µs but can slightly change depending on the load (generally speaking the higher the power of the machine,

_____

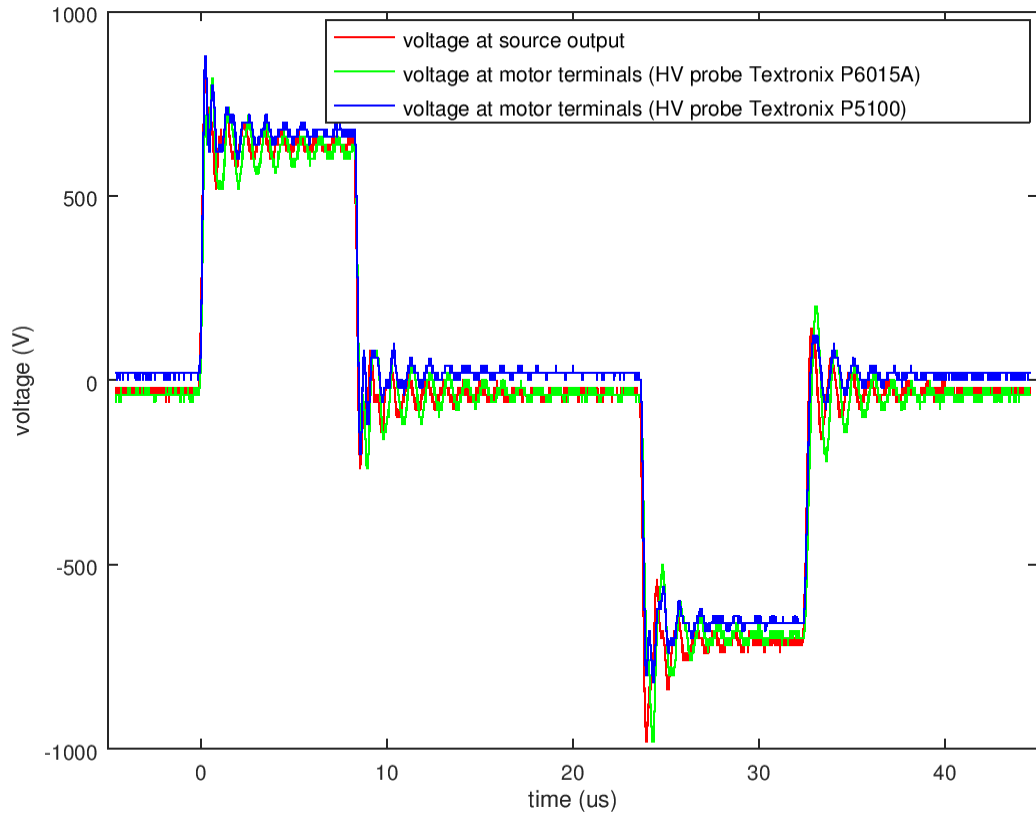the lower its input impedance and thus the higher the rise time at the machine terminals).

Figure 2.35. Pulse waveform used during the partial discharges measurements.

2.4.5.2.   *Test protocol*

For the insulation system in electric machines there are 3 configurations that need to be tested during PD measurements: phase-to-ground, phase-to-phase and turn-to-turn. The two first ones can be tested using sine voltage (see section 2.4.5.2.1), while the last one can be tested in most of machines only using short rise time repetitive voltage pulses (see section 2.4.5.2.2).

2.4.5.2.1.   *Test protocol for tests in sine mode*

Once star point is disconnected, the voltage is applied to tested phase, while other phases are connected to ground. For phase-to-ground test the frame is grounded as well, which is not the case for phase-to-phase mode. The test is repeated for all permutations in order to measure the PDIV for each phase and phase-to-phase configurations. Figure 2.36 shows the connections diagram for those two tests.
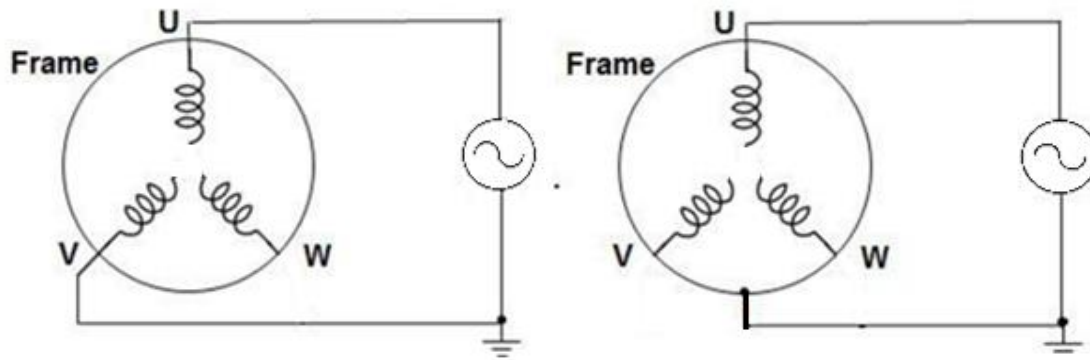
Figure 2.36. Connections for phase-to-phase (phase U / phase V; left) and phase-to-ground (phase U / ground; right) PD measurement.

The test begins by applying 500V (RMS value) sine voltage to a phase under test. The voltage is applied for 1s and during this time the number of partial discharges is registered. Naturally, at the beginning the applied voltage is too low to initiate any partial discharges activity. In the following steps (each lasting 1s) the voltage RMS value is increased by steps of 20 V. For each voltage level, the total number of detected partial discharges is stored. If the number of partial discharges at a given voltage level exceeds the chosen maximum (here fixed at 200 DPs per 1s, what gives on average 4 discharges per sinus period). This value was chosen to assure that the PDs are sufficiently numerous to have quite high PD activities yet still not harmful for the machine, even after several test repetitions. The test is stopped not to damage the machine under test.

2.4.5.2.2.   *Test protocol for tests in pulse mode*

Testing the turn-to-turn insulation of a standard winding requires using short rise time impulses with the star point connected. The connections stay the same as for the phase-to-ground test: voltage impulses are injected to the tested phase, while other phases and the frame are grounded. Figure 2.37 shows the connections diagram for this test.
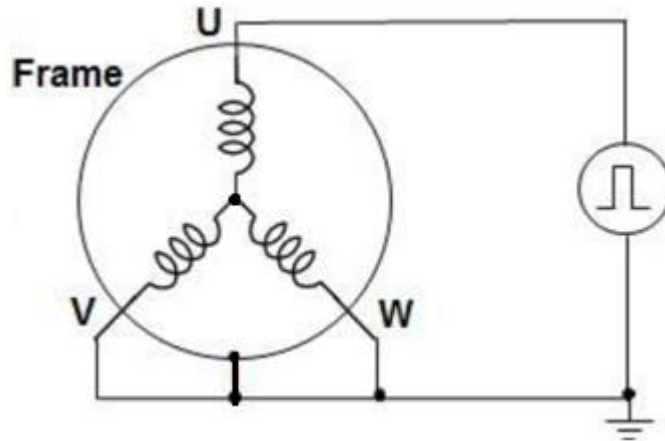
_____

Figure 2.37. Connection for turn-to-turn PD measurement [81].

The test protocol for this mode is the same as for the sine mode (see 2.4.5.2.1), although instead of using RMS value, the voltage amplitude is controlled. Per each sequence of 2 impulses, positive and negative, the program counts maximally 1 partial discharge, even if the detector enables to detect more. This means that each sequence of 2 pulses is judged either as "pass" (no DPs) or "fail" (at least 1 DP), as it is defined in the standard [14]. As there are exactly 50 pulses sequences per voltage level, the counter number of DPs divided by 50 gives the percentage of "failed" pulses. If it is greater than or equal to 50%, the RPDIV (repetitive partial discharge inception voltage, [14]) is equal to the corresponding voltage level.

2.4.5.3. Example of results

In order to provide reliable PDIV values, each measurement is repeated 10 times. Each test gives the number of partial discharges detected for each voltage level. Figure 2.38 shows the example of results of all 10 repetitions superimposed on each other. A rolling average of all 10 series enables to find the true value of PDIV. This approach allows to significantly limit the influence of possible noise on the final PDIV results much more effectively than a sample average of 10 PDIVs found for each individual test. It enables to obtain reliable PDIV results even for highly automated measurements without the expert analysis of each protocol.
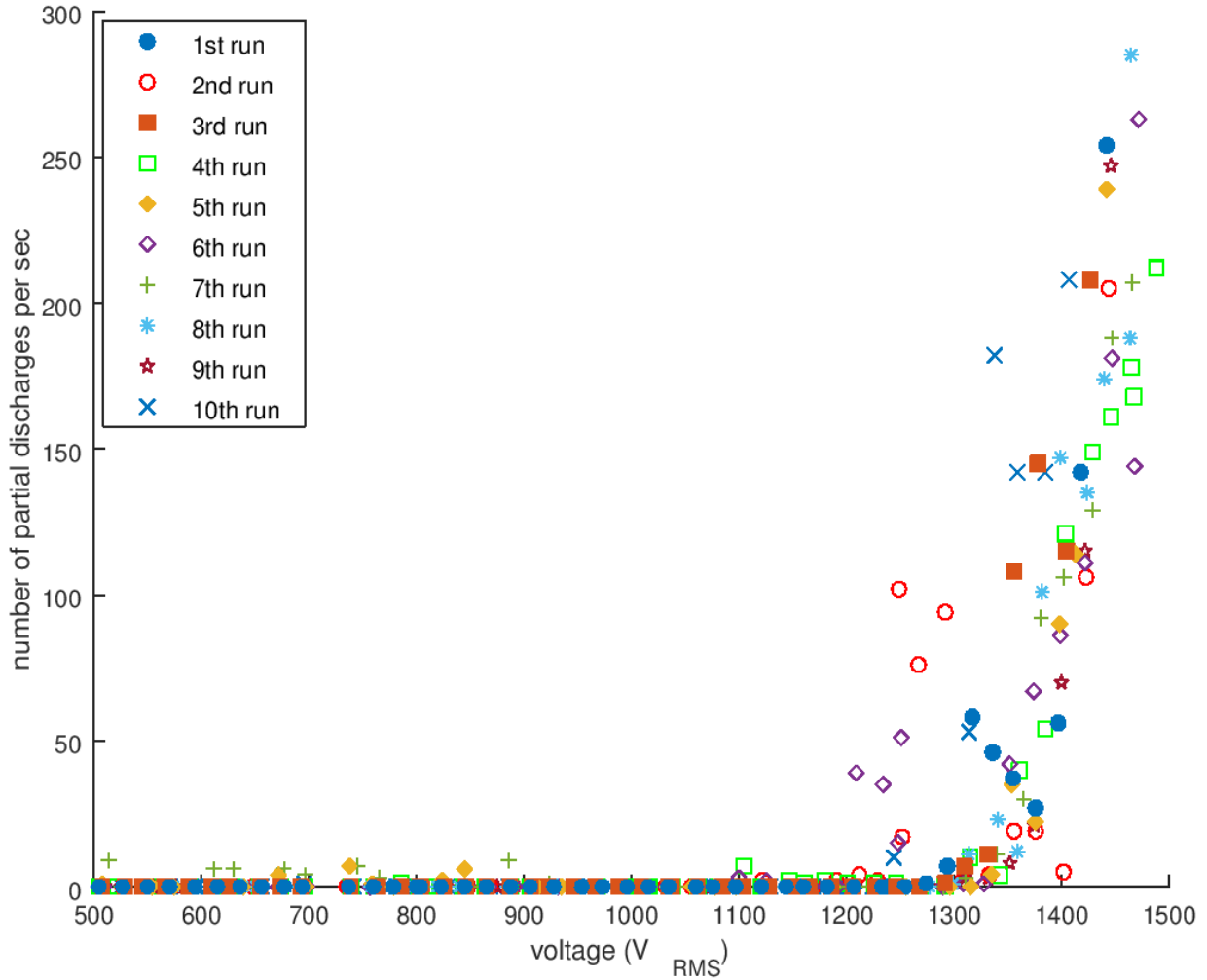
Figure 2.38. Number of partial discharges as a function of voltage level for all 10 repetitions (phase-to-ground measurements).

Rare and sparse PD activity for lower voltages (up to ≈1200 V_{RMS}) can be considered as external noise. Indeed, due to technical limitations of the test bench motor under test cannot be placed inside a Faraday cage. Under voltage levels between 1200 and 1350 V_{RMS} for some repetitions we registered numerous partial discharges, for others PD activity was still negligible. Lowest PDIV, registered for the 6th run was at 1180 ± 20 V_{RMS}, while highest for the 9th run was at 1320 ± 20 V_{RMS}. Finally, PDIV level determined using rolling average was 1185 V_{RMS}.

Partial discharge measurements are often subjected to important dispersions, especially in complex systems such as stators, due to the perturbed industrial environment. During two consecutive runs, PDs do not necessarily take place in the same area due to basic PD physics. As it can be seen in Figure 2.38 the difference from lowest to highest value of PDIV (140 V_{RMS}, thus over 11% of the average PDIV) is

_____

quite significant. This difference cannot be explained by differences in the experimental conditions (different temperature, humidity, air pressure etc.).

2.4.6. Partial discharges measurements as a method for winding fault detection

Partial discharges measurements are an excellent method for detecting any weak points of the insulation system of a machine. They are widely used in high voltage machines. Off-line measurements (see e. g. [82]) play an important role in quality control, while on-line measurements (see e. g. [83]) give invaluable information concerning the aging process of the insulation and help to organize the maintenance work in order to prolong the lifespan of the machine.

Partial discharges measurements on low-voltage machines are far less common and are applicable only for machines fed by inverters. The standard [14] from 2014 introduces off-line PD measurements for type I electrical insulation systems (see chapter 1) for qualification and quality control tests. According to this standard, such machines should be partial discharges free, which means that we need to assure that partial discharge inception voltage is always higher than the maximum voltage seen by the insulation system.

Quality control of the electrical insulation system is a very important part of the end-of-line test of electrical machines. PD measurements can give lots of complementary information to those tests and enables to detect insulation faults difficult or even impossible to detect by other methods.

2.4.6.1. PD test measurements

In order to test the efficiency of PD measurements as a quality control test, a group of low-voltage asynchronous machines was tested. All of them have successfully passed all of the quality and end-of-line tests.

Each machine underwent the test procedure described in paragraph 2.4.4. The complete procedure was repeated for the second time after 2 weeks to assure that the obtained results were significant as well as to verify how the change of the environmental conditions influences the results. The phase-to-phase PDIV values for each configuration and both repetitions are presented in Table 2.9.

Table 2.9. Phase-to-phase PDIV values for faulty stator winding

Connections		Phase-to-phase PDIV [V$_{RMS}$] (average of 10 runs)	
High voltage	Ground	First test	Second test
Phase U	Phase V	1173	1222
Phase V	Phase W	655	630
Phase W	Phase U	1338	1321

We can easily remark that the PDIV value for interphase VW is significantly smaller than those for 2 other interphases. The measured values of PDIV are close to those of a twisted pair (see section 2.4.3.3). This may signify that the phase separator between phases V and W is locally torn, misplaced or even missing. Such winding fault will almost inevitably lead to a partial discharges activity if the machine is fed by an inverter, significantly reducing its lifespan.

This machine was closely examined by a winding specialist who was able to find a probable source of a low PDIV values for interphase VW: a wire from phase V was misplaced and was in contact with the coil of phase W at end winding. Figure 2.39 shows this winding fault.

Figure 2.39. Stator winding fault in a low-voltage asynchronous motor: wire from phase V is misplaced and is in contact with a coil of phase W

_____

This type of winding faults cannot be detected using other standard end-of-line tests, such as surge test. The thin layer of enamel on the magnet wire can easily withstand the voltage applied during surge test ($2 \cdot U_n + 1000$ V, where U_n is machine's rated voltage [84]) during the short test time. Nevertheless, in case of the configuration presented in Figure 2.39, the voltage can easily exceed the PDIV value if the machine is powered by an inverter. The enamel on the magnet wire cannot withstand the partial discharges activity for a long time, which will inevitably lead to its degradation and as a result to the premature breakdown of the machine. By using PD measurements, this fault may be easily detectable and can be repaired before the client will receive his machine.

2.4.7. *Discussion over the test parameters in pulse mode*

On the one hand, the test conditions should be as close as possible to the normal working conditions. On the other hand, taking into consideration the large number of parameters to be adjusted as well as the wide range of machines types and their rated powers, it would have been difficult to construct the test bench enabling the control of all the characteristic for a reasonable price. Moreover, the impact of each of these parameters on the measured PDIV (individually or combined) is not yet well understood.

The EIC/TS 61934 standard [48] from 2011 defines the following parameters, amongst other factors, to be included in the specification of the pulse generator used for PD measurements:

- impulse rise time;
- impulse voltage polarity;
- impulse voltage repetition rate;
- impulse width;
- impulse duty cycle.

This standard gives the range of pulse characteristics without load (see Table 2.10). As the impulse waveform can change significantly with load, the standard strongly recommends to observe the impulses with a wide band oscilloscope.

Table 2.10 Example of parameters values of impulse voltage waveform without load [48].

Characteristic	Range of values
Impulse rise time	0.04 µs – 1 µs
Impulse repetition rate	1 Hz – 10 000 Hz
Impulse width	0.08 µs – 25 µs
Shape	Square or triangular
Polarity	Unipolar of bipolar (bipolar preferred)

As mentioned before, the IEC 60034-18-41 standard [14] from 2014 introduces more severe characteristics concerning the waveform of the voltage impulse: impulse rise time equal to 0.3 ±0.2 µs and specific impulse shape defined using forbidden zone (see Figure 2.34).

The IEC 60034-27-5 standard, currently under preparation (working draft [81]) will compile and further specify the requirements of standards [48] and [14].

Some preliminary partial discharges tests performed on low-voltage machine stators using different commercially available equipment for pulse mode showed that the PDIV or RPDIV[1] values can be significantly different from one test equipment to another. If PD measurements are only comparative, i.e. are used just to verify if the PDIV for newly developed machine is same of higher than the existing design, those differences are not really problematic. Unfortunately standard [14] introduces IVIC[2] classes that require absolute RPDIV values. Different PD test equipment use different voltage waveforms (naturally all meet the requirement of standards [48] and [14]), different test protocols and different PD detection techniques. Small differences in the PDIV or RPDIV values can be easily explained by the difference in the test conditions (temperature, humidity, air pressure, etc.) as it was not possible to perform the test in a

---

[1] RPDIV (repetitive partial discharge inception voltage) - minimum peak-to-peak impulse voltage at which more than five PD pulses occur on ten voltage impulses of the same polarity. This is a mean value for the specified test time and a test arrangement where the voltage applied to the test object is gradually increased from a value at which no partial discharges can be detected [20].

[2] IVIC (impulse voltage insulation class) - safe peak to peak voltage assigned by the manufacturer in relation to the nominal voltage for a specified converter-driven machine and indicated in its documentation and on its rating plate. There are 4 IVIC classes: A – low stress (overvoltage factor OF ≤ 1.1), B – medium stress (1.1 < OF ≤ 1.5), C – high stress (1.5 < OF ≤ 2.0) and D – extreme stress (2.0 < OF ≤ 2.5) [20].

_____

climatic chamber (it is rare in industrial environment to perform such PD measurements). But sometimes the difference is more than double between the one test equipment and the other. What is more, the results were not repeatable in case of some equipment. The difference in PDIV in sine mode (verified for those equipment which provided both sine and pulse voltage source) was negligible.

In order to investigate how the partial discharges activity changes with voltage, we performed a series of tests at different voltage levels. In this case, the voltage was increased by only 10 V with each step lasting 15 s. We have analyzed the PD patterns from the first level where PD activity was observed up to the level where almost all impulses resulted with partial discharges. Using a high bandwidth oscilloscope we have recorded the waveforms of 500 impulses of the fixed amplitude as well as the signals from the partial discharges detector. The impulses were superposed in order to see the dispersion of the voltage waveforms. PD signals were analyzed and every detected partial discharge was presented on a scatter plot as a point for the corresponding time and energy (here understood as the amplitude of the PD signal in mV). Figure 2.40 shows the PD patterns from the lowest voltage (A) to the highest (H).

One can see that generally speaking the higher the voltage, the more high energy PD signals. For negative impulse, mostly at the descending slope, some at the ascending slope and only few on the negative plateau. For positive pulses the PD signal are far more dispersed, but still the majority of them are right after the ascending slope.

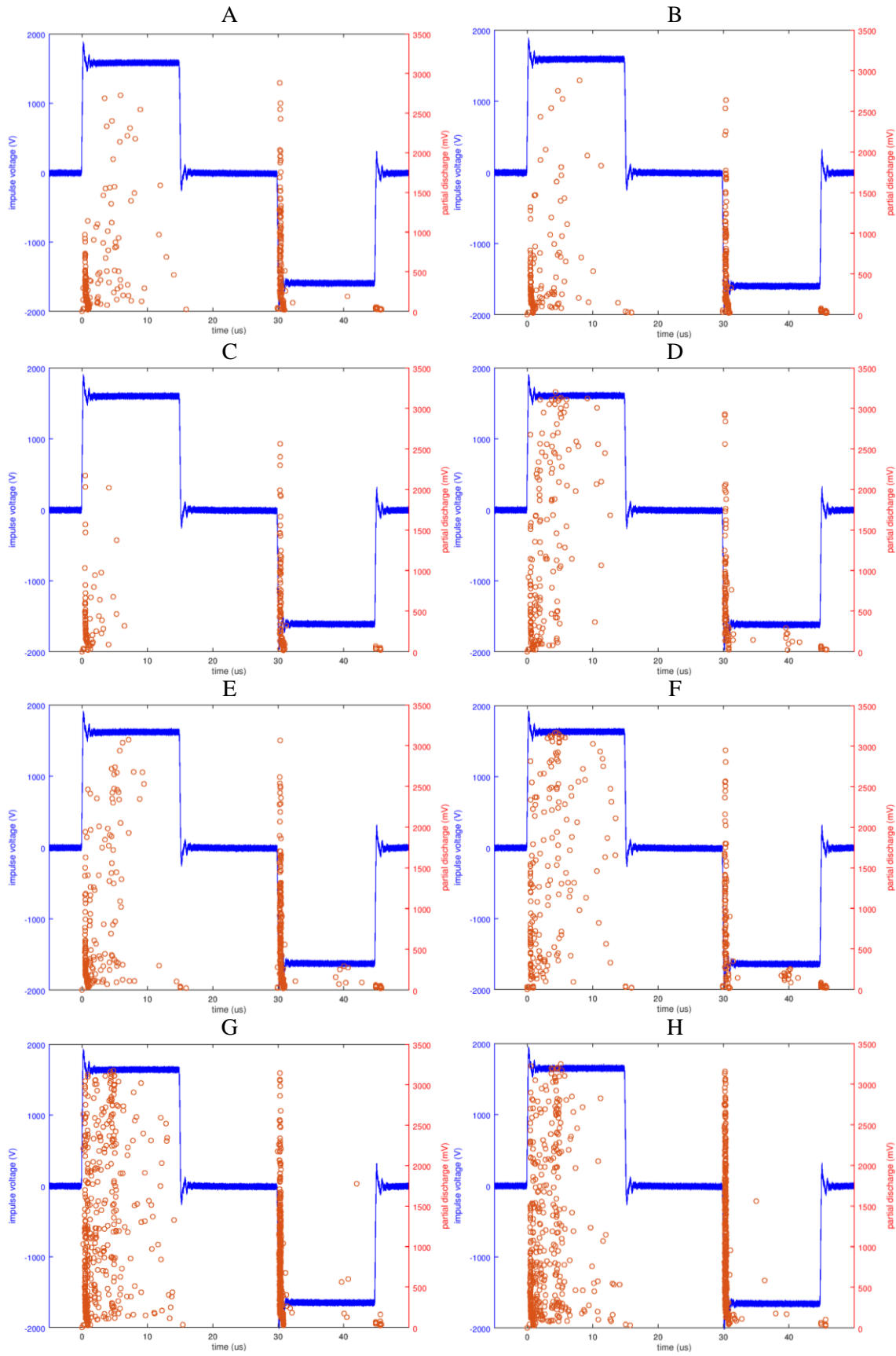Table 2.11 shows detailed data concerning those PD patterns.

Figure 2.40. PD pattern for phase W of a stator winding tested under bipolar impulses.

Table 2.11. Detailed data concerning PD patterns of Figure 2.40

PD pattern (Figure 2.40)	Positive peak value [V]		Negative peak value [V]		Peak-to-peak voltage [V]		Per cent of impulses resulting with PDs [%]		
	min	max	min	max	min	max	both positive and negative	only positive	only negative
A	1832	1879	-1906	-1951	3753	3813	53.6	35.4	35.8
B	1838	1880	-1918	-1962	3768	3827	51.2	26.6	35.4
C	1852	1902	-1924	-1976	3793	3858	31.0	16.8	22.0
D	1864	1911	-1939	-1981	3813	3874	37.0	32.2	23.8
E	1866	1912	-1949	-1994	3830	3898	71.0	39.2	52.0
F	1879	1923	-1955	-2011	3853	3916	59.0	35.4	46.2
G	1894	1930	-1971	-2017	3871	3935	96.6	73.6	82.8
H	1901	1946	-1981	-2028	3887	3961	96.4	79.4	84.6

One can see that the applied voltage is not perfectly symmetrical, as the negative impulse has peak values about 4% higher than the positive one. This may explain why for most cases there are more PD activity for negative impulses was higher. For this studied case, the PDIV and RPDIV levels are the same, as the very first voltage level with PD activity gave rise to partial discharges for at least 50% of impulses. Surprisingly, for patterns C and D, although the applied voltage was higher, the PD activity was smaller than for A or B. For the last 2 voltage levels tested, G and H, almost every impulse gave rise at least one PD.

As even for as many as 500 impulses per voltage level do not provide unequivocal RPDIV level, the minimum number of 10 impulses suggested in [14] seems insufficient.

Difference in PD patterns may signify that the impulse polarity might influence the measured value of the PDIV or RPDIV. Existing studies concerning this topic, e.g. [85] and [86], concentrates on tests performed using twisted pairs which may not be representative for measurements on stators. Further studies are needed to better understand how different test protocols can influence the measured PDIV or RPDIV.

2.5. Life data analysis

The results of all measurements are somehow vitiated by the measurement uncertainty, called also measurement error. There are 2 principle sources of errors:

- the systematic errors, also known as measurement or statistical bias, are attributed to the used experimental setup and influence the accuracy. Accuracy, called also trueness, describes a difference between a result and a true value (value we would be able to measure using perfectly unbiased method). This term is related to the concept of replicability, meaning the ability to independently achieve similar conclusions using different samples, test procedures or methods of data analysis.
- contrary to systematic error, the random errors describe the statistical variability of achieved data. They are described by the measurement precision and repeatability, so the variations in measurements taken in the same test conditions.

Naturally the measurements should be as accurate and precise as possible. Unfortunately, in case of accelerated aging tests, the random errors are significant and one can normally expect as much as ten-to-one difference in the lifetime of "same" samples tested in the same conditions [61]. The aging process is influenced by many factors. From the technical point of view it is almost impossible to precisely control all the test parameters. Some secondary factors have to be neglected.

2.5.1. Lifetime distributions

For such extremely variable test results as lifespan data, specialized statistical methods, like those presented in this section, are needed to analyze the results. Thanks to them, we are able to determine whether the observed differences between the series are statistically significant or are just a scatter of results.

In reliability engineering and lifetime data analysis, the output is always only an estimate. The true value of failure probability, reliability (probability of success), the mean lifetime or any other applicable parameter is never known and almost certainly will remain unknown to us for any practical purposes.

_____

In order to treat the statistical data we need a statistical distribution function, usually called probability density function *f(t)* or simply PDF. Different distribution exists, such as normal (Gaussian), exponential, Weibull, etc., with their predefined forms of *f(t)*. Some distributions tend to better represent lifetime data and thus are often called lifetime distributions.

Normal (Gaussian) distribution is probably the best known and its parameters, such as mean value or standard deviation, can be easily calculated. Unfortunately it is usually not appropriate to electrical breakdown data, as its probability density function is by definition positive for every value from -∞ to ∞. It would mean that for negative aging time there would be a positive failure probability, which is physically impossible [87].

Distributions typically used for electrical breakdown data are: Weibull, Gumbel and lognormal distribution [87]:

The **Weibull distribution** [88], due to a after Swedish mathematician: Waloddi Weibull [1887-1979], is one of the most widely used lifetime distributions in reliability engineering, commonly used for solid insulation. It is a type of extreme value distribution, which means that the system failure is defined by the failure of the weakest link [87].

The probability density function (PDF) for Weibull 2-parameter distribution is defined as [89]:

$$f(t) = \begin{cases} \dfrac{\beta}{\alpha}\left(\dfrac{t}{\alpha}\right)^{\beta-1} \cdot \exp\left[-\left(\dfrac{t}{\alpha}\right)^{\beta}\right] & t \geq 0 \\ 0 & t < 0 \end{cases} \qquad (2.1)$$

where:

$\alpha > 0$ – scale parameter (characteristic life for aging tests)

$\beta > 0$ – shape parameter or slope

t – measured variable, here: time to breakdown (lifespan), but can be also e.g. breakdown voltage

_____

There exists also a 3-parameter Weibull distribution, for which the PDF is defined as [89]:

$$f(t) = \begin{cases} \dfrac{\beta}{\alpha}\left(\dfrac{t-\gamma}{\alpha}\right)^{\beta-1} \cdot \exp\left[-\left(\dfrac{t-\gamma}{\alpha}\right)^{\beta}\right] & t \geq \gamma \\ 0 & t < \gamma \end{cases} \tag{2.2}$$

where:

$\gamma \in \mathbb{R}$ – location parameter (represents a time shift; the probability of failure is zero for $t < \gamma$); if $\gamma < 0$ - an indicative of quiescent failures, i.e. failures that occur before a product is used for the first time, such as manufacturing, packaging or shipping problems.

The **Gumbel distribution**, due to a German mathematician: Emil Julius Gumbel [1891-1966], is also an extreme value distribution. It is usually applicable to breakdown involving percolation, in liquids and in cases where fault sites, such as voids, are exponentially distributed.

The probability density function (PDF) for Gumbel distribution is defined as [90]:

$$f(t) = \frac{1}{b} \cdot \exp\left[-\left(\frac{t-u}{b}\right) + \exp\left(-\frac{t-u}{b}\right)\right] \tag{2.3}$$

where:

$b > 0$ – scale parameter

$u \in \mathbb{R}$ – location parameter

The **lognormal distribution**, introduced by an English statistician Francis Galton [1822-1911] (thus it is occasionally referred to as the Galton distribution), may be used for cases where specimens breakdown is due to unrelated causes or mechanisms.

The probability density function (PDF) for lognormal distribution is defined as [89]:

$$f(t) = \frac{1}{\sigma\sqrt{2\pi}} \cdot \exp\left[-\left(\frac{(\log t - \mu)^2}{2\sigma^2}\right)\right] \tag{2.4}$$

where:

μ – logarithmic mean (scale parameter)

σ – logarithmic standard deviation (shape parameter)

_____

As stated before, for solid breakdowns the 2-parameter Weibull distribution is most commonly used, thus other distributions presented briefly in this chapter will not be further discussed. Detailed information concerning Weibull distribution can be found in section 2.5.3.

2.5.2. Censoring

Some aging test, especially those performed for stress levels close to nominal working conditions, can be especially time consuming. Normally all the samples need to break down in order to start the data analysis. This 'complete' set of data, where the lifespan (or breakdown voltage) is known for all the samples, is called uncensored. If, however, the test was suspended for some of the samples from the tested lot, the data are 'incomplete' or **censored**. For such a test, the number of samples that broke down r is smaller than the total number of tested samples n.

Electrical insulation breakdown data can be **right-censored**, which means that a data point is above a certain value but is not known exactly. For example, if a sample has a lifespan of at least 100 h (the test was suspended after 100 h without the sample breakdown), but we do not know whether it is e.g. 101 h or 250 h. In case of breakdown strength measurement, the censored data can be obtained if the applied voltage was lower than a certain value (e. g. due to source limitations): for example the breakdown voltage is at least 10 kV, but we do not know whether it is e.g. 10.5 kV or 20 kV.

If the test for all samples was started and continued simultaneously, the data obtained after the test suspension will be *slightly censored*, which mean that all the previous specimens had broken down (the suspended sample are 'stronger' than the others). For *progressively censored* data the test has suspended at different moment for different samples, i. e. some samples were suspended at the time (or voltage) lower that the maximum lifespan (or breakdown voltage) for non-suspended samples.

In this thesis, only non-censored or slightly censored data were used. The approach presented in further paragraphs applies to such data and should be adopted in case of progressively censored data, which will not be described here.

2.5.3. Weibull statistical distribution

The use of the 2-parameter Weibull distribution for breakdown data is discussed in this section.

2.5.3.1. Cumulative distribution function

The cumulative distribution function [3] (CDF) for 2-parameter Weibull distribution is defined as:

$$F(t) = 1 - \exp\left[-\left(\frac{t}{\alpha}\right)^{\beta}\right] \tag{2.5}$$

By transforming the equation (2.5) one can obtain:

$$-\ln[1 - F(t)] = -\left(\frac{t}{\alpha}\right)^{\beta} \tag{2.6}$$

$$\ln\{-\ln[1 - F(t)]\} = \beta \cdot \ln t - \beta \ln \alpha \tag{2.7}$$

As shown in the equation (2.7) the cumulative distribution function can be linearized:

$$\underbrace{\ln\{-\ln[1 - F(t)]\}}_{Y} = \underbrace{\beta}_{m} \cdot \underbrace{\ln t}_{X} - \underbrace{\beta \ln \alpha}_{n} \tag{2.8}$$

2.5.3.2. Empirical cumulative distribution function

In order to apply the Weibull statistics to the samples, i. e. to find the parameters α and β, one must somehow obtain empirical cumulative distribution function $\hat{F}$. There are various approaches to estimate it [91] [92].

The test data should be placed in the order from the 'weakest' with the rank $i = 1$ (shortest lifespan or lowest breakdown voltage) to the 'strongest'.

Equation (2.9) shows the empirical cumulative distribution function approximation as advised in [87].

---

[3] Cumulative distribution function F of continuous random variable t is defined as the integral of its probability density function $f(t)$:

$$F(\tau) = \int_{-\infty}^{\tau} f(t) dt$$

$$\hat{F}(i,n) = \frac{i - 0.44}{n + 0.25} \times 100\% \tag{2.9}$$

where:

$i = \{1, 2, \dots, r\}$ – rank of the broken down sample

r – number of broken down samples (for uncensored data $r = n$)

n – total number of tested samples

2.5.3.3. Weibull plot

As shown in the equation (2.10) the Weibull distribution becomes linear if the on axis of abscissa we will present $\ln t$ and on axis of ordinates $\ln\{-\ln[1 - F(t)]\}$. A graph in this coordinate system is often called Weibull plot. One can also find Weibull papers with already printed Weibull scale.

In order to present the experimental data on the Weibull plot one must assign the coordinates of each point as in (2.10):

$$\begin{cases} x_i = \ln(t_i) \\ y_i = \ln\{-\ln[1 - \hat{F}(i)]\} \end{cases} \tag{2.10}$$

If the points are distributed according to the Weibull function they should be aligned. In order to verify it the correlation coefficient [4] R should be calculated. Demanding on the number of specimens broken down r, there is a minimum correlation coefficient assuring the collinearity of points. Figure 2.41 shows the goodness of fit of a 2-parameter Weibull distribution as a function of number of specimens broken down r. If the fit is sufficiently good the statistical distribution of results can be analyzed using Weibull equations.

---

[4] Pearson correlation coefficient R for n points of coordinated (x,y) is defined as:

$$R = \frac{n(\sum xy) - (\sum x)(\sum y)}{\sqrt{[n\sum x^2 - (\sum x)^2][n\sum y^2 - (\sum y)^2]}} \in \langle -1, 1 \rangle$$

If $|R| = 1$ – perfect linear correlation (positive of negative)
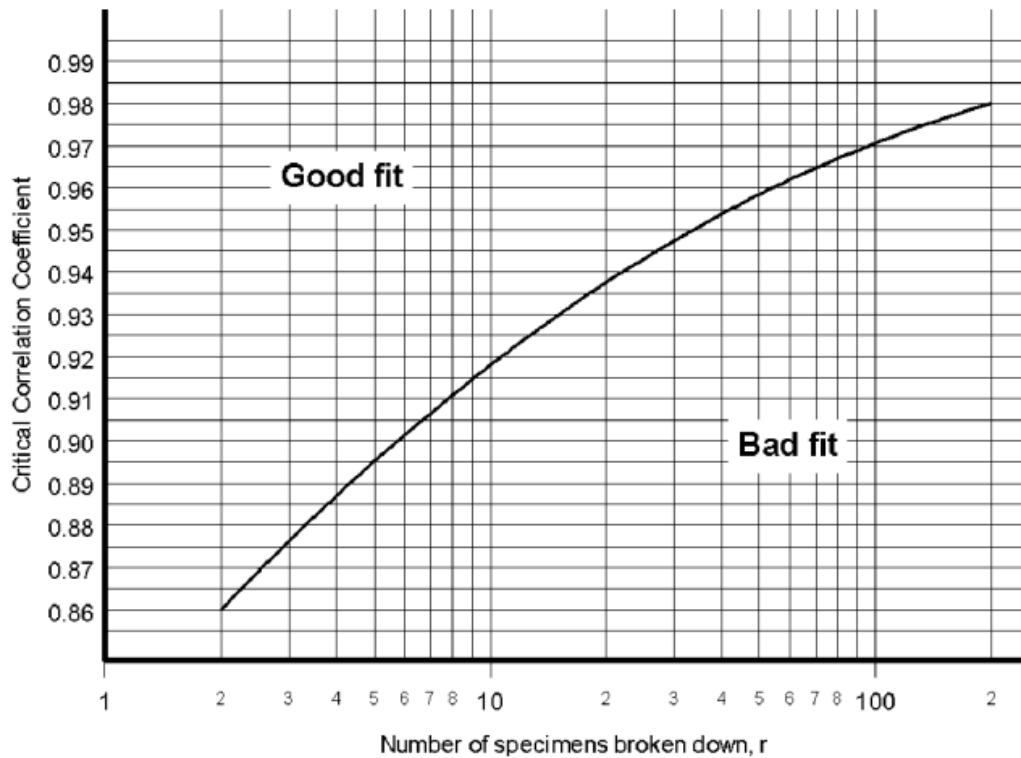
$R = 0$ – no linear correlation

Figure 2.41. Goodness of fit of a 2-parameter Weibull distribution [87]

2.5.3.4.   *Weibull parameters estimation*

If the experimental data can be approximated by Weibull distribution one need to find its parameters: scale parameter α and shape parameter β. They can be found using the following techniques:

2.5.3.4.1. Graphical estimates of Weibull parameters

First one should mark the experimental data points on the Weibull paper. Then the straight line should be fitted by eye to those points. The estimate for the scale parameter α is the time (or voltage) corresponding to $F(t) = 63.2\%$. Usually this probability value is clearly marked to facilitate the estimation of α. The value of the shape parameter β is estimated from the slope of the line. Typically Weibull papers have special scale allowing to directly estimate it.

However, this approach may be useful only if the rough estimates of parameters are required or where there are a large number of data points falling on a good straight line with very limited censoring.

Nevertheless, plotting the data on a Weibull plot is recommended so that the adequacy of the distribution may be assessed.

2.5.3.4.2. Computational techniques for Weibull parameters estimation for large data sets

As shown in equation (2.10) the cumulative distribution function can be linearized.

Using a least squares linear regression one can calculate the slope m and the y-intercept n of the regression line according to equation (2.8):

$$m = \frac{\sum(x_i - \bar{x})(y_i - \bar{y})}{\sum(x_i - \bar{x})^2}$$

$$n = \bar{y} - m\bar{x}$$

(2.11)

where:

$\bar{x} = \frac{\sum x_i}{r}$ – mean of abscissa

$\bar{y} = \frac{\sum y_i}{r}$ – mean of ordinates

r – number of broken down samples

In such a case the slope m of the regression line is equal to β, and the y-intercept n is equal to $-\beta \cdot \ln\alpha$. The Weibull distribution parameters can be thus calculated as shown in the equation (2.12):

$$\begin{cases} \alpha = \exp\left(-\dfrac{n}{m}\right) \\ \beta = m \end{cases}$$

(2.12)

This approach should be applied for larger data sets, typically with more than 20 breakdowns. For smaller data sets, the more adapted technique is presented in section 2.5.3.4.3.

2.5.3.4.3. Computational techniques for Weibull parameters estimation for small data sets

For data sets smaller than 20-30 breakdowns, it may be inaccurate to use the standard least-squares regression technique, as described in section 2.5.3.4.2. In such

_____

case different points need to be allocated different weightings, depending on the number of samples tested.

Table 2.12 presents the weighting for the test of 8 samples depending on the rank. The complete table of weightings can be found in [87].

Table 2.12. Weighting for the test of $n = 8$ samples [87] [93]

Rank	Weightings for the test of 8 samples
i	w_i
1	0.607927
2	1.546985
3	2.510036
4	3.447632
5	4.316695
6	5.041186
7	5.448119
8	5.011059

In order estimate the values of Weibull parameters one must first calculate the weighted averages as shown in (2.13) [87]:

$$\bar{x} = \frac{\sum_{i=1}^{r}(w_i \cdot x_i)}{\sum_{i=1}^{r}(w_i)}$$

$$\bar{y} = \frac{\sum_{i=1}^{r}(w_i \cdot y_i)}{\sum_{i=1}^{r}(w_i)}$$

(2.13)

Than the $\hat{\alpha}$ and $\hat{\beta}$ can be calculated as presented in (2.14) [87]:

$$\hat{\beta} = \frac{\sum_{i=1}^{r}[w_i \cdot (y_i - \bar{y})^2]}{\sum_{i=1}^{r}[w_i \cdot (x_i - \bar{x}) \cdot (y_i - \bar{y})]}$$

$$\hat{\alpha} = exp\left[\bar{x} - \frac{\bar{y}}{\hat{\beta}}\right]$$

(2.14)

For even smaller data sets, with less than 5 breakdowns, this method should not be applied as it can give rise to erroneous parameter estimates. Naturally it is strongly

_____

advised to obtain more data, but if it is not possible appropriate methodology is proposed in [93].

2.5.3.5.   Estimation of confidence intervals for the Weibull function

As stated before aging test results can be very scattered and thus the estimated Weibull parameters differ from the unknown true, especially for small set of data. To take into consideration this dispersion and present a range with highest probability of the true value of parameters, confidence intervals are commonly used. Generally speaking, the more specimens are tested, the closer the parameter estimates are to the true values and thus the narrower the confidence intervals are.

There exist multiple methods of calculating the confidence intervals [94] [95] [91] [90]. In this work we use the approach suggested in [87]. All confidence intervals calculated here are 90% bilateral confidence intervals[5] using coefficients calculated using a Monte-Carlo method and are to be accurate to within 1% for data sets used here.

Table 2.13 presents coefficients used for to calculate lower and upper bounds of 90% bilateral confidence intervals.

Table 2.13. 90% confidence intervals coefficients for α and β for of $n = 8$ samples [87]

Sample size		90% confidence intervals coefficients			
Total number n	Broken down r	α lower $W_{\alpha l}$	α upper $W_{\alpha u}$	β lower $W_{\beta l}$	β upper $W_{\beta u}$
8	3	0.2239	5.609	0.4273	5.178
	4	0.3291	3.021	0.4847	3.366
	5	0.4078	2.263	0.5292	2.67
	6	0.4669	1.970	0.5674	2.236
	7	0.4973	1.836	0.6024	2.025
	8	0.5135	1.782	0.6361	1.824

_____

[5] 90% bilateral confidence intervals exclude the highest 5% and lowest 5% of the distribution of the variable

_____

Lower and upper confidence bounds for α and β can be calculated as presented in (2.15):

$$\widehat{\alpha_l} = \hat{\alpha} \cdot W_{\alpha l}^{\frac{1}{\hat{\beta}}}$$

$$\widehat{\alpha_u} = \hat{\alpha} \cdot W_{\alpha u}^{\frac{1}{\hat{\beta}}}$$

$$\widehat{\beta_l} = W_{\beta l} \cdot \hat{\beta}$$

$$\widehat{\beta_u} = W_{\beta u} \cdot \hat{\beta}$$

(2.15)

2.5.3.6. *Weibull percentiles and their confidence intervals coefficients*

2.5.3.6.1. *Estimation of Weibull percentiles*

In life data analysis is it sometimes useful to use percentiles or so-called B-lives. For example B10 life, or 10th percentile, will signify the time at which 10% of the samples, at a given (constant) stress level, will break down.

The pth percentile can by calculated using the equation (2.16):

$$\hat{t}_p = \hat{\alpha} \cdot \left[-\ln\left(1 - \frac{p}{100}\right)\right]^{\frac{1}{\hat{\beta}}}$$

(2.16)

where:

p – percentage

2.5.3.6.2. *Confidence intervals for the Weibull percentiles*

Same as for *α* and *β*, the 90% bilateral confidence intervals can be estimate also for Weibull percentiles. The coefficients were calculated using Monte-Carlo method and are to be accurate to within 1%. Table 2.14 presents coefficients used for to calculate lower and upper bounds of 90% bilateral confidence intervals.

Table 2.14. 90% confidence intervals coefficients for Weibull percentiles for of $n = 8$ samples [87]

Sample size		90% confidence intervals coefficients											
		0.1% percentile		1% percentile		5% percentile		10% percentile		30% percentile		95% percentile	
Total number n	Broken down R	lower W_{tl}	upper W_{tu}	lower W_{tl}	upper W_{tu}	lower W_{tl}	upper W_{tu}	lower W_{tl}	upper W_{tu}	lower W_{tl}	upper W_{tu}	lower W_{tl}	upper W_{tu}
8	3	3.83×10^{-7}	0.1226	8.17E-05	0.2093	0.003411	0.3307	0.01617	0.4249	0.1126	0.9038	0.3458	64.5
	4	1.33×10^{-6}	0.0814	0.000149	0.1726	0.004041	0.3092	0.01662	0.4164	0.129	0.8217	0.5793	24.38
	5	3.01×10^{-6}	0.059	0.000227	0.1479	0.004724	0.2926	0.01747	0.4065	0.1331	0.8067	0.8093	13.95
	6	5.61×10^{-6}	0.04265	0.000316	0.1245	0.005374	0.2735	0.01841	0.3966	0.133	0.8056	1.04	9.773
	7	9.52×10^{-6}	0.03431	0.000425	0.1109	0.006195	0.261	0.01987	0.3866	0.1326	0.8048	1.222	7.544
	8	1.55×10^{-5}	0.02602	0.000567	0.09433	0.007086	0.2404	0.02146	0.3678	0.1323	0.8004	1.411	6.22

Lower and upper confidence bounds for t_p can be calculated as presented in (2.17):

$$\hat{t}_l = \hat{\alpha} \cdot W_{tl}^{\frac{1}{\hat{\beta}}}$$

$$\hat{t}_u = \hat{\alpha} \cdot W_{tu}^{\frac{1}{\hat{\beta}}}$$

(2.17)

_____

2.6. Conclusion

This chapter presented some general information concerning accelerated aging tests on insulating materials.

As showed in the first part the list of factors, which can influence the lifespan of the insulating system of a machine is very long. Those factors can interact with each other, thus the study of each of them individually is under no circumstances sufficient for lifespan assessment. The study of the influence of all the factors would be almost impossible due to their large number, thus some most important ones were chosen for the following tests. The results of some preliminary tests are presented in chapter 3, while the lifespan models using the 3 most important ones: voltage, frequency and temperature, are presented in chapter 4.

The second section, where the detail description of the designed test bench was presented, showed how technically complicated it is, even for the limited number of factors that were tested.

The third part, dedicated to partial discharges measurements, presented some PDIV results, as these values were essential for correctly choosing the stress levels for all the following tests. The results of some preliminary PD tests performed on the electric machines showed how efficient this technique can be in fault detection, but at the same time highlighted some possible problems with experimental data analysis.

Finally, the last section explained in details the statistical analysis of lifespan data, crucial for all the accelerated aging tests presented in the following chapters.

CHAPTER 3

Factors influencing the lifespan of insulating materials

Table of content

_____

3. CHAPTER 3: FACTORS INFLUENCING THE LIFESPAN OF INSULATING MATERIALS

This chapter presents the results and the analysis of some preliminary tests, prior to lifespan modeling.

Section 3.1 is dedicated to the choice of samples for accelerated aging tests. Sections 3.2 to 3.5 cover the influence of the most important factors that can influence the lifespan of an electrical insulation, respectively: temperature, power source parameters, environmental conditions and surface state. The study of all these factors individually is necessary to the construction of consistent multi-factors lifespan models.

3.1. Sample choice for accelerated aging tests

3.1.1. General requirements

The choice of a sample for accelerated aging tests is not a simple task. A good sample needs to meet several requirements, expressed in the features listed below:

- Representative
  - The chosen sample type should be as good representation as possible of the aging process inside a real object, in our case an electric machine. This study is dedicated to aging due to a partial discharges activity, so a sample should enable to model the same partial discharges aging mode as seen in the working machine. The "further" the sample is from it, the more difficult it would be to draw any conclusion considering the final product.
  - Naturally, the most representative sample would be a complete machine in its normal working conditions, but due to multiple problems, mentioned later in this paragraph, it is often impractical, even almost impossible, to perform accelerated aging study on it. In a study dedicated to investigate a particular aging mechanism, such as partial discharges activity, all other failure modes need to be withdrawn from the results pool.

- Reproducible
  - As stated before in chapter 2, the accelerated aging results tend to be quite strongly dispersed. A particular attention should be paid to the sample initial characteristics. If, for example, the PDIV values are strongly dispersed even before the aging test, it is highly probable that the accelerated aging results will be even more strongly scattered. Too dispersed data might make it impossible to draw pertinent conclusions.
  - The dispersion in the sample properties is a result of differences in the properties of primary materials (different batches of "the same" product can vary significantly and even the beginning and the end of the same batch) and the sample manufacturing process. Generally speaking the more complex the sample is, the harder it is to assure the same, or at least as similar as possible, parameters of each sample as it uses more different materials and its manufacturing process has more stages.
- Reasonable
  - Accelerated aging tests can be particularly time and energy consuming. A well-chosen sample should allow to obtain the tests results in a reasonable period of time.
  - Naturally, the economical aspect of a sample choice cannot be neglected. As accelerated aging is often a destructive test, the sample cannot be reused. Taking into consideration an important number of samples needed in order to obtain reliable results, a sample unitary cost should be as low as possible. Generally speaking, higher complexity and more rigorous parameters control, the higher this cost is. However the total cost of testing depends also on the necessary equipment. Bigger and heavier samples require more voluminous climatic chambers and, depending of its parameters, more powerful source.

_____

3.1.2. Overview of existing samples of insulation system

There are multiple different sample types that are used for accelerated aging tests of insulating materials. This paragraph presents the overview of those most commonly used.

3.1.2.1.   "Sandwich"-type samples

A so-called "sandwich" samples consists of an insulation layer (or multiple layers) inserted in-between two electrodes. Such sample offers a very good control of all geometrical dimensions, such as insulation layer thickness, electrodes geometry, as well as a mechanical pressure applied while assembling the sample.
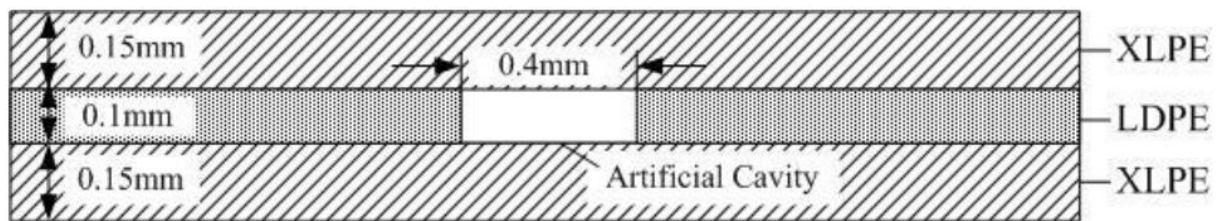
Figure 3.42. The example of "sandwich" sample [96]

However, it is quite far from the real-life conditions seen by the insulation system in the machine. If used for varnish or enamel, the polymer deposition and curing process need to be modified. As already explained in chapter 1, the manufacturing process has a great influence on the final properties of the insulation system, thus a sample may not be sufficiently representative for an aging process in an electric machine.

This type of sample is most commonly used to study the aging process of impregnating varnish, resin or solid insulators [96] [97]. It is rarely used for enamels, as a multistage deposition and curing process, seen by the magnet wire, would be difficult to reproduce.

3.1.2.2.   Crossed wires

The simplest sample using a magnet wire is a crossed wire. It is just two pieces of magnet wire being in contact in only one point, as shown in Figure 3.43.
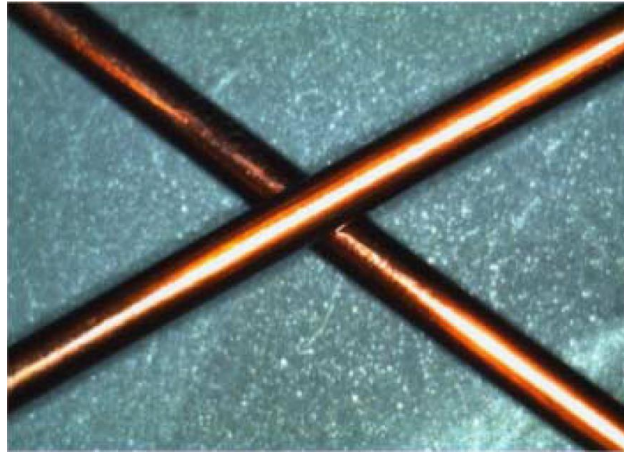
Figure 3.43. Crossed wires as a type of a magnet wire sample [98]

The biggest advantage is its simplicity. However it tests only one point of contact along the wire, so it would be required to test lots of samples to give an overview of the enamel state. It might be also problematic to apply adequate mechanical tension to, on the one hand, assure the contact between the wires and, on the other, to be representative for the one used during the winding process [99].

3.1.2.3.   Twisted pairs

Twister pair is the most commonly used sample to test the magnet wire quality. Its manufacturing is controlled by the standard [100], as it was primarily designed for testing the breakdown voltage. Table 3.15 presents the load applied to the wire and number of twists depending on the conductor nominal diameter.

Table 3.15. Loads applied to the wire and number of twists (extract from [3])

Nominal diameter of conductor [mm]		Load [N]	Number of twists [-]
Higher than	Up to (and included)		
0.355	0.500	3.40	16
0.500	0.710	7.00	12
0.710	1.060	13.50	8
1.060	1.400	27.00	6

The device used for manufacturing of twisted pairs is shown in Figure 3.44.

Figure 3.44. Device used for manufacturing of twisted pairs.

Thank to well-established manufacturing protocol, twisted pairs have quite good reproducibility. On the other hand, they are relatively delicate and requires care while manipulating (especially for smaller diameter magnet wires), which may lead to increased dispersion of final results. Some other factors that may influence this scatter, such as humidity, ozone concentration and surface state, are discussed in section 3.4 and 3.5.

Twisted pair is advised as one of the sample types for turn-to-turn insulation tests in standard [14].

However, a basic twisted pair cannot simulate the effect of impregnation on turn-to-turn insulation. Naturally it is possible to impregnate a twisted pair, typically by dipping method. Unfortunately such samples present much more dispersion due to manufacturing process, mostly vertical curing process which results in uneven varnish distribution. Moreover such samples are especially delicate as polymerized varnish is very brittle.

Some preliminary tests showed, that due to transportation and manipulations with impregnated twisted pairs, the PDIV values on some samples from the batch were

_____

relatively high (over 2 kV$_{RMS}$) while others presented much lower values (around 800 V$_{RMS}$), typical for non-impregnated samples. After closer analysis it was stated that in those samples which presented low PDIV samples, the varnish was missing between the wires, especially between the "legs" of a twisted pair. Naturally the lifespan tests on such a dispersed population would have pointless, as at the given voltage level the aging mechanism for these 2 types of samples (correctly impregnated and faulty ones) would be completely different.

3.1.2.4. *Winded elements*

The other sample that may be used to test the magnet wire properties is a small coil or other winded element. This type of sample on the one hand enables to simulate the mechanical stress seen by the magnet wire (tension during winding and resulting elongation), on the other hand, is relatively easy to manufacture which can limit the dispersion in the results, as there are fewer parameters than cannot be precisely controlled. The advantage of such samples is that they offer lower PDIV values and shorter lifespans (in given conditions) than a twisted pair (about the half those of a twisted pair), as (taking as an example the sample presented in Figure 3.45) only one, not two, layer of enamel is exposed to stress. This enables to lower the voltage for accelerated aging and using cheaper sources.

_____
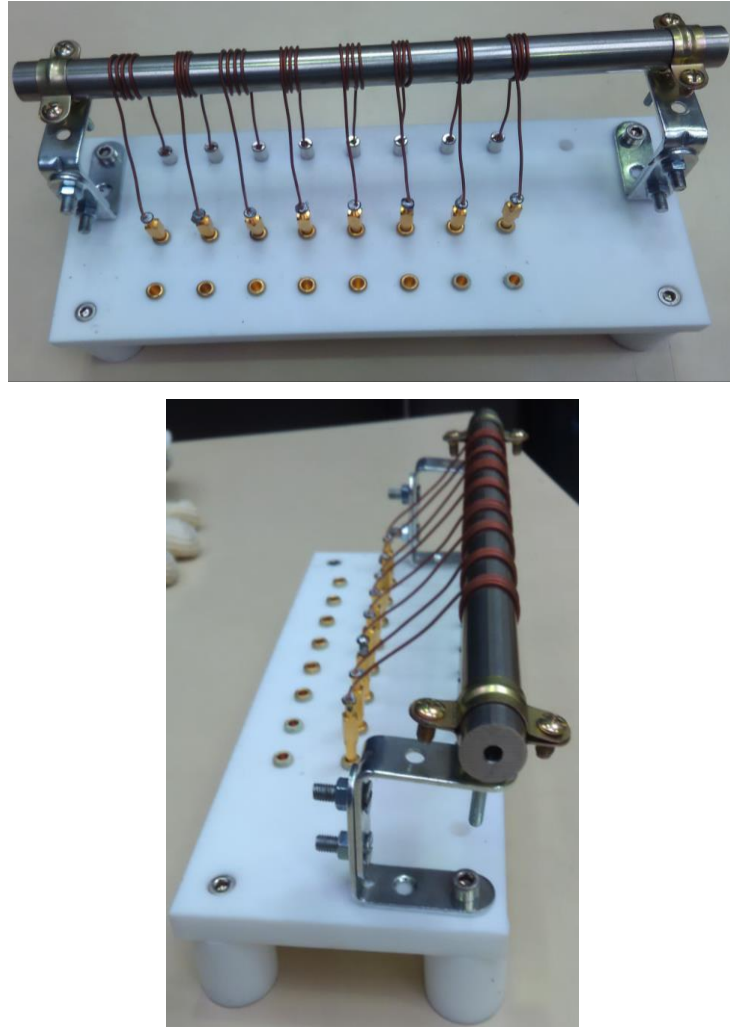
Figure 3.45. The example of winded samples. The voltage is applied between the coil (high voltage) and the metal rod (ground)

However this sample is not adapted to test the influence of impregnation on the PDIV and lifespan. Moreover, the mechanical tension is difficult to control during temperature cycling due to thermal expansion of both the magnet wire and the rod.

3.1.2.5. *Motorettes*

Motorette is a special test model used for the evaluation of the electrical insulation system of random-wound windings [47]. It is typically used for its thermal evaluation. Its manufacturing is controlled by standards [101] and [102].
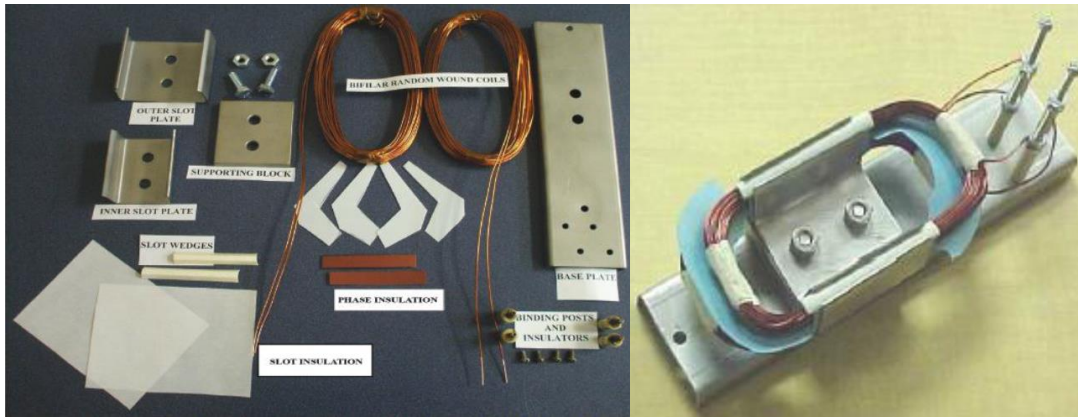
Figure 3.46. Components of a motorette before final assembly (left) and completely assembled and varnished motorette (right) [102]

An equivalent of motorette for form-wound windings is a formette [47] [27].

As a motorette is composed of the same insulating materials as a real machine, it enables to test all of them at the same time. It also possible to study the interaction between different insulating materials, for example: enamel and varnish or varnish and insulating papers. Motorette (or formette) is advised as one of the sample types for turn-to-turn, phase-to-ground and phase-to-phase insulation tests in standard [14].

The complexity of motorettes, both in materials used and manufacturing process, may cause important dispersion in initial properties and, as a result, in aging results.

3.1.2.6. *Statorettes, stators or complete machines*

Naturally the most representative test sample is a complete machine. It enables to study the behavior of all insulating materials exposed to real-life stresses and their interactions. Unfortunately, as already expressed before, the test on complete machine would be particularly time-consuming (lifespan of the machine in the typical working conditions is in the order of tens of years) and costly (machine cost but, above all, the test equipment and the consummated energy). Due to high complexity of such sample and resulting dispersion, it would be difficult to draw any pertinent conclusions. This cost can be slightly reduced by using only stators. However, the final dispersion will still be significantly higher than for other less complex samples.

Some manufacturers use a "mélange" of motorette and a complete stator, called statorette. Instead of using an artificial slot of motorette and downscaled coils and insulators, it uses a full scale coils inserted inside a stator core or its part. Such a sample

_____

is more representative than a motorette and generally easier (and cheaper) to manufacture that a complete stator. However, in most cases the so-called statorette is used for high-voltage winding (Figure 3.47) or for low-voltage flat wire winding.
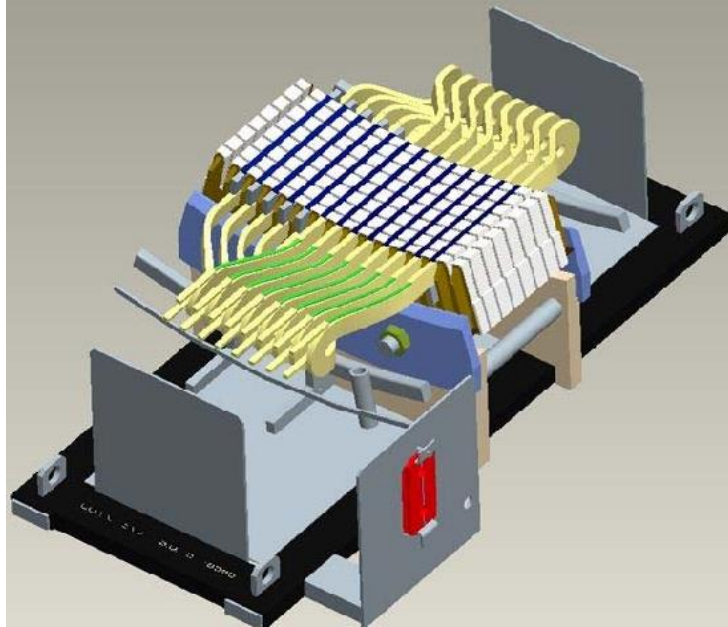
Figure 3.47. 3-D model of a 13.8 kV statorette [103]

3.1.2.7.   Choice of the aging sample - conclusions

Taking into consideration all the aspects presented in this section it was decided to perform accelerated aging tests mostly on twisted pairs. As mentioned before it offers a good compromise between the representativity (it models the worst case scenario of turn-to-turn insulation, when the first and last coils are adjacent and impregnating varnish is missing), good reproducibility (thanks to well defined manufacturing protocol – see also section 3.5.2) and offers reasonably low test costs. It is also the sample the most commonly used in the literature.

3.2. Influence of temperature on the lifespan of insulating materials

Temperature, beside voltage (see section 3.3.1), is probably the most recognized cause of insulation deterioration. This section is dedicated to a new and original study of its influence on the lifespan of insulating materials.

3.2.1. Temperature distribution in the electric machine; thermal class

The temperature seen by the insulation system is a resultant of multiple losses in the machine, such as [2]:

- Resistive losses (so-called copper losses or I^2R) in the stator and rotor circuit
- Iron losses due to eddy currents in the stator core
- Mechanical losses due to friction in the bearings and windage (due to air turbulence and shear because of relative movement of rotor and stator)
- Stray losses (e.g. higher harmonic losses in stator core).

This heat is than dissipated thanks to ventilation and via the stator frame. The heat transfer rate depends also on the ambient temperature and other environmental conditions.

The increased temperature accelerates the chemical reaction of polymer chain scission and oxidation (in air-cooled machines). As a result the insulation becomes more brittle and prone to damage, while insulating "papers" may start to delaminate due to loss of bonding strength or impregnating compound. Moreover, as due to the differences of coefficients of thermal expansion between the copper and insulating materials, the additional shear stress will appear during thermal cycling. The higher this temperature difference is, the sooner the failure appears. However no simple relationship relating the number of cycles with failure rate has been developed yet [6].

Moreover, in a transient situation the copper winding temperature increase much faster than this of the insulation system. This results in a shear stress between the conductors and the insulation as the copper grows more quickly than the groundwall insulation. In stator windings, after many thermal (i.e., load) cycles, the bond between the insulation and the copper may break, as a function of temperature. However, the

_____

higher the temperature difference between the insulation and the copper, the fewer the number of cycles to failure. [104]

The temperature is not uniformly distributed inside the machine. The parts closer to the fan are cooler than those on the other side. Also, parts closer to the frame have lover temperature than those further from it. The points of the machine where the temperature is higher than the mean value are called hot-spots. They can be found at coils outhangs or inside the slot, thus significantly increasing the thermal stress on the insulation system. Even the temperature inside the coil is not uniform, as the center of the coil is usually slightly hotter than the outside [105]. Figure 3.48 shows the increase of the temperature in different parts of electric machine.
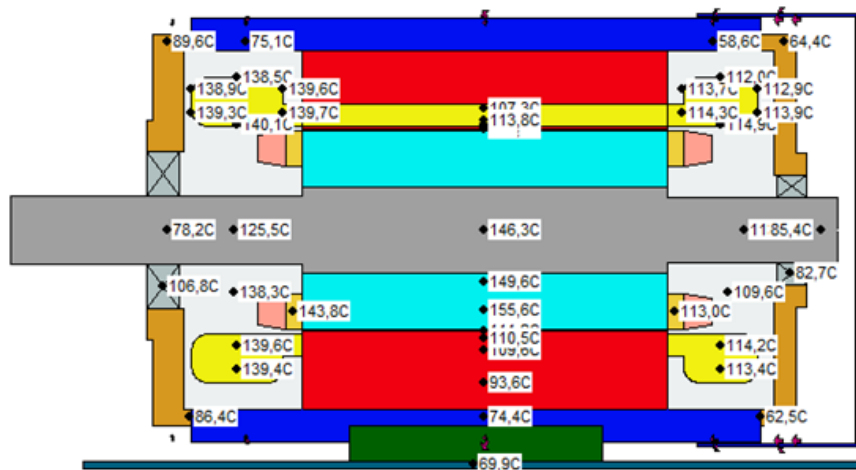
Figure 3.48. Results of the simulation of temperature increases in an electric machine
[courtesy of C. Neacsu]

The most commonly used model describing the effect of temperature on the lifespan of the insulation is based on the Arrhenius law, as presented in equation (3.1) [6] [106] [107]:

$$L = A \cdot e^{\frac{B}{T}} \qquad (3.1)$$

where:

L – the lifespan of the insulation

A, B – constants

T – absolute temperature [K]

The influence of the thermal stress on the lifespan of the insulation system elements is usually presented as a thermal class (see chapter 1). According to the definition, it denotes the temperature (in ℃) corresponding to the lifespan of 20 000 h. The maximum allowed temperature increase in the electric machine is typically 50℃ lower than the thermal class, as it takes into consideration the rated ambient temperature of the machine (40℃) and the safety margin for the hot-spot (10℃).

The study of thermal aging of impregnating varnishes is presented in [97]. It shows that for the temperatures significantly higher than the thermal class the aging mechanisms are different and as a result the extrapolation of Arrhenius law model is no longer correct. In this work the studied range of temperature will not exceed the limit of thermal class.

The equation (3.1) becomes linearized in log(L)-reciprocal(T) plot. This is particularly important for the design of experiment method (DoE) – see chapter 4. This linearity was experimentally verified on accelerated aging test bench (see chapter 2) on twisted pairs (1.12 mm, grade 2, PEI/PAI 200℃ corona resistant magnet wire) in the wide range of lifespans. Figure 3.49 presents this graph.
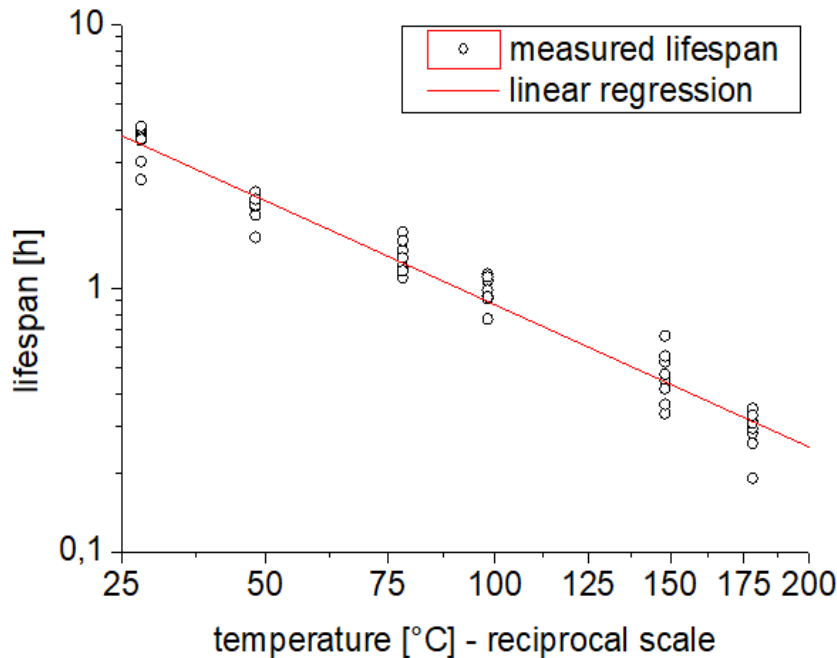
Figure 3.49. The experimental verification of the linearity of the function between the lifespan and the temperature in log-reciprocal plot (other constraint factors are constant: $V = 1.75$ kV, $f = 10$ kHz).

_____

3.2.2. Influence of the temperature on the partial discharges activity

The definition of a thermal class takes into consideration only the thermal aging. However, the temperature influences also other aging modes.

As presented in [108] the partial discharge inception voltage changes as a function of temperature. Figure 3.50 shows the PDIV (phase-to-ground; sine 50Hz; RMS values) as a function of the temperature for different types of stators: not impregnated, dipped impregnated (polyester resin) and potted one (epoxy resin).
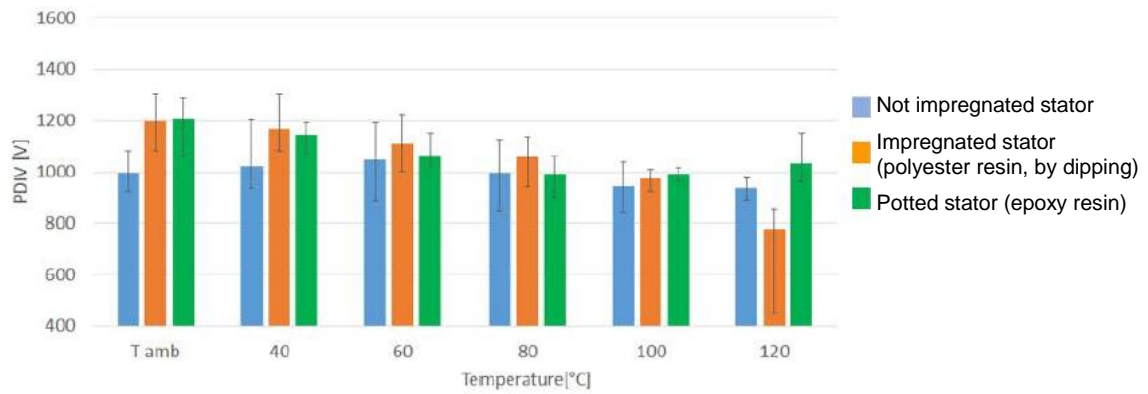
Figure 3.50. Average PDIV (phase-to-ground; sine 50Hz; RMS values) at different temperatures for each kind of insulating system (error bars show the measurement uncertainties) [108]

One should notice also the error bars of the measured PDIV. They are in the same order of magnitude as the ones achieved by our industrial measurements (see chapter 2). If we take them into consideration the relation between the PDIV and the temperature is not always statistically clear.

Figure 3.51 shows the RPDIV (turn-to-turn; weakest phase) for the same 3 stator for 3 different temperatures.
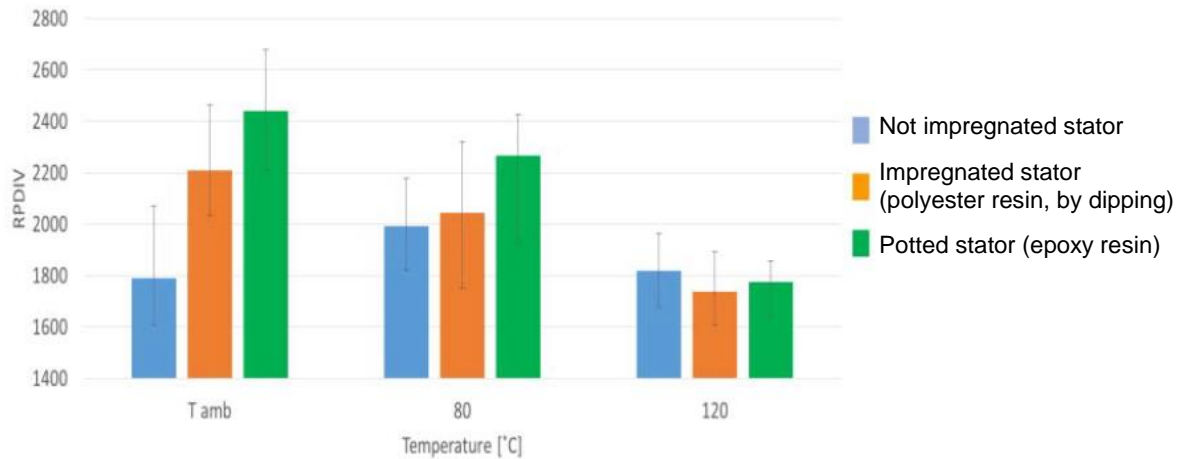
Figure 3.51. Average RPDIV (pulse voltage) at different temperatures for each kind of insulating system (error bars show the measurement uncertainties) [108]

As it can be seen, the PDIV, generally speaking, decreases with the increase of temperature. Higher temperature increases electron thermal agitation which increases the probability of finding the germ electron to start the partial discharge activity. This effect, however, is not the clear for the 3 stators tested ([108]) in the whole range of temperatures, especially in we take into consideration the measurement uncertainties). The decrease of PDIV with the increase of temperature can mean that, even if at ambient temperature the machine is exempted from partial discharges, at operating temperature they can appear. In such a case, the aging rate would increase [15] dramatically, as the PD deterioration rate is usually significantly faster than the thermal one.

The phenomenon needs to be coupled with the humidity level, which was not controlled in this test (see section 3.4.2), as the higher temperature can have drying effect which is not the same for not impregnated, impregnated and potted stator.

In same specific conditions the influence of the temperature can be beneficial. Higher temperature can prevent moisture from condensing on the winding, which reduces the risk of failure (see section 3.4.2). Because of thermal expansion the elements can also "swell" reducing the size of air pockets in the insulation and lower the risk of partial discharges. In low temperatures polymer materials, especially those in varnish, are far more brittle and prone to mechanical damages than in higher temperatures.

The temperature was included as one of the aging factors in the lifespan model presented in chapter 4.

The influence of the temperature cycling was not included in this study, but it is planned to be included in the following works.

3.2.3. Local overheating due to a partial discharges activity

Not only the temperature influences the partial discharges activity, but also the partial discharges activity may locally increase the temperature.

When electric charges accelerated by the electric field are bombarding the surface of the insulator, part of the energy is dissipated as heat. Taking into consideration poor thermal conduction of insulating materials, the increase of the temperature is localized to the zone closest to where partial discharges occur. This local overheating will even further increase the degradation rate of the insulation.

For a relatively low partial discharges activity and voltages close to PDIV, this phenomenon is hard to observe, as the temperature rise is negligible. For this reason it has not been stated on conventional magnet wires. For low voltage stress levels the difference in the temperature is too low, while for high voltage stress levels the lifespans are too short to observe the temperature rise.

However, for corona resistant wires this phenomenon can have significant influence on the resulting lifespan.

In some preliminary tests, 8 twisted pairs of corona resistant magnet wire (1.12 mm, grade 2, PEI/PAI 200ºC) were tested in a small (32L) non-ventilated oven at very high stress level (voltage amplitude 2.5 kV, frequency 10 kHz). For such a high stress level, the measured lifespan was in the order of 20 minutes, but during this short time the sample temperature increased so drastically that the temperature measured by the temperature probe increased by almost 30ºC. Figure 3.52 shows the picture of the test bench with the exact position of the PT100 temperature probe. The same test performed in a ventilated oven (but still without cooling) showed that the temperature rise was limited to just few degrees and measured lifespan (Weibull characteristic value α of 8 samples) were 18% longer. The test performed in the climate chamber, where the

temperature was kept stable (±0.5ºC), the lifespan (α of 8 samples) was even longer (by 9%).
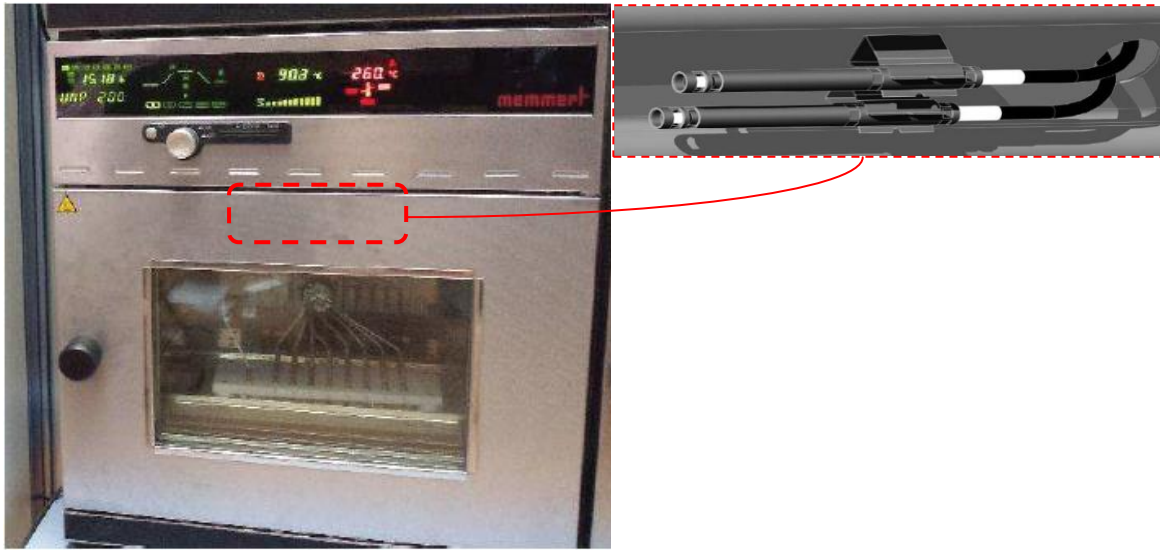
Figure 3.52. Laboratory non-ventilated oven used for some preliminary tests. The position of the PT100 temperature probe (zoom on the right) is marked in red.

Figure 3.53 shows how the temperature changed during the preliminary test in the non-ventilated and ventilated oven.
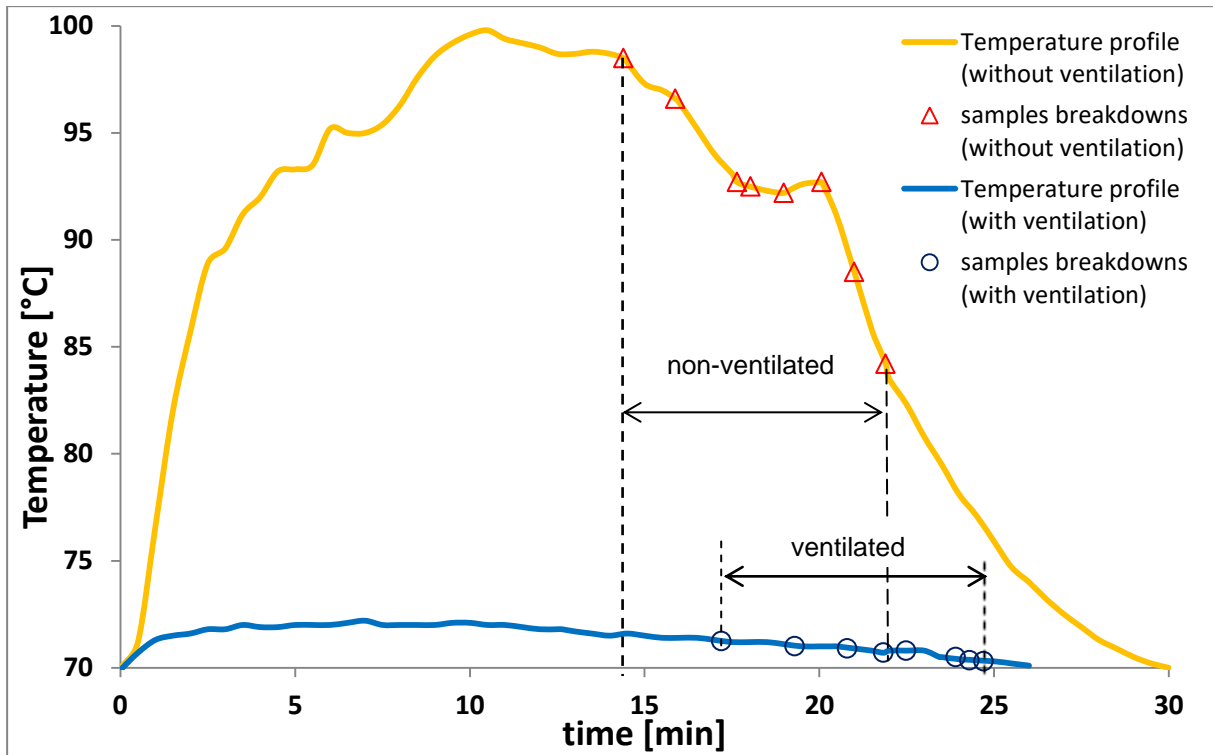
Figure 3.53. Temperature changes in the non-ventilated and ventilated oven during accelerated preliminary aging test.

_____

As it can be seen in Figure 3.53 the temperature rose very quickly right after the test was started to exceed by almost 30ºC the initial value. As the samples started to breakdown the temperature started to diminish and reached the initial level 8 minutes after the last sample broke down. The temperature withstood by the 8 samples was thus different throughout the aging process, hence influencing their lifespan.

For the purpose of lifespan modeling, the temperature must be kept at a precisely chosen level during the whole aging test. Then, in order to assure the stability of temperature, all future accelerated aging tests were performed only in the climate chamber, which allowed to quickly dissipate the extra heat generated by intense partial discharge activity.

3.3. Influence of powering parameters on the lifespan of insulating materials

3.3.1. Voltage amplitude

Electrical stress is a typical aging mode with threshold [109]. For voltages lower than the PDIV the aging process is significantly slower. The properties and thicknesses of insulation system elements are determined by thermal and mechanical considerations. Once the voltage is high enough to start the partial discharges activity, the aging rate is significantly higher and electrical stress becomes the primary source of failure.

As already explained in chapter 1, the type I insulation system [14] is composed exclusively of organic polymer materials. Those materials, when exposed to a partial discharge activity, deteriorate quickly due to scission of chemical bonds causing erosion [6].

The most commonly used model describing the effect of the electric stress on the lifespan of the insulation in the presence of partial discharges is an inverse power model, as presented in equation (3.2) [6] [106] [107]:

$$L = c \cdot E^{-n} \tag{3.2}$$

where:

L – the lifespan of the insulation

c, n – constants

E – electric field strength

The power law constant n is relatively high, for machines is usually reported to range from 8 to 12 [6] [110] [111]. Such a high value signifies a very powerful influence of the electric stress (in the presence of partial discharges) on the insulation lifespan.

The equation (3.2) can be linearized in a log-log plot. This is particularly important for the design of experiment method (DoE) – see chapter 4. This linearity was experimentally verified on accelerated aging test bench (see chapter 2) on twisted pairs (1.12 mm, grade 2, PEI/PAI 200ºC corona resistant magnet wire) in the wide range of lifespans (3 orders of magnitude). Figure 3.54 presents this graph.
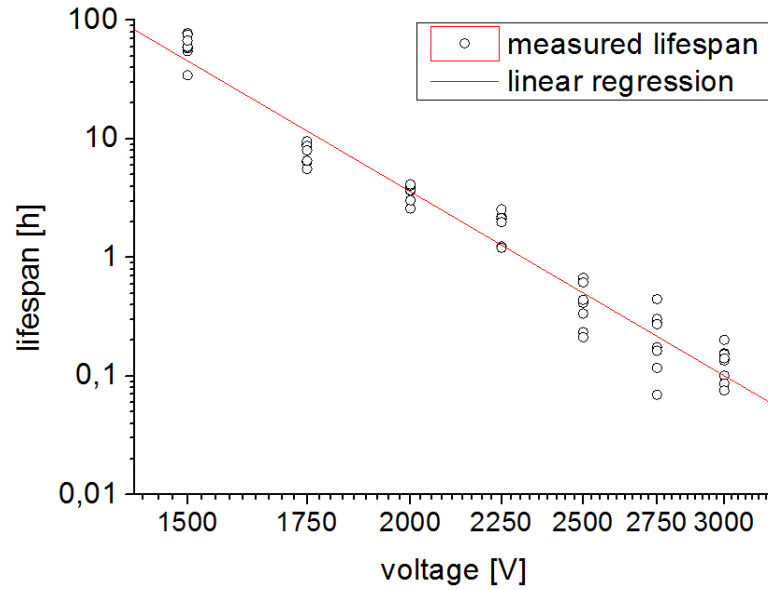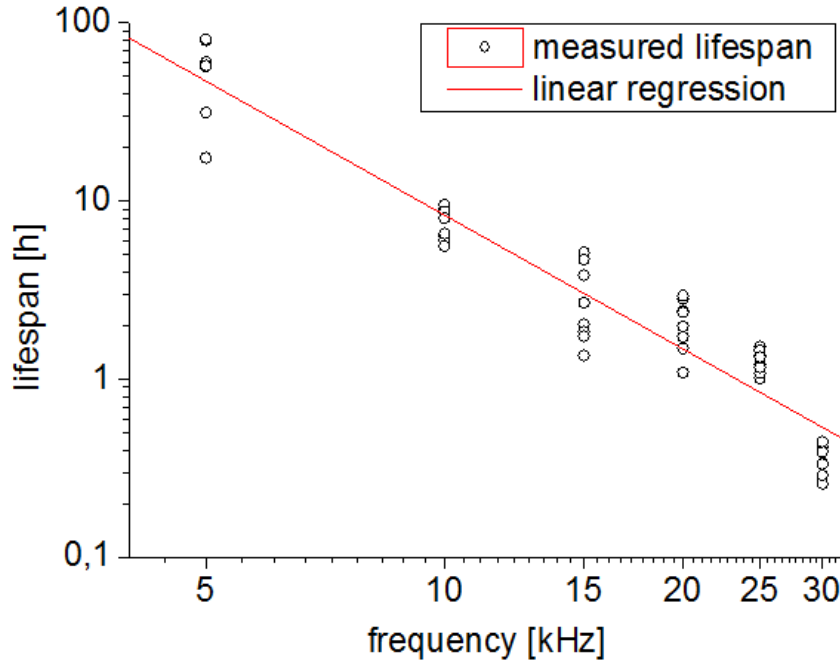
Figure 3.54. The experimental verification of the linearity of the function between the lifespan and the voltage in log-log plot (other constraint are constant: f = 10 kHz, T = 30ºC)

The experimentally found power law constant *n* from the equation (3.2) was around 8.9, so it fits the values found it the literature.

The voltage level was included as one of aging factors in the lifespan model presented in chapter 4.

3.3.2. Frequency

Another factor that can significantly influence the insulation degradation rate is the frequency. In inverter-fed machines, this degradation rate will be much faster than in the one powered from sinusoidal power source, even for the same peak-to-peak voltage at the terminals. The PWM signals have high switching frequencies and the surges of high voltages are repeated even tens of thousands times per second.

However, the relation between the lifespan and the switching frequency is not linear. The studies [112] [113] have shown that this function, shown in eq. (3.3) has the same nature as the one for the voltage amplitude.

$$L = c \cdot f^{-n} \tag{3.3}$$

where:

L – the lifespan of the insulation

c, n – constants

f – switching frequency

Same as for temperature and voltage amplitude, the equation (3.3) needs to be linearized for the design of experiment (DoE) model – see chapter 4. This linearity was experimentally verified on accelerated aging test bench (see chapter 2) on twisted pairs (1.12 mm, grade 2, PEI/PAI 200ºC corona resistant magnet wire) in the wide range of lifespans. Figure 3.55 presents this graph.

Figure 3.55. The experimental verification of the linearity of the function between the lifespan and the frequency in log-log plot (other constraint factors are constant: V = 1.75 kV, T = 30ºC)

The frequency was included as one of aging factors in the lifespan model presented in chapter 4.

3.4. Influence of environmental factors on the lifespan of insulating materials

3.4.1. Ozone concentration

Partial discharge activity in the presence of oxygen (e.g. in the air) can lead to bonds in oxygen molecules O_2 being broken by high energy electrons, thus creating oxygen radicals $O\bullet$ [114]. Those radicals are highly reactive and can attack either the polymer chains on the magnet wire or the other O_2 molecules, which creates an ozone molecule O_3. Ozone is known as a highly reactive gas. It may lead to ozonolysis reaction with the polymer chains [115] or it can react with nitrogen in the air creating different nitrogen oxides (NO_x). In the presence of humidity in the air, nitric acids may be created and deteriorate the motor's electrical insulation.

Those three degradation mechanisms mentioned above: directly by oxygen radicals, through ozonolysis and by nitric acids are competitive but are not equally harmful. Oxygen radicals are far more reactive and are most harmful for the enamel polymer. At the same time, they are the least stable and have lifetime so short, that it can be assumed that they are present only during PD activity. Ozone is less detrimental for the polymer but at the same time its lifetime is significantly longer and can react with the polymer up to 2-5 days after the end of PD activity (depending on the environmental conditions, such as humidity or temperature). Nitric acids are least reactive but at the same time are chemically stable and can act on the polymer properties a long time after the partial discharges were stopped [114][20] [116].

Monitoring the ozone concentration can be used as a partial discharges detection method that can also enable their localization [117]. The ozone concentration can reach significant levels, especially in the closed, non-ventilated machines, increasing the deterioration rate of the insulating properties of used materials [20].

In order to evaluate the influence of ozone concentration on the lifespan of magnet wires a special test was designed. Four different types on insulating enamels were tested: 3 conventional ones and 1 corona-resistant one, from different thermal classes. All wires were of the same diameter (0.5 mm) and same enamel grade (2). Table 3.16 shows the summary of the tested magnet wires.

Table 3.16. List of tested magnet wires

Type	1	2	3	4
Diameter	0.5			
Enamel grade	2			
Corona resistant	No	No	No	Yes
Enamel material	PEI (THEIC) (basecoat) PAI (overcoat)	PAI	PI	PAI with inorganic nanoparticles
Thermal class	200	220	240	220

The samples were divided into 2 series in order to evaluate the influence of ozone:

- Inside a close, non-ventilated climate chamber to allow the ozone to reach as high concentration as possible; this model represents a closed machine where ozone concentration can reach significant values

- Inside an open, highly ventilated climate chamber to assure that the ozone produced during the test was extracted as quickly as possible; this model represents a ventilated machine[6]

In each series up to 8 samples were tested in order to be able to perform a statistical analysis of the experimental data.

The test conditions were chosen in order to recreate the real-life stress submitted to the insulation of an inverter-fed machine. The voltage amplitude was set to 800 [V] to assure that for all the samples, it exceeds the PDIV. What is more, as we compare conventional and corona-resistant wires, the voltage level needs to provide sufficiently long lifespan for standard wires so that the measurements can be precise and reasonably not too long lifespans for corona resistant wires. The temperature was set to a classical ambient level (27ºC) to assure that the effect of ventilation will not influence significantly the temperature of the twisted pair surface. A pyrometer was used to prove that the temperature of the twisted pair varies less than 10ºC during the aging test. The influence of such a low change of temperature on the measured lifespan can be

---

[6] In an air ventilated machine the ozone concentration is not perfectly homogenous (the concentration around the 'source' of the ozone will be higher), however it is far more uniform than in closed, non-ventilated machine. Those differences in the ozone concentration can be used for localizing partial discharge activity in machines [119].

_____

neglected (see section 3.2, especially Figure 3.49). Table 3.17 shows the summary of the test conditions.

Table 3.17. Test conditions

Parameter	Series	
	non-ventilated	ventilated
Voltage amplitude	800 ± 10 [V]	
Frequency	15 ± 0.001 [kHz]	
Waveform	Square	
Duty cycle	50 ± 0.5 [%]	
Temperature	27 ± 0.5 [ºC]	
Ventilation of climate chamber	no ventilation	highly ventilated
Measured ozone concentration	200 ± 50 [ppm]	0.5 ± 0.2 [ppm]

The measurements of ozone concentration were conducted using an Oldham CTX300 electronic ozone detector (for the series in the ventilated climate chamber) and 10/A Dräger Ozone Tubes (non-ventilated climate chamber). Figure 3.56 shows the ozone detectors used.

Figure 3.56. Ozone detector Oldham CTX 300 O_3 0.00 – 1.00 ± 0.01 [ppm] (left) and 10/A Dräger Ozone Tubes 20 – 300 ± 50 [ppm] (right) [118] [119]

For each magnet wire (1-4) used in this tests, the Weibull plot is presented with both the series with ventilated and non-ventilated climate chamber. For each series the scale factor α (characteristic value of the lifespan) is calculated as well as its 90% confidence bounds.

_____

Figure 3.57 shows the Weibull plots, while Table 3.18 presents the test results for all 4 magnet wires.

Magnet wire 1 (PEI-PAI)

Magnet wire 2 (PAI)

Magnet wire 3 (PI)

Magnet wire 4 (PAI with nanoparticles)

- ● Data for non-ventilated climate chamber
- ◆ Data for ventilated climate chamber
- —— Weibull best fitting line for non ventilated climate chamber
- —— Weibull best fitting line for ventilated climate chamber
- - - - confidence bounds for non-ventilated chamber
- - - - confidence bounds for ventilated chamber

Figure 3.57. Weibull plots for series made in ventilated and non-ventilated climate chamber for magnet wire number 1-4

_____

Table 3.18. Weibull scale factor for series made in ventilated and non-ventilated climate chamber for magnet wires 1-4

Magnet wire	Ventilation	Weibull scale factor α [h]	90% confidence bounds [h]	Decrease in lifespan due to ozone concentration
1 (PEI-PAI)	Non-ventilated	0.361	(0.348; 0.376)	17.9 %
	Ventilated	0.440	(0.430; 0.451)	
2 (PAI)	Non-ventilated	0.250	(0.239; 0.261)	14.9 %
	Ventilated	0.294	(0.283; 0.306)	
3 (PI)	Non-ventilated	0.233	(0.229; 0.237)	3.4%
	Ventilated	0.241	(0.238; 0.237)	
4 (PAI with nanoparticles)	Non-ventilated	273.7	(259.5; 289.4)	24.1 %
	Ventilated	360.3	(347.2; 375.3)	

The results presented above show that high ozone concentration can affect the lifespan of samples, as for all 4 magnet wires studied in this article, the lifespan of the samples exposed to ozone was shorter than for not exposed ones.

The highest differences (of almost 25%) between the lifespans of 2 series were measured for the corona resistant wires (number 4). Due to its higher resistance PDs, hence, its much longer lifespan for the given test conditions, this wire was exposed to ozone for much longer (about 1000 times longer) than the other wires.

The smallest, almost negligible difference (3.4%) between the two compared series, was measured for the magnet wires of the highest thermal class of the studied materials – 240 (number 3). At the same time, this magnet wires presented the shortest lifespan of all the tested wires, thus its exposition to ozone was the shortest.

In comparison to other parameters affecting the lifespan of the electrical insulation, such as voltage, frequency or temperature level (see sections 3.2-3.3), the ozone impact seems to be much smaller, as the difference of the ozone concentration between the two analyzed series is very significant, while the change in the lifespan not so much.

This work was published during 35th IEEE Electrical Insulation Conference in Baltimore (2017) [120].

3.4.2. Humidity

The influence of the humidity on the partial discharge inception voltage of the twisted pairs is quite complex.

As water has very high relative permittivity ($\varepsilon_r = 80$), moisture absorbed by the enamel can increase its relative permittivity. As shown in [121] enamel ε_r can increase by approximately 0.4 when it is exposed to 95% relative humidity (at 30ºC) during time higher than 30 minutes. Increased ε_r results in higher field strength between the wires and thus PDIV is lower. Moreover, moisture absorption can increase surface conductivity, which increases the PDIV.

Water molecules suspended in the air can attach electrons and hence quench discharge activities. At higher temperatures, water concentration (absolute humidity) is high even for quite low relative humidity, so the humid air is becoming more and more electro-negative.

The last, but not the least factor, is wettability of the magnet wire. For very high relative humidity, water droplets can condensate on the enamel surface. The electric field is intensified, which can easily trigger a partial discharges activity. Moreover, electrokinetic forces can attract water to the high electric field strength area [122].

Figure 3.58 shows how PDIV changes as a function of relative humidity for 3 different temperatures for both conventional and nanocomposite (corona-resistant) wires.

_____
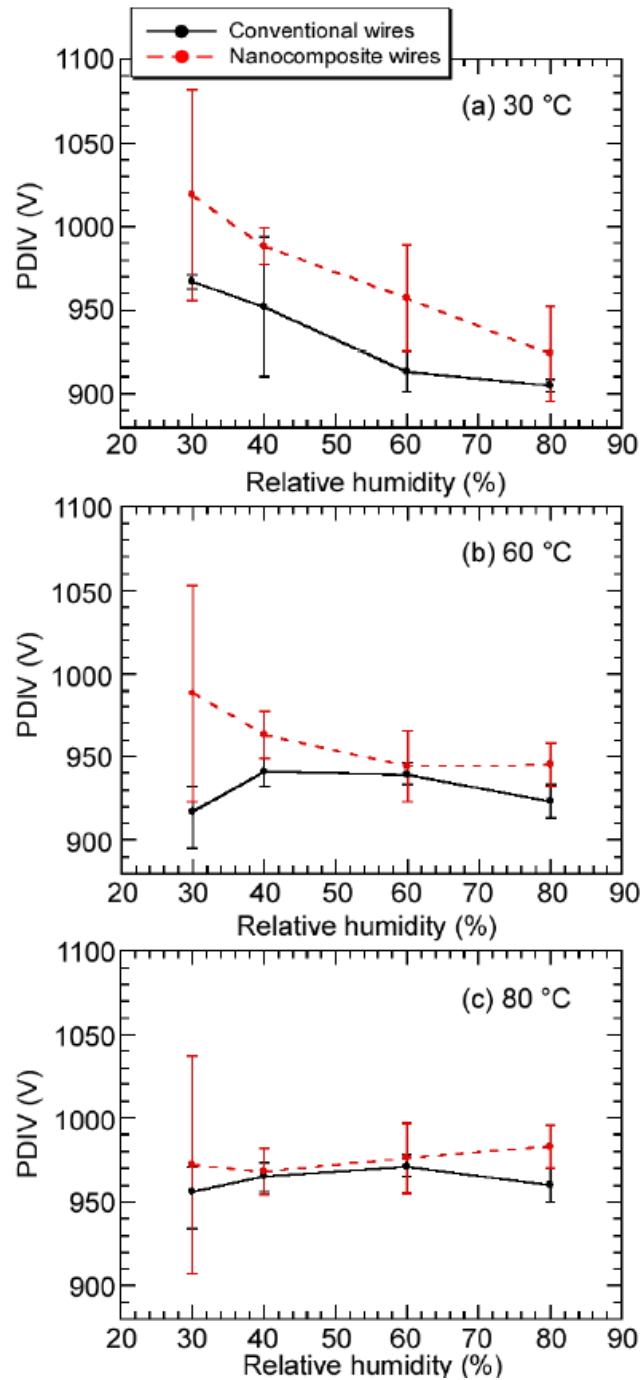
Figure 3.58. PDIV (RMS value; 60Hz sine voltage) as a function of the relative humidity with changing temperature (30-80°C); black solid line shows the results for conventional wire, dashed red one – nanocomposite (corona-resistant) [121]

Unfortunately the climate chamber used for the accelerating aging tests was not equipped with humidity regulation. For this reason the humidity variation can be treated as one of sources of results dispersion. Especially during long time aging tests the samples are exposed to multiple humidity variations.

3.5. Influence of the surface state on the lifespan of insulating materials

3.5.1. Influence of wire surface contamination

Preliminary tests have shown some important dispersion in results. To some extent they might have been attributed to humidity variation (see section 3.4.2). But it was decided to study how the sample manufacturing process and the wire storage conditions can influence the results.

Some papers, e.g. [123], show that the surface contamination, especially highly conductive (such as salt ions), can strongly influence the PDIV (sine 50 Hz) values. Figure 3.59 shows how the PDIV can vary between cleaned and contaminated magnet wires (here PPS insulated rectangular wire) in function of relative humidity (at 25ºC).
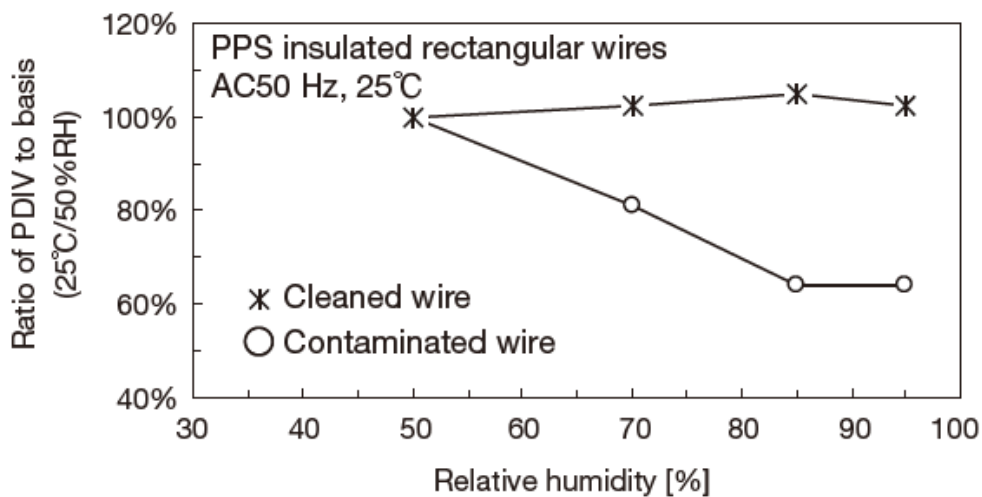
Figure 3.59. Effect of both surface contaminants and humidity on PDIV [123]

In order to test the hypothesis of how surface contamination influence on the lifespan of the samples, 3 series of samples were prepared:

- Twisted pairs prepared according to standard protocol,
- Twisted pairs prepared according to standard protocol and left for 2 weeks in the open air exposed to dust deposition,
- Twisted pairs prepared just before the test with magnet wire cleaned with 96% ethanol solution; all manipulations were done in gloves to prevent any additional contamination.

_____

All those 3 series were tested in the same conditions (voltage amplitude: 2.25 kV, square waveform; frequency: 10 kHz; temperature: 30ºC). Figure 3.60 shows the Weibull plots comparing those 3 series of samples.
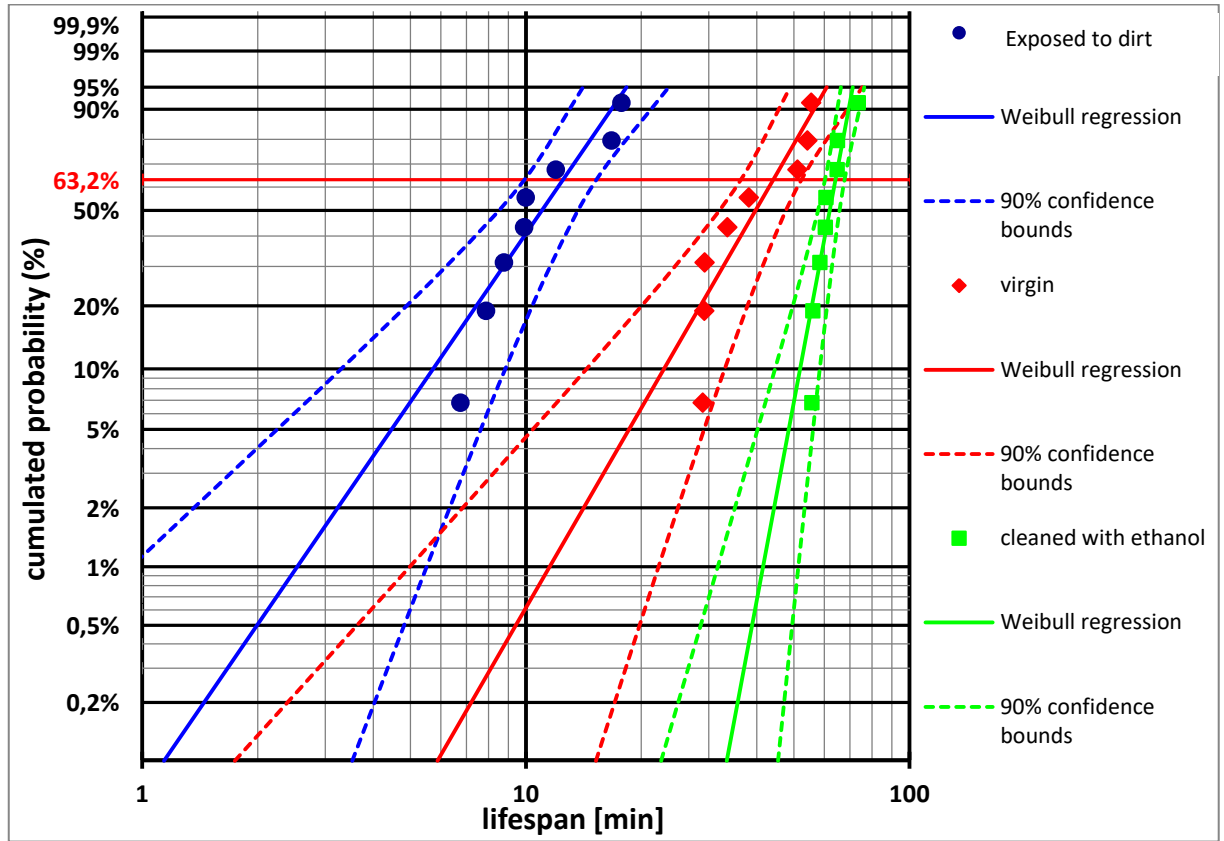
Figure 3.60. Weibull plots showing the influence of the surface state on the measured lifespan

The Weibull parameters (see chapter 2) calculated for each series are presented in Table 1.4.

Table 3.19. Weibull parameters for 3 series of samples, showing the influence of surface state

Test series	Weibull parameters	
	α [min]	β [-]
Standard (virgin) samples	44.2	3.4
Samples exposed to dust for 2 weeks	12.5	2.9
Samples cleaned with 96% ethanol solution	64.2	10.6

As it can be seen in Table 1.4 the samples prepared with cleaned magnet wires had longer lifespan and, what is even more important, were far less dispersed (higher β). Samples exposed to dust depositions were the most dispersed and had significantly shorter lifespans.

Those results shows how important the sample preparation protocol can be. As a result sample preparation protocol was modified in order to provide more reliable and reproducible results.

3.5.2. Protocol of samples preparation

As shown in previous paragraph, the contaminations on the enamel surface can significantly change test results, both concerning PDIV and lifespan measurements. In order to minimize this influence on the results, the protocol of sample preparation was slightly modified:

- All the manipulations with the magnet wires are done with gloves to avoid any additional contamination,

- Each magnet wire is cut to the proper length and its terminals are stripped; thanks to that there are fewer manipulations needed with a pair one it is twisted,

- All the wires are cleaned with 96% ethanol solution just before the preparation of twisted pairs. Thanks to that, most of the contaminations are cleaned from the enamel surface, even those that result from wire stripping. Cleaning wires with compressed air did not prove to be as effective, as expected,

- Twisted pairs are manufactured according to the standard [3] requirements (see section 3.1.2.3),

- In order to provide good and reliable electrical contact during the whole aging process, the gold-plated connectors are soldered to the twisted pair terminals,

- All the samples are prepared right before the test, not in advance, so that they are not exposed to contamination. They have been stored in a clean and dry place.

3.6. Conclusions

As explained in section 3.1 twisted pairs were chosen as most convenient samples for the accelerated aging tests. It seems to be a good compromise between the representativity (worst case scenario of turn-to-turn insulation, when the first and last coils are adjacent and impregnating varnish is missing), has a good reproducibility (thanks to well defined manufacturing protocol) and offers reasonably low test costs.

The temperature is clearly one of the most influential factors for the insulation deterioration rate. The most commonly used Arrhenius law was experimentally confirmed as a lifespan model. Temperature can also influence other aging modes (as e.g. PDIV value changes with temperature) or be influenced by them (local overheating due to partial discharge activity).

Voltage amplitude and frequency are, along with the temperature, other main factors to be included in the lifespan models, as their influence is far from being negligible. In machines where a partial discharges activity can appear, the deterioration rate is mostly dependent on this phenomenon.

The influence of environmental factors (humidity and ozone concentration) as well as surface state have secondary influence compared to the three factors mentioned before, however they can generate significant dispersion. In order to limit their influence, all the aging tests were performed in a climate chamber with scrupulously prepared samples.

The study of the ozone influence showed that it depends on the type of insulating material (enamel) as well as on the time exposition to this gas. However, generally speaking, the impact of ozone on the lifespan of insulating materials is significantly smaller than other factors (temperature, voltage, etc.). On the other hand the surface state of the samples has non negligible effect on the dispersion of the results, making life data analysis far more difficult. As a result, we established a special protocol of samples preparation in order to reduce this scatter.

The influence of air pressure was not studied in this chapter, as this work is dedicated for application areas where the differences of the air pressure and their influence of the insulation lifespan can be neglected. In case of e.g. aircraft equipment

the decrease in air pressure becomes one of the main issues influencing the insulation deterioration rate.

The information presented in the first two chapters allowed to identify the most probable sources of low voltage machines premature breakdowns and presented the appropriate background for the identification of aging factors and life data analysis. This chapter was devoted entirely to preliminary studies for accelerated aging test campaign. In the next chapter that information will be applied in order construct the lifespan models. The chosen methodology allows to include as many aging factors as needed (we showed the experimental results for 2- and 3-factors models) as well as to take into consideration the interaction between those factors. The experimental results show how efficient this technique can be in lifespan prediction, even far from the factor levels studied in the learning set.

CHAPTER 4

Lifespan modeling

Table of content

_____

4. CHAPTER 4: LIFESPAN MODELING

4.1. Introduction

This chapter shows the possible applications of the Design of Experiments (DoE) method as a modeling tool used for the lifespan prediction.

The first part presents the brief overview of existing lifespan models. It shows the advantages of developing a new another approach to lifespan modeling presented in this thesis.

Part 4.3 gives a detailed historical and theoretical introduction to the DoE technique. It explains step by step how the DoE model is defined and calculated. It also gives the experimental results used for the construction of the short-time DoE models.

The forth subchapter is dedicated to the use of DoE method for long lifespan prediction. Those predictions are based exclusively on short-time measurements up to 100 times shorter than the predicted lifespan, which is an original and unique approach. This section gives also the methodology of scatter analysis, which enables to enrich the DoE prediction with some confidence bounds. Finally all the predictions are verified experimentally in order to check how efficient this method really is.

The last subchapter explains how the DoE can be used as a comparative method. It shows the methodology to compare e.g. different material manufacturers based only on short-time measurements. Same as for the previous section, those short-time models are extrapolated towards much longer lifespans and compared with the experimental results in order to verify the accuracy of this prediction.

4.2. Overview of existing lifespan models

4.2.1. Single factor models

The vast majority of the lifespan models existing in the literature take into consideration only one aging factor. The most commonly recognized stress types in case of electric machines are, so-called TEAM stressed (Thermal, Electrical, Ambient (environmental) and Mechanical). In order to evaluate their effect on the lifespan numerous standards were developed. They define the test conditions as well as some requirements toward insulating materials. Table 4.20 presents a summary of these standards divided into the four stress categories mentioned above.

Table 4.20. The standard requirements towards accelerated aging tests of insulating materials [68].

Type of stress	Standards (examples)	Example of test conditions
Thermal stress (constant temperature)	[101] [124] [125] [126]	At least 3 values of different temperature tested At least 5 samples per each temperature Expected lifespans: 100-5000 h Standard atmospheric conditions Extrapolation according to Arrhenius law (see chapter 3)
Electrical stress	[15] [127] [128] [129]	Comparison of lifespans between the tested material and the reference sample (both tested in the same conditions) At least 3 values of voltage tested Expected lifespans: 100-3000 h Extrapolation according to the inversed power law (see chapter 3)
Ambient (environmental) stress	[130]	Samples exposed to weekly cycles of ambient constrains (3-6 cycles to be applied) 3 levels of relative humidity (30%, 60%, 95%) 2 levels of temperature (55°C, 70°C) Possibility of UV radiation
Mechanical stress	[131] [132]	Test of tensile strength (elongation) Tests of compressive strength Tests of flexural strength (bend strength)

According to those standards in can be seen that they are based almost entirely on the Arrhenius law (thermal stress) and inversed power law (electrical stress). The

_____

variation of the factor level (e.g. thermal cycling) is rarely present. They do not cover the possibility of interactions between several factors and often do not precise the specific test conditions (e.g. ambient conditions).

4.2.2. Two factors models

As stated before in chapter 3 the lifespan of the insulating materials is often the function of multiple stress factors. For this reason the single factor models are insufficient to properly model the aging process. In the literature we can find some 2 factors models, that are based on the 2 most widely recognized aging factors: temperature and electric field. They are all somehow inspired by Arrhenius law (thermal aging) and inversed power law (electrical aging). Examples of such models are presented below [68] [133]:

- Crine's model [134]
    - This model is based on the hypothesis that most of the aging processes of dielectrics are thermally activated. He assumes that the changes of material properties are due to the variation of Gibbs free energy *ΔG* and not to the activation energy *ΔE*. This means that the entropy of activation *ΔS* cannot be neglected.
    - For the combined thermal and electrical stress, the lifespan is modeled as (4.1):

$$L = \frac{h}{kT} \exp\left(\frac{\Delta G - e\lambda E}{kT}\right) \tag{4.1}$$

where:

h – Plank constant,

k – Boltzmann constant,

e – electric charge,

λ – width of the barrier (scattering length),

E – electric field strength,

T – absolute temperature.

- Simoni's model [109] [135]

  o This model is based on the thermodynamic laws in order to describe the degradation speed of the insulating material under thermal and electrical stress. Thermal aging is described by Arrhenius law, while electrical aging is described by exponential law, with the parameter depending reciprocally on the temperature.

  o The proposed model is presented in (4.2):

$$L = A\exp\left(\frac{B}{T}\right)\exp\left(-\left(a + \frac{b}{T}\right)(E - E_0)\right)$$
(4.2)

  where:

  A, B, a, b – constants to be experimentally found for each material,

  E – electric field strength ($E > E_0$),

  E_0 – electric field strength threshold,

  T – absolute temperature.

- Ramu's model [133]

  o This model was obtained by multiplication of 2 models: thermal model (based on the Arrhenius law) and electrical model (based on the inversed power law). The interaction between those 2 aging factors is considered in exponent on power law describing the electrical aging.

  o The proposed model is presented in (4.3):

$$L = c(T)\exp\left(-B\left(\frac{1}{T} - \frac{1}{T_0}\right)\right)\left(\frac{E}{E_0}\right)^{-n(T)}$$
(4.3)

  where:

$$c(T) = \exp\left(c_1 - c_2\left(\frac{1}{T} - \frac{1}{T_0}\right)\right),$$

$$n(T) = n_1 - n_2\left(\frac{1}{T} - \frac{1}{T_0}\right),$$

  c_1, c_2, n_1, n_2 – constants to be experimentally found for each material,

  E – electric field strength ($E > E_0$),

  E_0 – electric field strength threshold,

  T_0 – ambient temperature,

  T – absolute temperature.

_____

- Fallou's model [136]
  - Fallou proposed a semi-empiric model based on the Arrhenius law for thermal stress and the exponential law for electrical stress without the notion of threshold value E_0.
  - The proposed model is presented in (4.4):

$$L = \exp\left(A(E) + \frac{B(E)}{T} \right) \tag{4.4}$$

where:

$A(E) = A_1 + A_2(E),$

$B(E) = B_1 + B_2(E),$

A_1, A_2, B_1, B_2 – constants to be experimentally found for each material.

4.2.3. Summary

The lifespan of any components is rarely depending on only one factor, but usually is a complex function of many factors. The factors influencing the lifespan of electric machines were listed in chapter 2 and the most significant ones were analyzed in chapter 3.

The models presented in the literature take into consideration on maximum two aging factors, most often the temperature and the electric field. They cannot easily be adapted to include other factors, such as e.g. switching frequency or even the periodic changes of the studied factors, i.e. thermal cycling. Moreover, they do not take into consideration the economic aspects of the tests required. Finally, they were developed only for the purpose of modeling the aging of insulating materials and the conclusions cannot be generalized for other domains.

The methodology of lifespan modeling presented in the next section of this chapter is based on the Design of experiments. The examples and experimental results are presented for 2 and 3 factors, but the model can be easily adapted for a higher number of factors. This method automatically takes into consideration the possible interactions between the studied factors. The number of needed aging tests is also reduced in order to limit the total cost.

_____

Although this work is entirely devoted to the study of aging of insulation materials used in the electric machines, the same technique can be used for modeling the lifespan of other components used in electrical engineering, such as e.g. the OLEDs, as shown in [68].

4.3. Design of experiments

4.3.1. Definition and general information

Most commonly used test methods change only one factor, while other are kept constant (so called One Factor At Time, or OFAT). If it is needed to test the influence of several factors, the test must be repeated for each factor separately.

The DoE method uses a different approach. At the same time, all factors do have a significant role and all of them might be changed from one experimental point to the other. Interaction may exist between factors, consequently the effect of two (or more) combined factors may be larger, or smaller, than the sum of the two (or more) effects taken separately. The DoE method can take into account these interactions between the factors.

Thanks to this approach, we can significantly reduce the number of the experiments and at the same time increase the analysis accuracy as well as draw more persistent conclusions from the test campaign.

The DoE is thus a very efficient method to organize the experiments allowing to process optimization or model estimation.

The DoE method was first introduced by R.A. Fisher in 1935 [137] but actually his previous work from 1926 [138] already included the idea of "complex" design of experiments (although the term DoE was used officially 9 years later). The first use was related to the agriculture, since then, the DoE was used in multiple different domains.

The method has already proven its potency in many different fields of electrical engineering [139, 140, 141, 142], also for modeling the insulation lifespan [143] [144] [145]. DoE is a very cost-effective and efficient approach, as it allows to strictly limit the number of needed experiments.

4.3.2. Model construction – theoretical introduction

The DoE model describes the relationship between the response of the system Y (a function of an observable, e.g. lifespan) and the levels of the factors X_i influencing it (factors that can change the value of an observable, e.g. temperature, voltage). The

effect of each of those factors and the interactions between them is denoted by the coefficients in an "effect" vector E. The general matrix equation is shown in (4.5).

$$[Y] = [X] \cdot [E] \qquad (4.5)$$

The coefficients in the "effect" vector E must be calculated, based on the experimental data of system responses Y. If $[X]$ is square matrix, by the simple modification of the above equation, one gets (4.6).

$$[E] = [X]^{-1} \cdot [Y] \qquad (4.6)$$

A design, in which all combinations of factors are investigated in each replicate of the experiment, is called a full factorial design or full factorial experiment. It is the only means to completely and systematically study interactions between factors in addition to identifying significant factors [146].

The most widely used parametrical model is based on 2 levels of each factor. In case of k factors the model requires 2^k parameters and thus 2^k experimental points. The model equation in this situation is shown in (4.7). [147]

$$Y = M + \sum_{i=1}^{k} E_i X_i + \sum \sum_{i=1<j}^{k} I_{ij} X_i X_j + \sum \sum \sum_{i=1<j<l}^{k} I_{ijl} X_i X_j X_l + \cdots + I_{12\ldots k} \prod_{i=1}^{k} X_i \quad (4.7)$$

where:

M – the mean system response (the value of system response Y when all the factors X_i are equal to 0)

E_i – effect of the factor X_i (taken individually)

I_{ij} – effect of the second order interaction, i.e.: between 2 factors: X_i and X_j

I_{ijl} – effect of the third order interaction, i.e.: between 3 factors: X_i, X_j and X_l

…

I_{ijl} – effect of the interaction of the k-th order, i.e.: between all k factors: X_1 to X_k

It should be noted that the interactions are usually much smaller than then the effects of factors taken individually. Generally speaking the higher the order of the

interaction, the lower its effect. Moreover, the interactions of factors with high individual effect are typically higher than those of smaller effect [143] [144] [145].

Naturally there are more complex models of 3 and more levels for several (or all the) factors. Unfortunately, they require far more experiments: for full factorial design n^k experiments are needed, were k is the number of factors and n the number of their levels. For this reason, 2-level models offers the best compromise between the number of required tests and the model precision. The 2-level factorial design can be also used as a preliminary test to identify the most influencing factors and eliminate those with negligible effect. Afterwards the new multi-level factorial design can be proposed in order to study the influence of just those important factors more closely.

In this work, we are using 2 or 3-factor, 2-level models. These 2 levels correspond to 'high' (maximum) and 'low' (minimum) level of each factor. They are noted as '+1' and '-1', respectively.

For 2 factors, noted as A and B, the DoE model can be simplified to (4.8).

$$Y = M + E_A X_A + E_B X_B + I_{AB} X_A X_B \qquad (4.8)$$

As before M denotes the mean system response, E_A and E_B denote the individual effect of factors A and B, respectively, while I_{AB} the interaction between them. All these 4 coefficients can be calculated by solving the system of equations presented in the matrix (4.9).

$$\begin{bmatrix} Y_1 \\ Y_2 \\ Y_3 \\ Y_4 \end{bmatrix} = \begin{bmatrix} +1 & -1 & -1 & +1 \\ +1 & -1 & +1 & -1 \\ +1 & +1 & -1 & -1 \\ +1 & +1 & +1 & +1 \end{bmatrix} \cdot \begin{bmatrix} M \\ E_A \\ E_B \\ I_{AB} \end{bmatrix} \qquad (4.9)$$

In order to obtain the coefficient vector E, we need the vector of 2^2 system responses Y. These 4 experiments need to be performed for the factor levels at the vertexes of the square of the full factorial design, thus for $\{X_A = -1; X_B = -1\}$, $\{X_A = -1; X_B = +1\}$, $\{X_A = +1; X_B = -1\}$ and $\{X_A = +1; X_B = +1\}$, where '+1'stands for maximum level and '-1' for minimum. Their results are noted as $Y_1 - Y_4$. Figure 4.61 shows the plot of the full factorial design for such a factorial experiment.
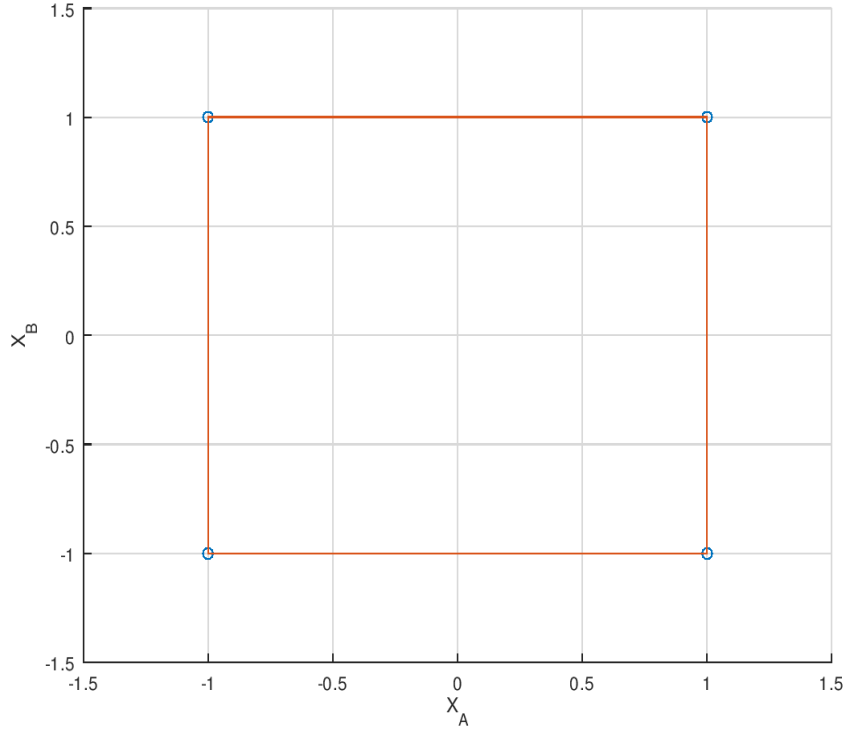
Figure 4.61. Plot of full factorial design for 2-factor 2-level model.

In case of three factors (A, B and C), the DoE model becomes:

$$Y = M + E_A X_A + E_B X_B + E_C X_C + I_{AB} X_A X_B + I_{AC} X_A X_C + I_{BC} X_B X_C + I_{ABC} X_A X_B X_C \qquad (4.10)$$

In this case there are three individual factor effects E_A, E_B and E_C, three second order interactions (I_{AB}, I_{AC} and I_{BC}) and one third order interaction of all three factors I_{ABC}. All of those coefficients, as well as the mean system response M, can be calculated from the matrix equation (4.11).

$$
\begin{bmatrix} Y_1 \\ Y_2 \\ Y_3 \\ Y_4 \\ Y_5 \\ Y_6 \\ Y_7 \\ Y_8 \end{bmatrix} =
\begin{bmatrix}
+1 & -1 & -1 & -1 & +1 & +1 & +1 & -1 \\
+1 & -1 & -1 & +1 & +1 & -1 & -1 & +1 \\
+1 & -1 & +1 & -1 & -1 & +1 & -1 & +1 \\
+1 & -1 & +1 & +1 & -1 & -1 & +1 & -1 \\
+1 & +1 & -1 & -1 & -1 & -1 & +1 & +1 \\
+1 & +1 & -1 & +1 & -1 & +1 & -1 & -1 \\
+1 & +1 & +1 & -1 & +1 & -1 & -1 & -1 \\
+1 & +1 & +1 & +1 & +1 & +1 & +1 & +1
\end{bmatrix} \cdot
\begin{bmatrix} M \\ E_A \\ E_B \\ E_C \\ I_{AB} \\ I_{AC} \\ I_{BC} \\ I_{A8C} \end{bmatrix} \qquad (4.11)
$$

The factors levels X become a $2^3 \times 2^3 = 8 \times 8$ matrix. Its first column refers to the mean value of all the system responses M. The next three columns describe the levels of

_____

factors *A* to *C*. Columns 5 to 7 describe the interaction between two of the factors, respectively *AB*, *AC* and *BC* and their level *X* is a simple multiplication of the corresponding factors levels. Last column is the interaction of the three factors A, B and C.

As it can be seen, in order to solve this equation we need 2^3 experiments performed at the vertexes of the cube of 3-factor full factorial design, i.e. for all the eight variations of $\{X_A = \pm 1; X_B = \pm 1; X_C = \pm 1\}$, where '+1'stands for maximum level and '-1' for minimum. Figure 4.62 shows the plot of full factorial design for such a factorial experiment.
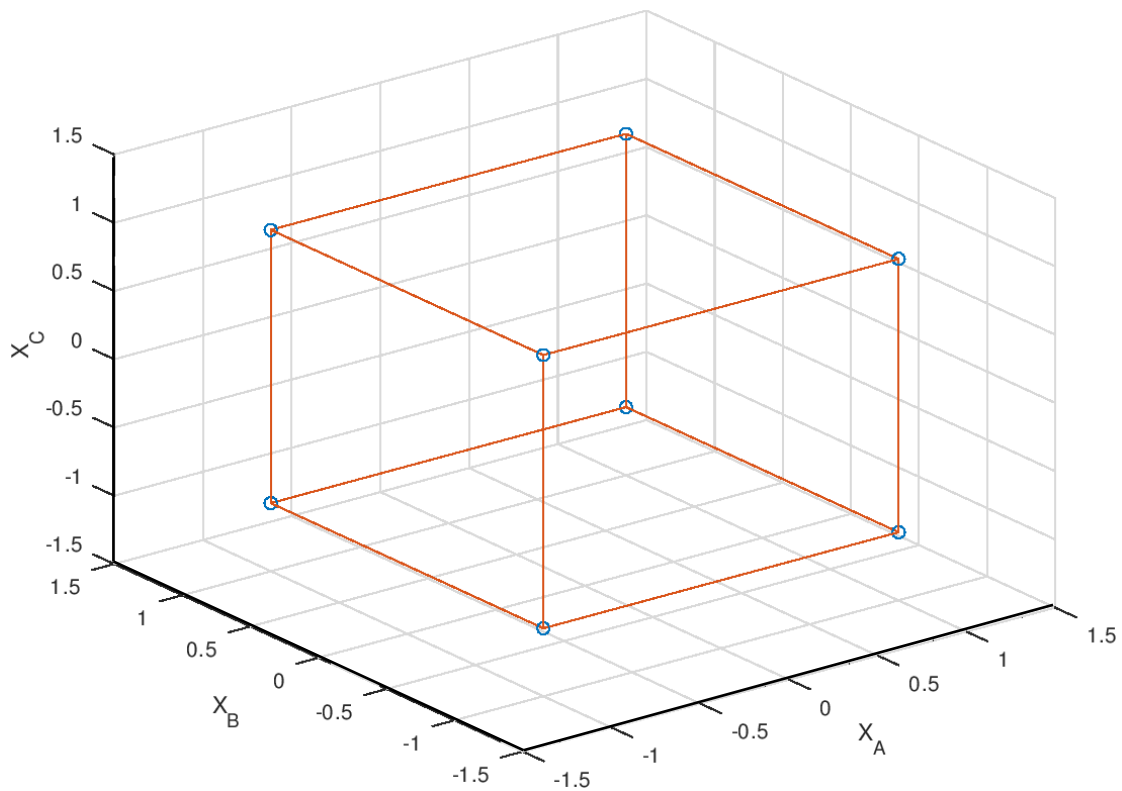
Figure 4.62. Plot of full factorial design for 3 factors – 2 levels model.

4.3.3. 2- and 3-factor short time lifespan models

According to information presented in chapter 3, three factors were selected as they show the most significant impact on the insulation lifespan of inverter-fed low voltage machines. Those factors are: the voltage level, the switching frequency and the operating temperature.

Those models are called 'short-time', as they are defined for relatively high stress levels, typically far bigger than the nominal stress of the electrical insulation system of low voltage motors. As a result the measured lifespan are quite short. Such short lifespans enable to perform multiple tests needed for the model construction in a relatively short time, thus significantly reducing the experimental cost.

The stress levels were chosen so that the lifespan of all experimental points are in the order of a few tens of minutes to few hours. Thanks to that, the end-of-life time is measured with enough precision for high stress levels (as presented in chapter 2 the aging time is measured with the precision of 1s), while the tests for low stress levels are not excessively long.

Those short-time models are the basis for the extrapolation hypothesis, explained in detail in section 4.4.

Each experimental point consisted in eight samples tested simultaneously under the same constraints in order to be able to perform a statistical analysis of the experimental data.

4.3.3.1. *Sample details*

As discussed in chapter 1, the electrical insulation system of low voltage inverter-fed machines is primarily endangered in turn-to-turn. As explained in chapter 3, the choice of sample geometry can have significant effect on the quality of the DoE model. All lifespan test presented in this chapter were performed on twisted pairs prepared according to the improved manufacturing protocol (see chapter 3). They are simple, cheap and easily repeatable models of winding, widely used in accelerated aging tests.

In order to be able to obtain both short- and long-term results (see section 4.4) it was not possible to use standard magnet wires. Indeed, for standard wires in a partial discharge regime, the lifespan does not exceed few hours. However, the wires covered with enamel with inorganic nano-fillers, called 'corona-resistant' (see chapter 1), can sustain a partial discharges activity up to 1000 times longer than the standard ones. Thus, for this campaign of measurements, a corona resistant wire was chosen. All information concerning the used magnet wore are presented in Table 4.21.

_____

Table 4.21. Properties of tested magnet wire

Parameter	Value
Conductor material	Copper
Conductor diameter	1.12 mm
Conductor diameter tolerance	0.011 mm
Enamel grade	2
Outer diameter of enameled wire	Min. 1.185 mm Max. 1.217 mm
Enamel material	PEI (THEIC) (basecoat) PAI (overcoat)
Thermal class	200°C

4.3.3.2. Short time lifespan models- experimental data

4.3.3.2.1. 2- factor DoE model

For this DoE model two factors, voltage level and switching frequency, were chosen to build the full factorial design. As shown in chapter 3 the temperature can strongly influence the lifespan results. In order to stabilize it all the tests were performed inside a climate chamber. Strong ventilation enabled to minimize the effect of local overheating during a partial discharges activity, as mentioned in chapter 3.

The experimental conditions for the DoE tests are presented in Table 4.22. The chosen parameters allowed to keep the experiments short, yet still providing the necessary interval between the results achieved for the different tests in the DoE matrix.

Table 4.22. Test conditions for 2 factors model

Parameter	Minimum level (-1)	Maximum level (+1)
Voltage amplitude [kV]	2.00 (±0.01)	2.25 (±0.01)
Frequency [kHz]	5.00 (±0.0001)	10.00 (±0.0001)

*The duty cycle was set to 50% (±0.5%)
** The temperature was set to 30ºC (±0.1ºC)

As shown in the theoretical introduction (see section 4.3.2), the 2 factor model can be developed as:

$$Y = \log(L) = M + E_V X_V + E_f X_f + I_{Vf} X_V X_f \qquad (4.12)$$

As discussed, the voltage and frequency cannot be included directly in the model, but only using their dimensionless levels normalized to [-1,+1] range: X_V for the voltage amplitude and X_f for the switching frequency. As already explained in section 4.3.2, the relation between the system response and factor levels must be linearized. As already shown in chapter 3, for both voltage and frequency levels the relation between the lifespan and their influence is linear in a log-log scale. Hence voltage and frequency levels X_V and X_f can be calculated as shown in equations (4.13) and (4.14) respectively:

$$X_V = \frac{2}{\log\left(\frac{V_{max}}{V_{min}}\right)} \cdot \log(V) + \left(1 - \frac{2\log(V_{max})}{\log\left(\frac{V_{max}}{V_{min}}\right)}\right) \qquad (4.13)$$

where:

V is the voltage amplitude in volts

V_{max} and V_{min} are, respectively, the maximum and minimum voltage levels (in volts) as shown in Table 4.22

$$X_f = \frac{2}{\log\left(\frac{f_{max}}{f_{min}}\right)} \cdot \log(f) + \left(1 - \frac{2\log(f_{max})}{\log\left(\frac{f_{max}}{f_{min}}\right)}\right) \qquad (4.14)$$

where:

f is the frequency in Hertz

f_{max} and f_{min} are, respectively, the maximum and minimum frequencies (in Hertz) as shown in Table 4.22

As explained in section 4.3.2, 4 tests, performed at the vertexes of the square of the full factorial design, are needed in order to find the coefficient vector E. Table 4.23 presents the results of those experiments. Each experimental value consisted of 8 samples tested simultaneously. The Weibull analysis was applied to the 4 tests, according to instructions in chapter 2. The characteristic value α, expressed in minutes, was taken into consideration while constructing the model and calculating the model coefficients.

_____

Table 4.23. Experimental results for 2-factor DoE model

No.	Voltage level X_V [-]	Frequency level X_f [-]	Lifespan – characteristic value α [min]	System response $Y_i = \lg(\alpha)$ [lg(min)]
1	-1	-1	435.0	2.64
2	-1	1	300.1	2.48
3	1	-1	180.1	2.26
4	1	1	122.4	2.09

The values of the coefficients denoting the influence of each factor were calculated according to equation (4.9). Figure 4.63 shows the values of the 4 coefficients for this model
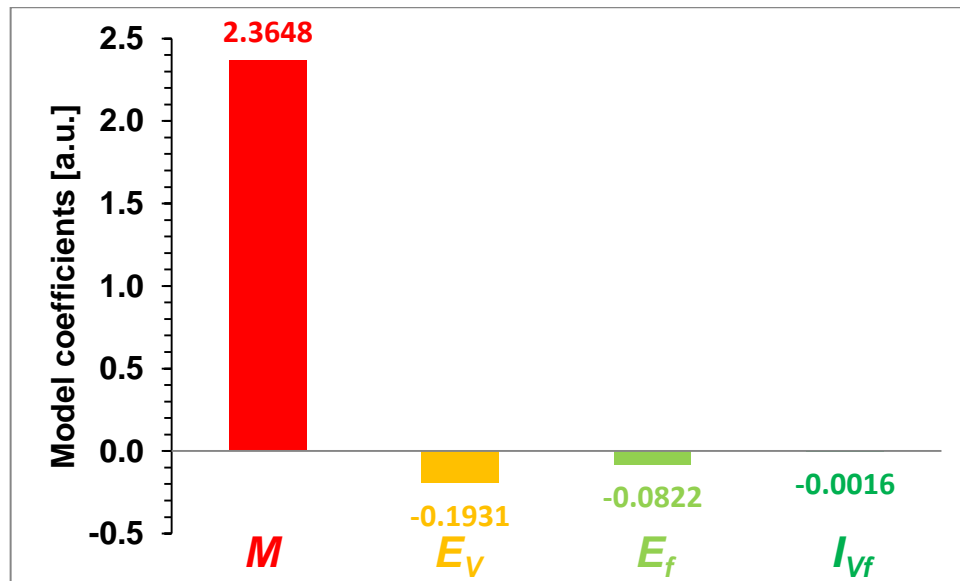
Figure 4.63. The coefficients denoting the influence of voltage amplitude (E_V), frequency (E_f) and their interaction (I_{Vf}). M denotes the average lifespan (logarithmic scale).

The results presented in Figure 4.63 show that in the chosen range of both voltage and frequency, the influence of the voltage amplitude is more than twice as important as the influence of frequency. The interaction between the voltage and frequency has secondary influence, even negligible.

_____

4.3.3.2.2. 3- factor DoE model

For this DoE model all three factors mentioned before, i.e.: voltage level, switching frequency and temperature, were chosen to build the full factorial design. Same as for 2-factor DoE model, all tests were performed in a ventilated climate chamber in order to minimize the effect of local overheating during partial discharge activity (see chapter 3).

The experimental conditions for the tests for the DoE are presented in Table 4.22. Same as for the previous model, the test parameters are chosen to keep the experiments reasonably short, while assuring the necessary distance between the results achieved for the different tests in the DoE matrix is maintained.

Table 4.24. Test conditions for 3 factors model

Parameter	Minimum level (-1)	Maximum level (+1)
Voltage amplitude [kV]	2.00 (±0.01)	2.25 (±0.01)
Frequency [kHz]	5.00 (±0.0001)	10.00 (±0.0001)
Temperature [ºC]	30.0 (±0.1)	100.0 (±0.1)

*The duty cycle was set to 50% (±0.5%)

According to section 4.3.2 the 3-factor model can be developed as:

$$Y = M + E_V X_V + E_f X_f + E_T X_T + I_{Vf} X_V X_f + I_{VT} X_V X_T + I_{fT} X_f X_T + I_{VfT} X_V X_f X_T \qquad (4.15)$$

As defined in section 4.3.3.2.1 in equations (4.9) and (4.10), the dimensionless stress levels X_V and X_f, normalized to [-1,+1] range stand for voltage and frequency respectively. As shown in chapter 3, the relation between the lifespan and (absolute) temperature is most often described by an Arrhenius law and thus can be linearized in $\log(L)$-reciprocal(T) scale. By normalizing this law to [-1,+1] range, one achieve the temperature level as shown in equation (4.16):

$$X_T = \frac{2 \cdot T_{max} \cdot T_{min}}{T_{min} - T_{max}} \cdot \frac{1}{T} + \left(1 - \frac{2 \cdot T_{min}}{T_{min} - T_{max}}\right) \tag{4.16}$$

where:

T is the absolute temperature in Kelvin

T_{max} and T_{min} are, respectively, the maximum and minimum absolute temperatures (in Kelvin) as shown in Table 4.24.

In order to find the coefficient vector, $2^3 = 8$ tests performed at the vertexes of the cube of the full factorial design are needed. Table 4.25 presents the results of those experiments. As for the 2-factor model, each experimental point consisted of 8 samples tested simultaneously and Weibull characteristic values α (see chapter 2), expressed in minutes, were taken into consideration while constructing the model and calculating the factor coefficients.

Table 4.25. Experimental results for 3-factor DoE model

No.	Voltage level X_V [-]	Frequency level X_f [-]	Frequency level X_T [-]	Lifespan – characteristic value α [min]	System response $Y_i = log(α)$ [log(min)]
1	-1	-1	-1	434.9	2.64
2	-1	-1	1	197.3	2.29
3	-1	1	-1	300.1	2.48
4	-1	1	1	142.8	2.16
5	1	-1	-1	180.1	2.26
6	1	-1	1	78.5	1.90
7	1	1	-1	122.4	2.09
8	1	1	1	52.2	1.72

The values of the coefficients denoting the influence of each factor were calculated according to equation (4.11). Figure 4.64 shows the values of all the eight coefficients for this model.
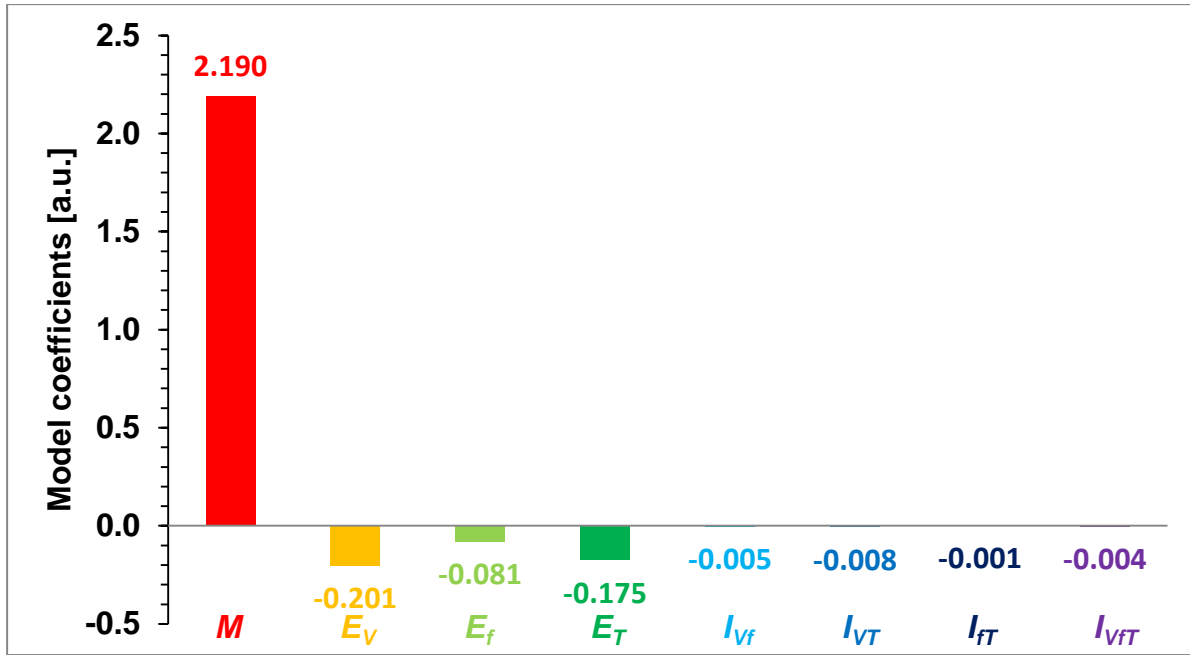
Figure 4.64. The coefficients denoting the influence of voltage amplitude (E_V), frequency (E_f), temperature (E_T) and their second and third order interaction (I). M denotes the average lifespan (logarithmic scale).

The results presented in Figure 4.64 show that in the chosen range of stress level, the influences of the voltage amplitude and temperature are the most important. The effect of frequency of the lifespan is about 2 times less important than those of the 2 factors.

The influence of the interactions is once again significantly smaller than these of the individual factor effects. The most important among the interactions is the one of voltage and temperature, which are the most influential factors. The heritage assumption is then verified. Anyway, in these lifespan models, those interactions would have secondary influence in comparison to "individual" effects of voltage, temperature and frequency.

4.4. Lifespan prediction

4.4.1. Model extrapolation

A standard DoE model is valid for the factor levels between the minimum and maximum chosen for its construction. This mean that, for each stress factor, the corresponding *Xi* level should be always within the range of [-1, 1].

If we were to cover the whole range of operating conditions within one factorial design, the tests for very low stress levels would be far too time and energy consuming and costly, while those for very high stress level might be too short to give reliable results. As it is necessary to control the stress parameter levels as precisely as possible, otherwise all the model experimental points would not be reliable, it might be necessary to use different test equipment for different tests thus adding additional source of results dispersion.

Short-time DoE models, as already presented in section 4.3.3.2.1 and 4.3.3.2.2, provide quick and reliable information about the lifespans for stress levels within the range of [-1, 1]. In this work we wanted to verify whether those short-time models can be used for predicting the lifespan of much longer tests. For this reason short-time models need to be extrapolated. The model extrapolation consists in choosing any stress level out of this natural range of [-1, 1]. In our case, the model is contracted for relatively high stress levels in order to assure that the needed experiments are as short as possible. It is particularly interesting to extrapolate the model towards longer lifespan. As a result the chosen factor levels will be smaller than the model's minimum "-1". Naturally, it is true only for factors, which when increased, decreases the system response, but this is the case for all three factors (voltage amplitude, frequency and temperature) studied here.

Naturally this approach must be limited to the reasonable range of stress levels. The aging mechanism must be at least similar for both short- and long-time results. As explained in chapter 3 some lifespan models (e.g. [109] [135] [148]) postulate the existence of a threshold level, below which no aging takes place. This effect can be totally neglected if we are far enough from this threshold, but if we operate close to it the DoE method might not be well adapted in such a case.

In the particular case of the voltage amplitude, the PDIV level for example can be considered as a threshold. On the other hand there are very few studies describing the influence of voltage without partial discharges activity on the lifespan of insulation systems. However, we know for sure that the aging mechanism with and without partial discharges is not the same, thus the PDIV level creates the natural barrier for model extrapolation.

Similarly for thermal aging, test performed at very high temperature levels will induce different aging mechanisms and activate different reactions than those performed at lower temperatures. The study [109] postulates the threshold at the room temperature level[7,8], however in case of electric machines, temperature rises quickly during operation, thus usually tests are achieved quite far from this threshold.

We can also apply simple mathematical consideration. In case of all the factors studied here we can assume that an increase in stress level should always decrease (or at least never increase) the lifespan of the samples.

Firstly, we will analyze the 2-factor model. As stated in section 4.3.3.2.1, it can be presented as shown in the equation (4.12). The partial derivatives of this model are as shown on the equation (4.17):

$$\begin{cases} \dfrac{\partial Y}{\partial X_V} = E_V + I_{Vf} X_f \\ \dfrac{\partial Y}{\partial X_f} = E_f + I_{Vf} X_V \end{cases} \qquad (4.17)$$

For both of these factors, the response of the system Y should decrease when the factor level X_i is increasing (otherwise it would mean that an increased voltage or a higher frequency can prolong the insulation lifespan, which is not the case). Thus both of these partial derivatives should be negative:

$$\begin{cases} \dfrac{\partial Y}{\partial X_V} = E_V + I_{Vf} X_f < 0 \\ \dfrac{\partial Y}{\partial X_f} = E_f + I_{Vf} X_V < 0 \end{cases} \qquad (4.18)$$

---

[7] By 'room temperature' the authors of [12] mean 'the temperature at which electrical tests without thermal aging are normally performed'

[8] It should be noted that the authors of [12] state that at room temperature the thermal aging, although very small, **is** not 0. However the room temperature is very often the lowest test temperature, and the usual distinction between threshold and no-threshold materials comes from the tests at this temperature.

___

As a result we obtain:

$$\begin{cases} I_{Vf}X_f < -E_V \\ I_{Vf}X_V < -E_f \end{cases} \qquad (4.19)$$

By using the coefficients found in section 4.3.3.2.1 we obtain:

$$\begin{cases} X_f > -120.6 \\ X_V > -51.3 \end{cases} \qquad (4.20)$$

Naturally, those results correspond to very low voltage and frequency levels, thus cannot be taken into consideration due to aging mechanism changes, as explained before. On the other hand, they show that the method is mathematically stable for a very wide range of stress levels.

By applying the same technique to a 3-factor model (see equation (4.15)), the partial derivatives are as shown in equation (4.22):

$$\begin{cases} \dfrac{\partial Y}{\partial X_V} = E_V + I_{Vf}X_f + I_{VT}X_T + I_{VfT}X_f X_T < 0 \\[2mm] \dfrac{\partial Y}{\partial X_f} = E_f + I_{Vf}X_V + I_{fT}X_T + I_{VfT}X_V X_T < 0 \\[2mm] \dfrac{\partial Y}{\partial X_T} = E_T + I_{VT}X_V + I_{fT}X_f + I_{VfT}X_V X_f < 0 \end{cases} \qquad (4.22)$$

All those three partial derivatives are function of 2 factors. The mathematical solution of this system does not exist, that is why they were plotted in order to solve this problem numerically.

Figure 4.65 shows the plots of partial derivatives as a function of the other 2 factor levels. If the partial derivative is negative (colored in shades of green or blue), the model extrapolation is mathematically stable. Otherwise, i.e. for positive partial derivative (colored in yellow, red or brown), the extrapolation cannot be used, because it would lead to erroneous predictions. The limit (derivative equal to zero) is marked with thick red dashed line.

As it can be seen on Figure 4.65 the model cannot be extrapolated when one of the factors is significantly below the short-time model minimum, i.e. -1, or while the other factor is significantly higher the maximum (+1).
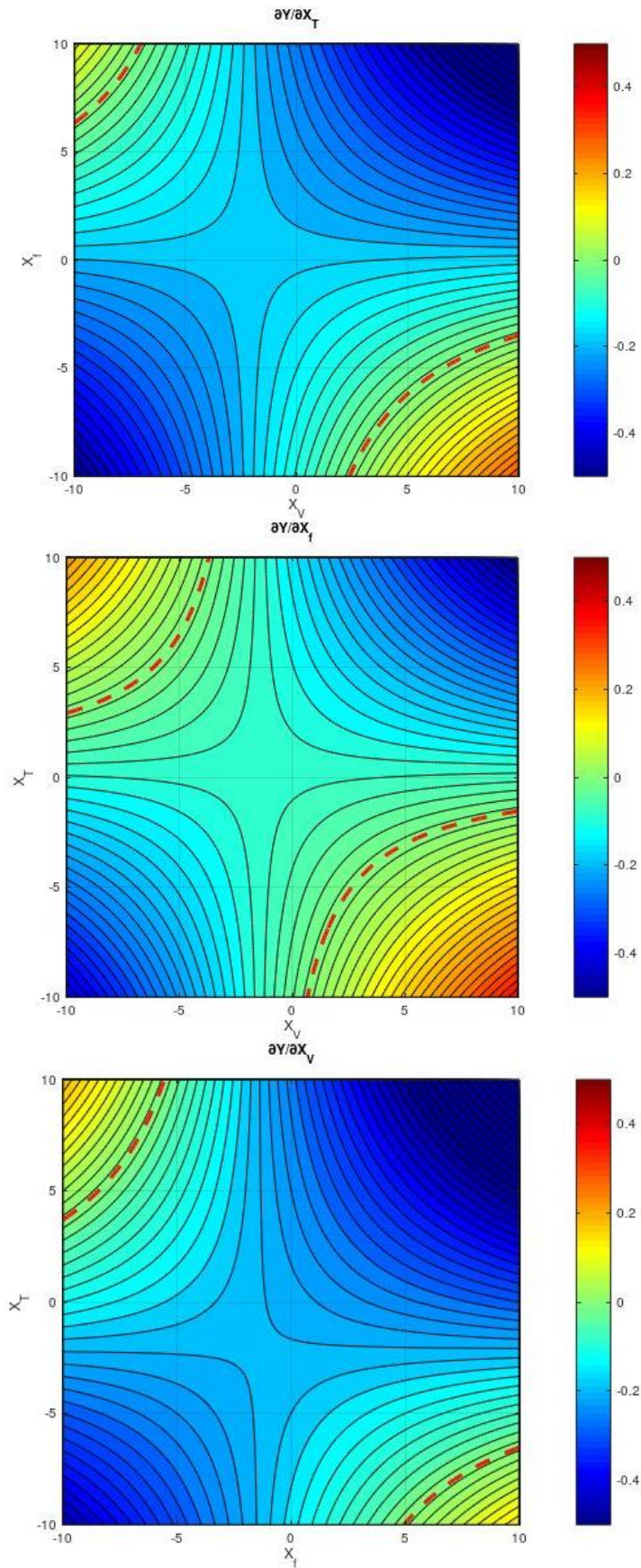
Figure 4.65. Plots of partial derivatives of the 3-factor models. Red dashed line shows the extrapolation stability limit (partial derivative equal to 0).

4.4.2. Prediction of results scatter

All experimental results are affected by measurement uncertainties. The outcome depends on many effects, such as the measurement procedure, the environmental conditions, the sample reproductivity, … Therefore, no measurement is perfectly repeatable or reproducible and the scatter of results is inevitable.

Lifespan measurements can be particularly dispersed due to a very complex aging phenomenon. The results can be influenced by many factors, some relatively easy to control, while others far more difficult, too expensive to precisely control or even not controllable (the microscopic structure of a polymer is messy while the dielectric breakdown is a localized phenomenon). As a result, the results are often strongly dispersed. For very simplified samples, where many technical details can be scrupulously verified, the scatter of results can be reduced. The disadvantage of those samples is that they might not be representative for real objects and the aging and breakdown mechanisms can be completely different from the final product. Generally speaking, the more complex the sample is, the better it represents the final product but usually at a price of higher dispersion. For electrical insulation system faults in motors, one can easily expect as much as ten-to-one difference between the lifespan of samples tested in the identical conditions [6].

Such a high result dispersion can significantly constrict the lifespan modeling and may bias the final conclusions. A standard DoE model enables only to predict the characteristic value (α), but cannot bring any confidence bounds of such prediction.

To enable the scatter prediction for the long-term experiments, it is only possible to base it on the scatter of the short-term results, which were used to obtain the DoE model. The coefficient of variation (CV), called also relative standard deviation (RSD), was chosen for this purpose. It is defined as the ratio of the standard deviation σ to the mean value (in case of normal distribution) or, as used here, to the characteristic value α in case of a Weibull distribution.

$$CV = \frac{\sigma}{\alpha} \tag{4.23}$$

For the Weibull distribution, it can be calculated as shown in equation (4.24):

$$CV = \sqrt{\frac{\Gamma\left(1 + \frac{2}{\beta}\right)}{\Gamma^2\left(1 + \frac{2}{\beta}\right)} - 1} \qquad (4.24)$$

where:

$$\Gamma(n) = \int\limits_{0}^{\infty} e^{-x} x^{n-1} dx$$

β - Weibull shape parameter calculated as presented in chapter 2.

According to the above equation the coefficient of variation is calculated for all the DoE short-time model experimental points. Table 4.26 and Table 4.27 show the values of these coefficients for the 2- and 3-factor models respectively. .

Table 4.26. Coefficients of variation for the 2-factor model

No.	Voltage level	Frequency Level	β [-]	CV [%]
1	-1	-1	8.50	16.4
2	-1	1	3.82	29.4
3	1	-1	5.34	21.7
4	1	1	3.71	30.1

Table 4.27. Coefficients of variation for the 3-factor model

No.	Voltage level	Frequency Level	Temperature level	β [-]	CV [%]
1	-1	-1	-1	8.50	16.4
2	-1	-1	1	2.62	41.0
3	-1	1	-1	3.82	29.4
4	-1	1	1	9.48	12.7
5	1	-1	-1	5.34	21.7
6	1	-1	1	2.58	41.6
7	1	1	-1	3.71	30.1
8	1	1	1	3.28	33.5

The average of all those CVs is then assumed to describe the scatter of long-term results.

$$\overline{CV} = \frac{\sum_{i=1}^{n} CV_i}{n} \tag{4.25}$$

For the 2- and 3-factor models these values are equal to:

$$\overline{CV_{Vf}} = 24.4\%$$
$$\overline{CV_{VfT}} = 28.3\% \tag{4.26}$$

4.4.3. Experimental verification

In order to verify whether the predictions of lifespan made using the short-time DoE model are correct and if the scatter prediction is effective, several long-time experiments were achieved. In those experiments, the level of at least one aging factor, typically voltage amplitude, was significantly lower the natural validity range of DoE model, i.e. [-1, +1]. The other factor in some cases was higher than the +1 maximum in order to accelerate the test. Finally, factor levels were calculated using the equations (4.13) - (4.14).

Table 4.28 shows the experimental points used for this verification (test set).

Table 4.28. Experimental points used to verify the predictions

Test	Voltage amplitude V [kV]	Voltage level X_V [-]	Frequency f [kHz]	Frequency level X_f [-]
A	1.50	-5.88	10.000	1.00
B	1.50	-5.88	5.000	-1.00
C	1.36	-7.55	14.569	2.09
D	1.32	-8.06	12.487	1.64
E	1.09	-11.31	10.752	1.21
F	1.08	-11.46	12.691	1.69
G*	1.10	-11.15	8.914	0.67

*test G was not performed in the climate chamber but in a laboratory oven without the possibility of cooling; due to lack of ventilation, the temperature was not as stable as for the other tests.

All those tests, except the last one (G*), were performed in the climate chamber where the temperature was kept constant at 30°C (±2°C). Thanks to high ventilation, the influence of the local overheating of insulation due to partial discharge activity as well as ozone concentration on the test results was minimized.

The last measurement, noted as G* was on purpose not performed inside the climate chamber but in a laboratory oven without the possibility of cooling by ventilation. It was done so in order to verify whether at this relatively low stress level the temperature will be stable only thanks to heat dissipation losses. No significant increase of average temperature inside the oven was noted due to this test, however the fluctuations of temperature were higher than for climate chamber (±2°C in the oven in comparison to ±0.1 °C in the climate chamber). It is however highly possible that locally, on the sample surface, the temperature was slightly higher. The additional heat generated locally was not high enough to change the temperature inside the oven (as observed and discussed before in chapter 3), but were enough to bias the lifespan results (see Table 4.29).

For each of the experimental points A to G, the predicted lifespan was based only on the short-time 2-factor model extrapolation, as shown in (4.27).

$$Y_{prediction} = M + E_V X_V + E_f X_f + I_{Vf} X_V X_f$$
$$Y_{prediction} = \log(\alpha_{prediction}) \qquad (4.27)$$
$$\boldsymbol{\alpha_{prediction} = 10^{Y_{prediction}}}$$

Following the hypothesis about the constant coefficient of variation (see section 4.4.2), the standard deviation was calculated as (4.28).

$$\sigma = \overline{CV_{Vf}} \cdot \alpha_{prediction}$$
$$(4.28)$$

The calculated standard deviations were used to estimate the scatted of the results for the predicted lifespan values. Upper and lower limits of dispersions, here defined as α + σ and α - σ respectively, were also calculated.

_____

For each experimental point A to H also, the extrapolation factor was presented in order to show how much longer the predicted lifespan is in comparison to the average lifespan of short-time model:

$$\text{extrapolation factor} = \frac{\alpha_{prediction}}{\bar{\alpha}_{short-time}} = \frac{\alpha_{prediction}}{10^M} \tag{4.29}$$

The results are presented in Table 4.29.

Table 4.29. Prediction of the result scatter

Test	Predicted lifespan α [h]	Extrapolation factor [-]	Standard deviation σ [h]	Lower limit of dispersion α − σ [h]	Upper limit of dispersion α + σ [h]
A	44.66	11.6	10.89	33.77	55.56
B	62.48	16.2	15.24	47.24	77.72
C	78.98	20.5	19.26	59.71	98.24
D	106.6	27.6	26.01	80.63	132.7
E	492.5	127.6	120.2	372.3	612.7
F	492.5	127.6	120.2	372.3	612.7
G*	497.7	128.9	121.5	376.3	619.2

Finally, the results predicted by the model were compared with the experimental ones.

For all the seven experimental points A-G, the long-time aging tests were performed. In each test, up to eight samples were tested at the same time. All those results were then presented on Figure 4.66 as a scatter plot. Axis of abscissa represents the modeled lifespan (from the learning set), thus the one calculated in Table 4.29, while axis of ordinates shows the measured lifespan, thus the experimental data from the long-time measurements (test set). The diagonal, marked in red, shows the DoE model line. The dash line below and above it are the lower and upper limits of the predicted dispersion of results, based on the hypothesis explained in section 4.4.2. The experimental points used for the DoE model construction are marked in blue in the left

bottom corner of the graph. These points show how far are the long-time measurements from the short-time experiments which have been used to create the DoE model.
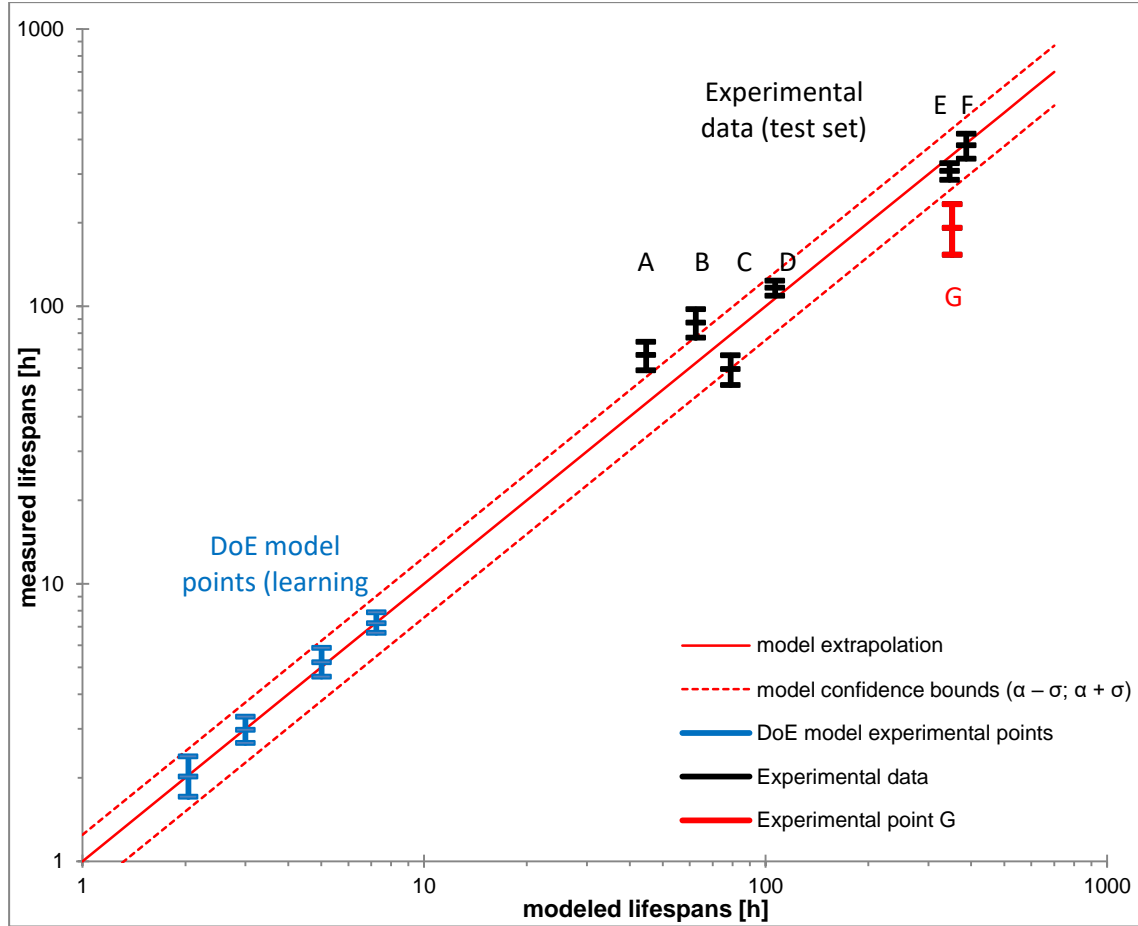
Figure 4.66. The comparison between the model predictions and the real experimental data.

The obtained results show that the proposed method is a very efficient tool for predicting much longer lifespan. The maximum relative error is 33% (excluding series G), which is similar the results obtained is some much more short-term studies [143] [113]. Taking into consideration that the analyzed stress levels are far from the range used to construct the model, with the extrapolation factor even **higher than 100** for the longest tests, the accuracy of the outcome is even more impressive.

The suggested methodology of including the scatter of the results has proven to be effective. The spans of the dispersion intervals of the test sets are close to the ones predicted by the model. Naturally not all the experimental points are included in the

predicted triangle of dispersion, but always some experimental points are within this zone (excluding series G).

In case of the G series, the error of prediction is visibly more important. All the experimental points had the lifespans shorter than model predictions, and none of them were in the zone predicted by the scatter analysis. As for this series the experiment was not conducted inside the climate chamber but in a laboratory oven, the temperature of enamel might have been locally slightly higher due to absence of ventilation. This temperature rise, undetectable at the scale of the oven (temperature sensor measures the average temperature inside the oven), might have been the cause of the lifespan shortening. These results show that even in the case of such a long test (predicted lifespan >400h) the temperature must be rigorously kept constant in order to assure the reliable results of accelerated aging tests.

In conclusion, the Design of Experiments (DoE) method proved to be effective even for the extrapolation of the model far from its initial range of validity. This shows that, based only on short-time results, it is possible to effectively predict both the lifespan value and scatter of results for the lifespans, tens of times longer than the duration of the needed experiments. This obviously means that the method is not only time- but also money-saving. The extrapolation permits also to approach much closer the nominal conditions of the machines exploitation.

This work was published during IAS Annual Meeting in Cincinnati (2017) [149].

4.5. Design of experiments as a comparative tool

In the previous chapter, we have already shown how effective the DoE method can be for preparing lifespan models but it can also be an efficient method of predicting the long-time results based only on short-time tests. As explained before, this methodology can significantly reduce the length and cost of experimental campaigns.

The prediction of the lifespan is only one of the concerns in the field of electrical insulation system of rotating machines. In this highly competitive market, the machine primary products, such as magnet wires, insulating papers or varnishes are constantly modified and improved. Naturally the price of each of these components changes also, it influences thereby the final price of the machine.

The design of the machine electrical insulation system is often based on the already existing solutions, only with some modifications, such as different magnet wire or different thickness of the insulating papers. As a product from the same manufacturer can differ from one batch to another, this will influence the final reliability of the machine. Regular quality control of those primary products is thus essential.

As stated before, it is not possible to test the machine in its nominal conditions each time any of its components changes. Such tests would be far too long and energy consuming. Therefore we need a quick and reliable comparative test in order to assure that the applied changes are for the better, not for worse.

This subchapter shows how the DoE methodology presented in the previous sections of this chapter can be implemented as an effective comparative tool between different materials.

4.5.1. Comparison of the short-time model coefficients

In order to be able to compare magnet wires of different lifespans, we have chosen three enameled wires (A-C) from the same thermal class, having the same enamel polymer but of three different diameters. The wire having the smallest diameter has the thinnest enamel which is supposed to be degraded faster than for wires with higher diameters. Hence, in given test conditions, the average lifespan of wire A (with thickest enamel) should be higher than this of B, and wire C (with thinnest enamel) should have the lowest lifespan.

_____

Table 4.30 presents the detailed information concerning the magnet wires used in these experiments.

Table 4.30. Properties of tested magnet wires

Parameter	Magnet wire		
	A	B	C
Conductor material	Copper		
Conductor diameter	1.12 mm	0.8 mm	0.5 mm
Conductor diameter tolerance	0.011 mm	0.008 mm	0.005 mm
Enamel grade	2		
Outer diameter of enameled wire	Min. 1.185 mm Max. 1.217 mm	Min. 0.856 mm Max. 0.884 mm	Min. 0.545 mm Max. 0.566 mm
Enamel material	PEI (THEIC) (basecoat) PAI (overcoat)		
Thermal class	200°C		

These sets of samples simulate three wires from different manufacturers but we know 'a priori' how their performances are ranked.

Same as for the other tests in this chapter, all experiments were performed on twisted pairs. As the wire diameter changes for wires A to C, the number of twists and mechanical load during twisted pair manufacturing were modified as well, according to standard [100]. See chapter 3 for more information.

We will use three separate short-time DoE models – each for one wire type. Two stress factors were used: voltage amplitude and frequency, same as already presented in section 4.3.3.2.1. The model equation was already presented in (4.8), while dimensionless and normalized stress level X_V and X_f can be calculated according to equations (4.9) and (4.10) respectively.

In order to calculate the coefficient vector one need to solve the matrix equation (4.2). For each magnet wire (A-C) the lifespan was experimentally measured for four

_____

experimental points at the vertexes of the factorial design square. Table 4.31 shows the conditions for these four tests.

Table 4.31. Test conditions for 2-factor models used for comparison of wires A to C

Parameter	Minimum level (-1)	Maximum level (+1)
Voltage amplitude [kV]	2.00 (±0.01)	2.25 (±0.01)
Frequency [kHz]	5.00 (±0.0001)	10.00 (±0.0001)

*The duty cycle was set to 50% (±0.5%)
** The temperature was set to 30ºC (±0.1ºC)

Table 4.32 presents the measured lifespan for all the three magnet wires and corresponding system responses.

Table 4.32. Test results for short-time DoE models for wires A to C

No.	Voltage level X_V [-]	Frequency level X_f [-]	Lifespan – characteristic value Wire A	Wire B α [min]	Wire C	System response Wire A	Wire B Y_i [-]	Wire C
1	-1	-1	435.0	201.1	196.7	2.638	2.303	2.294
2	-1	1	300.1	164.9	57.5	2.477	2.217	1.760
3	1	-1	180.1	66.8	61.2	2.256	1.825	1.787
4	1	1	122.4	61.2	18.3	2.088	1.787	1.262

Figure 4.67 presents the values of coefficients denoting the influence of each factor for all the three magnet wires.
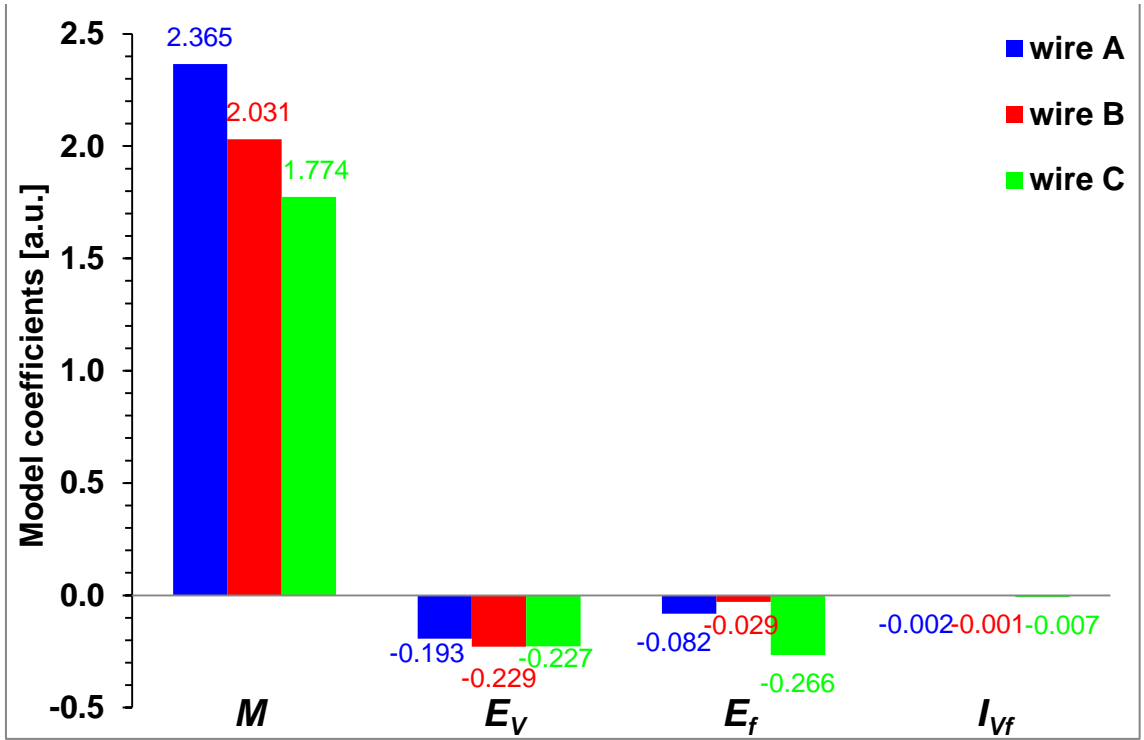
Figure 4.67. The coefficients for the three tested wires A to C denoting the influence of voltage amplitude (E_V), frequency (E_f) and their interaction (I_{Vf}). M denotes the average lifespan (logarithmic scale).

For wire A the influence of the voltage is more than twice as important as this of the frequency. This ratio is even more biased in favor of voltage for wire B. For the last tested wire, C, the influence of voltage and frequency are comparable, slightly higher for frequency. As seen before in section 4.3.3.2.1 the interaction between the voltage and frequency has almost negligible effect in comparison to single factors.

As predicted before, the mean system response M for magnet wire A (with the thickest enamel) was the highest, hence the mean lifespan $L_0=10^M$ [min] was the longest. Accordingly, for wire C (with the thinnest enamel) this mean lifespan was the shortest of the three tested wires.

In conclusion, according to those short-time models the wire A should withstand longer than wire B, while wire C would be the weakest of those three tested samples.

4.5.2. Scatter prediction

Using the same methodology as presented in section 4.4.2 we want to be able to predict the scatter of result for long-time predictions based only on the dispersion of short-time measurement.

_____

For each four experimental points of the three DoE models A to C, the Weibull shape parameter β (see chapter 2) and the coefficient of variation CV (see section 4.4.2) are calculated.

The same hypothesis was made in order to predict the long-time scatter of results: the coefficient of variation for all the predictions is constant and equal to the average coefficient of variation, calculated as a mean value of all 4 CVs from DoE model.

Table 4.33 presents the β and corresponding CV for each magnet wire A to C for the 4 points of DoE model. The average coefficient of variation is presented in the bottom line of this table.

Table 4.33. Coefficients of variations for magnet wires A to C

No.	Voltage level	Frequency level	Magnet wire					
			A		B		C	
			β [-]	CV [%]	β [-]	CV [%]	β [-]	CV [%]
1	-1	-1	8.50	16.4	4.26	26.50	2.24	47.21
2	-1	1	3.82	29.4	20.23	6.13	4.99	22.95
3	1	-1	5.34	21.7	3.65	30.47	10.14	11.87
4	1	1	3.71	30.1	11.18	10.83	7.17	16.43
Average coefficient of variation				24.4		18.48		24.62

4.5.3. Extrapolation towards long-time results

As shown in section 4.4, those short-time models calculated in the beginning of this paragraph can be extrapolated towards much longer lifespans.

One point was chosen to compare the DoE models predictions for all the 3 wires with experimental values. The test voltage was randomly chosen and fixed at 1.32 ($\pm$0.01) kV (peak-to-peak voltage 2.64 kV), which was significantly lower than any voltage amplitude used in the DoE tests. The corresponding voltage factor, calculated according to (4.13) was equal to -8.06, thus largely exceeds the natural validity range of DoE of [-1, 1]. The frequency was fixed at 12.487 ($\pm$0.001) kHz (the corresponding level, according to (4.14), was equal to $X_f = 1.64$). It was also outside the range of [-1, 1], this time slightly higher to accelerate the aging rate.

_____

As already stated in paragraph 4.4.2, standard deviation can be predicted by assuming that the coefficient of variation is constant and equal to its average value, calculated in Table 4.33 from the learning set.

The calculated standard deviations were used to estimate the scatted of the results for the predicted lifespan values. The results are presented in Table 4.34.

Table 4.34. Model predictions for $V = 1.32$kV and $f = 12.487$ kHz with dispersion prediction

Magnet wire	Predicted lifespan α [h]	Standard deviation σ [h]	Lower limit of dispersion $\alpha - \sigma$ [h]	Upper limit of dispersion $\alpha + \sigma$ [h]
A	106.6	26.01	80.63	132.7
B	73.51	13.58	59.92	87.09
C	29.60	7.22	22.38	36.82

Those predictions presented in Table 4.34 were confronted to the experimental values obtained for those conditions ($V = 1.32$ kV; $f = 12.487$ kHz). Finally, the results predicted by the model were compared with the experimental ones.

Figure 4.68 shows the experimental results for the 3 magnet wires A to C tested in the above-mentioned test conditions. They are presented as scatter points. Confidence intervals are presented as a line where bottom bar denotes $\alpha - \sigma$, upper $\alpha + \sigma$ and middle one characteristic lifespan α. The predicted intervals, presented in Table 4.34, are shown in blue and intervals for experimental points, calculated according to chapter 2 (Weibull α parameter) and (4.24) respectively are shown in red.
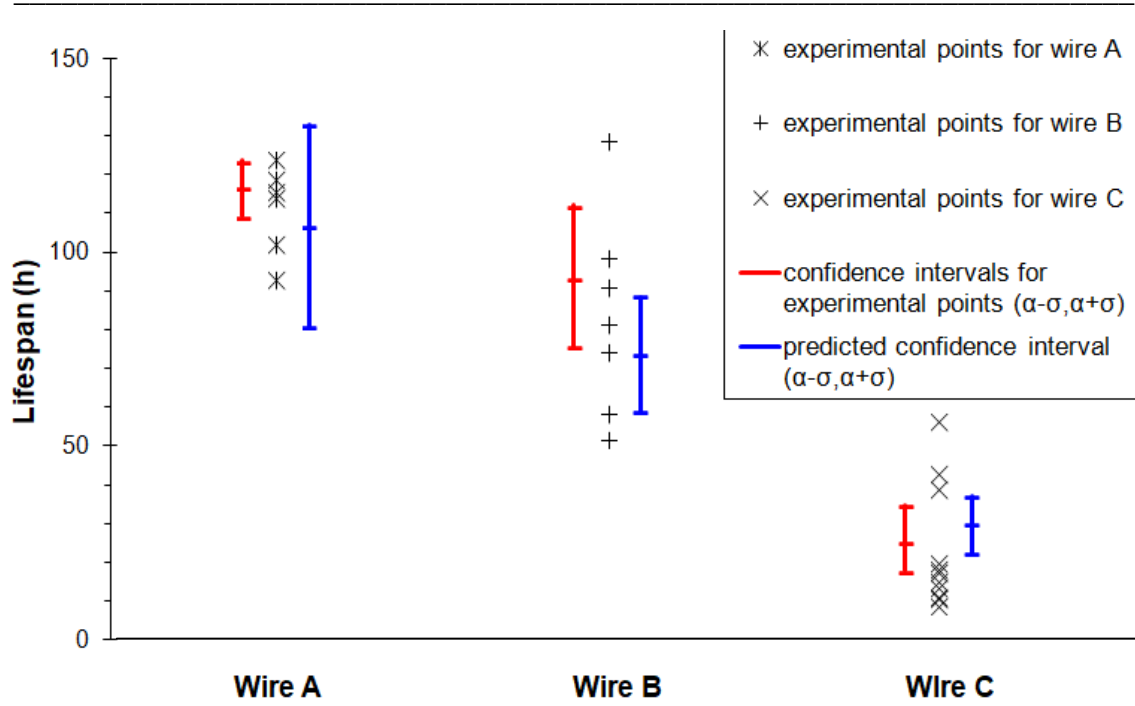
Figure 4.68. Comparison between the model predictions and the real experimental data for wires A-C at given stress level ($V = 1.32$ kV; $f = 12.487$ kHz).

As presented in Figure 4.68, the predicted model intervals always intersect with the experimental data. The sorting, established from the short-time DoE model (see section 4.5.1), where wire A has longer lifespan than wire B, and wire C being the "weakest" one, is confirmed for much longer lifespans.

If we take into consideration the whole confidence interval and not just the characteristic lifespans α, we can see that according to model prediction, wire A should present higher lifespans than B, but as there is an overlap between their corresponding confidence intervals the difference is not, statistically speaking, sufficient to always prefer wire A to B. Experimental points and their confidence intervals confirm this prediction: although characteristic lifespan α for wire A is higher than for wire B, some samples of wire B outperformed some wire A samples. The difference between A and B is thus statistically not significant enough. On the other hand if we compare wire A and C the difference is clear, as "weakest" samples of wire A have still longer lifespan than "strongest" ones of wire C. Accordingly, between wire B and C, only one sample of C reached the lifespan of "weakest" wire B samples. As both predicted and experimental confidence intervals are separate (no overlap) the difference between B and C is statistically significant.

_____

This work was published during IAS Annual Meeting in Portland (2018) [150].

4.6. Conclusion

The chapter presented the Design of Experiments as a very efficient tool for lifespan modeling.

As already shown in several publications on this topic, the DoE proved its usefulness in the field of modeling accelerated aging of different insulating materials. However, up to now, almost only short-time models were presented for which the stress levels have been significantly higher than those that might be seen by the insulation system during normal operating conditions in order to accelerate the test.

The results presented in this chapter show that DoE models can be successfully extrapolated towards much lower stress levels and that they give satisfyingly accurate predictions of much longer test results. Thanks to the original methodology proposed for the scatter of short-time results, the DoE model extrapolation was enriched with the prediction of the dispersion of long-time results. The predicted lifespans correspond well with the experimental data, especially if we take into consideration that the short DoE tests were in average up to 100 times shorter than the predictions.

Finally, the DoE short-time models can be used as a comparative tool for different products available on the market. Thanks to the proposed methodology it was possible to classify the products regarding their lifespan, from the best to the worst, using only a quick test campaign. This classification was confirmed by long-time predictions and correlated well with the experimentally obtain results for those points.

GENERAL CONCLUSION AND PERSPECTIVES

The problem of partial discharges in low-voltage machines is a burning issue for electrical insulation system designers. PWM voltage pulses cause significant overvoltages at the motor terminals, which could greatly exceed the rated values. As a result, partial discharges may occur, leading to fast degradation of the insulating properties, especially problematic for type I low-voltage machines. New inverters, based on wide band gap components, such as SiC or GaN, will even further increase the impulses steepness, thus rising the electric stress seen by the electrical insulation system. The existing solutions allowing to limit such a risk, such as dV/dt filters are not widely used due to their cost and weight. At the same time, the current standard requirements allow some PD activity, if the probability of their appearance is sufficiently low (<50%), as they use the classifying criteria based on the RPDIV (Repetitive Partial Discharge Inception Voltage) not the PDIV. Thus the aging process of the insulating materials in the presence of PD activity need to be studied.

One of the main problems with the choice of a suitable insulating material for each part of the insulation system is that two materials having similar initial characteristics can behave completely differently during the machine functioning. Even though the materials are compliant with the applicable standards requirements, this cannot guarantee their good quality in the final product during aging. For this reason, an appropriate testing method is needed in order to correctly asses the materials during aging and to be able to model their lifespan.

This thesis shows the Design of Experiments as an efficient tool in lifespan modeling. It has proved its usefulness in the field of modeling accelerated aging of different insulating materials, however, up to now, almost only short-time models were presented. For those tests the stress levels have been significantly higher than those that might be seen by the insulation system during normal operating conditions. Such aging tests were quick but not fully representative of the final object. A prediction technique was needed in order to approach the tests to more 'realistic' stress levels.

The results presented in this thesis show that DoE models can be successfully extrapolated toward much lower stress levels and give satisfyingly accurate predictions of much longer test results. Thanks to the methodology proposed the basic DoE model

was enriched with the prediction of the dispersion of long-time results, basing it only on the short-time results scatter. The predicted lifespans correspond well with the experimental data, especially if we take into consideration that the short DoE tests were in average up to 100 times shorter than the predictions. Thanks to this technique it is possible to give more reliable predictions of the insulation lifespan, while still keeping the test campaign time and money effective.

Finally, the presented methodology can be used as a comparative tool for different products available on the market. Thanks to this approach, it is then possible to classify the products from the best to the worst, using only quick test campaign. This classification was confirmed by long-time predictions and correlated well with the experimentally obtain results for those points. Such a comparison is much more reliable than the one based only on the initial material characteristics, as it tests the influence of several aging factors at the same time in the conditions much close to the ones seen by the material in the real machine than those of initial standard tests.

Due to constantly changing requirements and wide range of insulating materials needed to be tested, complementary studies are needed in order to better understand the aging phenomena in low voltage machines exposed to a partial discharges activity and to be able to establish better, more precise lifespan models. The work presented in this thesis could be continued and will be directed towards three main axes:

- Improvement of modeling techniques for other products and materials
  o As presented in this thesis the use of the Design of Experiments (DoE) method can be an effective tool in lifespan modeling as well as its prediction. Further work, in the form of another PhD dissertation, will verify if the methodology can be applied to other than insulating material domains, such as LEDs, OLEDs or fuel cells.
- Further analysis of PD activity in low voltage motors
  o As it was shown in chapter 2, the problem of a partial discharges activity in low voltage machines is far from being well understood. There is still lot of ambiguity of how exactly the PD tests should be performed on such machines, especially in industrial environment.

In the framework of my future work in the Institute of Research and Technology in Toulouse IRT Antoine de Saint Exupéry as part of the 'High Voltage project', the influence of external factors on the PD phenomena will be studied, especially this of temperature, humidity and air pressure. At the same time, the analysis of existing normalized test protocols will be conducted. New protocol, assuring better reproducibility of PD measurements will be developed and after round-robin test campaign suggestions will be presented in the IEC group working on new standards in this domain (especially the IEC60034-27-5).

- Wider range of tested materials
    o The study presented in this thesis was based entirely on the enameled wires and their insulation. Future work will be directed towards wider range of insulating materials in order to be able to study the aging of the insulating systems of low voltage machines as a whole. It will enable to analyze the behavior of each element of insulating system but also the interactions between them. This study will be also conducted in the IRT Antoine de Saint Exupéry as another part of the 'High Voltage project'.

REFERENCES

[1] Hughes A.: Electric Motors and Drives. Fundamentals, Types and Applications, Third edition, Elsevier, 2006.

[2] Fitzgerald A.E., Kingsley Ch. Jr., Umans S. D.: Electric Machinery, Sixth Edition, McGraw-Hill, 2003.

[3] Ronkowski M., Michna M., Kostro G., Kutt F.: Maszyny elektryczne wokół nas. Zastosowanie, budowa, modelowanie, charakterystyki, projektowanie. Wydawnictwo Politechniki Gdańskiej, Gdańsk, 2011.

[4] Kato Engineering Inc.: Engineering Report: Form-Wound Coils, Random-Wound Coils, 2001.

[5] Mihaila V.: Nouvelle conception des bobinages statoriques des machines à courant alternatif pour réduire les effets négatifs des dV/dt, 2011.

[6] Stone G. C., Boulter E. A., Culbert I., Dhirani H.: Electrical Insulation for Rotating Machines. Design, Evaluation, Aging, Testing, and Repair, Wiley, 2004.

[7] Catalog of Suzhou Smart Motor Equipment Manufacturing Co., Ltd.: SC160 Slot Insulation Paper Inserting Machine.

[8] Commercial materials from Elantas Electrical Insulation (http://www.elantas.com/beck-india/products-services/secondary-insulation-si/impregnating-resins.html).

[9] Commercial materials from GMR Electric Motors LTD (http://gmrelectric.com/Services/RewindDepartment.aspx).

[10] Tong W.: Mechanical Design of Electric Motors, CRC Press, Routledge, 2017.

[11] Grubic S., Aller J. M., Lu B., Habetler T. G.: A Survey on Testing and Monitoring Methods for Stator Insulation Systems of Low-Voltage Induction Machines Focusing on Turn Insulation Problems, IEEE Transactions on Industrial Electronics, Vol. 55, pp. 4127-4136, Dec. 2008.

[12] Celiński Z.: Materiałoznawstwo elektrotechniczne, Oficyna Wydawnicza Politechniki Warszawskiej, Warszawa, 2011.

[13] Neelakanta P. S.: Handbook of Electromagnetic Materials: Monolitic and Composite Version and Their Applications, CRC Press, 1995.

[14] IEC 60034-18-41:2014 Rotating electrical machines - Part 18-41: Partial discharge free electrical insulation systems (Type I) used in rotating electrical machines fed from voltage converters - Qualification and quality control tests,

2014.

[15] IEC 60034-18-42:2017 Rotating electrical machines - Part 18-42: Partial discharge resistant electrical insulation systems (Type II) used in rotating electrical machines fed from voltage converters - Qualification tests, 2017.

[16] Anton A., Steinle J. L.: Micas et produits micacés, Techniques de l'ingénieur, 1997.

[17] Bruins P. F.: Plastics for Electrical Insulation, Interscience Publishers, New York, 1968.

[18] Menguy C.: Mesure des caractéristiques des matériaux isolants solides, 1997.

[19] Arora R., Mosch W.: High Voltage and Electrical Insulation Engineering, IEEE Press, 2011.

[20] Dubois J. C.: Propriétés diélectriques des plastiques, Techniques de l'ingénieur, 2001.

[21] Shugg W. T.: Handbook of Electrical and Electronic Insulating Materials, Van Nostrand Reinhold, New York, 1986.

[22] Bureau J. M.: Propriétés diélectriques des polymères, Techniques de l'ingénieur, 2016.

[23] Anton A.: Matériaux isolants solides. Caractéristiques électriques, Techniques de l'ingénieur, 2003.

[24] IEC 60050-212:2010 International Electrotechnical Vocabulary – Part 212: Electrical insulating solids, liquids and gases, 2010.

[25] Dakin T. W.: Electrical Insulation Deterioration Treated as a Chemical Rate Phenomenon, Transactions of the American Institure of Electrical Engineering, vol. 67, pp. 113-18, 1948.

[26] IEC 60085:2007 Electrical insulation - Thermal evaluation and designation, 2007.

[27] IEC 60034-18-31:2012 Rotating electrical machines - Part 18-31: Functional evaluation of insulation systems - Test procedures for form-wound windings - Thermal evaluation and classification of insulation systems used in rotating machines, 2012.

[28] IEC 60216-1:2013 Electrical insulating materials - Thermal endurance properties - Part 1: Ageing procedures and evaluation of test results, 2013.

[29] Ohta S. : Temperature Classes of Electrical Insulators, Three Bond Technical News, December 1985.

[30] Anton A.: Émaux isolants et fils émaillés, Techniques de l'ingénieur, 2009.

[31] Chapman M., Frost N., Bruetsch R.: Insulation Systems for Rotating Low-Voltage Machines, IEEE International Symposium on Electrical Insulation, pp. 257-260, 2008.

[32] IEC 60317-0-1:2013 Specifications for particular types of winding wires - Part 0-1: General requirements - Enameled round copper wire, 2013.

[33] Commercial materials from Elektrisola Dr. Gerd Schildbach GmbH&Co. KG, http://www.elektrisola.com/us/ [access online 08/21/2017].

[34] Beeckman R.: NEMA Magnet Wire Thermal Class Rating. How to Use Then, and How They are Derived, Essex Group Inc.

[35] Pleşa I., Noţingher P. V., Schlögl S., Sumereder C., Muhr M.: Proprieties of Polymer Composites Used in High-Voltage Applications, Polymers 2016, vol. 8, issue 5, 173, 2016.

[36] Bartnikas R., McMahon E. J.: Engineering Dielectrics Volume I: Corona Measurement and Interpretation, American Society for Testing and Materials, Baltimore, 1979.

[37] ASTM D1868-73: Standard Test Method for Detection and Measurement of Partial Discharge (Corona) Pulses in Evaluation of Insulation Systems, 1973.

[38] Townsend J. S., Philosophical Magazine, vol. 1, p. 198, 1900.

[39] Loeb L. B., Meek J. M., The Mechanism of the Electric Spark, Stanford University Press, Stanford, 1941.

[40] Raether H., Electron Avalanches and Breakdown in Gases, Butterworths, London, 1964.

[41] Engelmann, Eberhard: A contribution to the discharge behavior of large electrodes having field distortions in air with positive switching surge, Dissertation, TU Dresden, 1981.

[42] Meek J. M., Craggs J. D.: Electrical Breakdown in Gases, John Wiley & Sons Ltd, 1978.

[43] Paschen F.: "Über die zum Funkenübergang in Luft, Wasserstoff und Kohlensäure bei verschiedenen Drucken erforderliche Potentialdifferenz, Annalen der Physik vol. 273 (5), pp. 69–75, 1889.

[44] Wittenberg H.: Gas tube design in Electron Tube Design, pp. 792-817, RCA Electron Tube Division, 1962.

[45] Sili E.: Etude et caractérisation des décharges partielles et du vieillissement du polyimide en environnement aéronautique, doctoral dissertation, Toulouse, 2012.

[46] IEC 60664-1:2007: Insulation coordination for equipment within low-voltage systems - Part 1: Principles, requirements and tests , 2007.

[47] IEC 60050-411:1996 International Electrotechnical Vocabulary - Chapter 411: Rotating machinery, 1996.

[48] IEC/TS 61934:2011 Electrical insulating materials and systems – Electrical measurements of partial discharges (PD) under short rise time and repetitive voltage impulses, 2011.

[49] IEC 60034-27-5:2017 (Working Draft 4) Rotating electrical machines - Part 27-5: Off-line partial discharge tests on winding insulation of rotating electrical machine during repetitive impulse voltage excitation, 2017.

[50] Wróblewski D.: Falownik bez tajemnic, Magazyn Przemysłowy, 2016.

[51] Rashid M. H. et al.: Power Electronics Handbook, Academic Press, 2001.

[52] Ginot N., Batard C., Lahaye P.: MOSFET et IGBT : circuits de commande, sécurisation et protection du composant à semi-conducteur, Techniques de l'Ingénieur, 2017.

[53] IEC 60050-131:2002 International Electrotechnical Vocabulary - Part 131: Circuit theory, 2002.

[54] Bolkowski S.: Teoria obwodów elektrycznych, Wydawnictwo Naukowo-Techniczne, Warszawa, 2001.

[55] Démoulin B.: Éléments sur la théorie des lignes de transmission, Techniques de l'Ingénieur, 2014.

[56] Persson E.: Transient Effects in Application of PWM Inverters to Induction Motors, IEEE Transactions on Industry Applications, vol. 28, no. 5, 1992.

[57] Neacsu C., Bidan P., Lebey T., Valentin M.: Presentation of a new off line test procedure for low voltage rotating machines fed by Adjustable Speed Drives (ASD), VIII IEEE International Power Electrics Congress CIEP 2002. Technical proceedings, 2002.

[58] Fabiani D.: Accelerated degradation of AC-Motor winding insulation due to voltage waveforms generated by adjustable speed drives, Ph.D. Thesis, University of Bologna, 2003.

[59] Taghia B., Cougo B., Piquet H., Malec D., Belinger A., Carayon J.-P.: Advanced Analysis of Transient Overvoltage in Electromechanical Chain Fed by SiC

Inverter, Electrimacs, 2017.

[60] Bidan P., Lebey T, Neacsu C.: Development of a New Off-line Test Procedure for Low Voltage Rotating Machines Fed by Adjustable Speed Drives (ASD), IEEE Transactions on Dielectrics and Electrical Insulation, vol. 10, no. 1, 2003.

[61] Stone G. C., Culbert I., Boulter E. A., Dhirani H.: Electrical Insulation for Rotating Machines. Design, Evaluation, Aging, Testing, and Repair, 2nd Edition, Wiley-IEEE Press, 2014.

[62] Moore B. J., Rehder R. H., Draper R. E.: Utilizing Reduced Build Concepts in the Development of Insulation Systems for Large Motors, Proceedings of IEEE Electrical Insulation Conference, CIncinnati, pp. 247-252, 1999.

[63] Recchioni M., Ardente F., Mathieux F.: Environmental Footprint and Material Efficiency Support for Product Policy, JRC Technical Report, 2016.

[64] Vassilious P., Mettas A., Understanding accelerated life-testing analysis, 2003 Annual Reliability and Maintainability Symposium, 2003.

[65] Escobar L. A., Meeker W. Q.: A review of accelerated test models, Statistical Science, vol. 21, no 2, pp. 552-577, 2006.

[66] ReliaSoft Corporation: Accelerated Life Testing Reference, Tucson, 2017.

[67] IEC 60505:2011, Evaluation and Qualification of Electrical Insulation Systems, 2011.

[68] Salameh F.: Méthodes de modélisation statistique de la durée de vie des composants en génie électrique, PhD Thesis, Toulouse, 2016.

[69] Commercial materials from Technix HV: DC High Voltage Generators SR Series, 2017.

[70] Commercial materials from DEI Scientific (now part of Litllefuse group), 2017.

[71] IEEE Standard 1434-2000 (R2005) Guide to the Measurement of Partial Discharges in Rotating Machinery, April 2000.

[72] Kreuger F. H.: Partial discharge detection in high voltage equipment, Butterworth-Heinemann Ltd, 1989.

[73] Giussani R., Cotton I., Sloan R.: Detection of corona with RF methods and spectra analysis, 2012 IEEE International Symposium on Electrical Insulation (ISEI), 2012.

[74] IEEE Std 286-2000: IEEE Recommended Practice for Measurement of Power Factor Tip-Up of Electric Machinery Stator Coil Insulation, 2000.

_____

[75] ASTM D3382 - 95: Standard Test Methods for Measurement of Energy and Integrated Charge Transfer Due to Partial Discharges (Corona) Using Bridge Techniques, 1995.

[76] Cartlidge D. M., Casson D. W., Franklin D. E., Macdonald J. A., Pollock B. C.: Machine condition monitoring: ozone monitor for air cooled generators, CEA Research Report Contract 9134G864, 1994.

[77] Wilson A.: Site discharge testing aids plant maintenance, Electrical Times, 1976.

[78] IEC 60270:2000 AMD1:2015 CSV (Consolidated version) High-voltage test techniques - Partial discharge measurements, 2015.

[79] Détecteur de gaz analogique CTX 300, Manuel d'utilisation, Oldham S.A.S., 2015.

[80] Benmamas L., Teste P., Krebs G., Odic E., Vangraefschepe F., Hamiti T.: Contribution to partial discharge analysis in inverter-fed motor windings for automotive application, IEEE Electrical Insulation Conference (EIC), Baltimore 2017.

[81] IEC 60034-27-5: Rotating electrical machines - Part 27-5: Off-line partial discharge tests on winding insulation of rotating electrical machine during repetitive impulse voltage excitation (Working Draft 4), 2018.

[82] IEC 60034-27-1:2017 Rotating electrical machines - Part 27-1: Off-line partial discharge measurements on the winding insulation, 2017.

[83] IEC TS 60034-27-2:2012 Rotating electrical machines - Part 27-2: On-line partial discharge measurements on the stator winding insulation of rotating electrical machines, 2012.

[84] EASA AR100-2015: Recommended practice for the repairs of rotating electrical apparatus, Electrical Apparatus Service Association Inc., 2015.

[85] Kaufhold M., Börner G., Eberhardt M., Speck J.: Failure Mechanism of the Interturn Insulation of Low Voltage Electric Machines Fed by Pulse-Controlled Inverters, IEEE Electrical Insulation Magazine, vol. 12 issue 5, pp. 9-16, 1996.

[86] Wang P., Hongying X., Wang J., Zhou W., Cavallini A.: The influence of Repetitive Square Wave Voltage Rise Time on Partial Discharge Inception Voltage, 2016 IEEE Conference on Electrical Insulation and Dielectric Phenomena (CEIDP), pp. 759-762, 2016.

[87] IEC 62539:2007, IEEE Std 930-2004: Guide for the statistical analysis of electrical insulation breakdown data, First edition, 2007.

[88] Weibull W.: A statistical distribution function of wide applicability, J. Appl.

Mech. - Trans. ASME, 18 (3), pp. 293-297, 1951.

[89] Leemis L. M.: Reliability - Probabilistic Models and Statistical Methods, Prentice Hall Inc., Englewood Cliffs, New Jersey, 1995.

[90] ReliaSoft Corporation: Life Data Analysis Reference, Tucson, 2017.

[91] Nelson W.: Applied Life Data Analysis, John Wiley & Sons Inc, 1982.

[92] Ross R.: Graphical methods for plotting and evaluating Weibull distributed data, Proceeding of the IEEE International Conference on Properties and Applications of Dielectric Materials, 1, pp. 250-253, 1994.

[93] White J. S.: The Moments of Log-Weibull Order Statistics, Technometrics, 11 (2), pp. 373-386, 1969.

[94] Abernethy R. B.: The New Weibull Handbook, second edition, 1996.

[95] Lawless J. F.: Statistical Models and Methods for Lifetime Data, John Wiley and Sons, New York, 1982.

[96] Wang L., Cavallini A., Montanari G. C., Testa L.: Patterns of Partial Discharge Activity in XLPE: from Inception to Breakdown, 10th International Conference on Solid Dielectrics (ICSD), Potsdam, Germany, July 4-9, 2010.

[97] Fetouhi L. Petitgas B., Dantras E., Martinez-Vega J.: Mechanical, dielectric, and physicochemical properties of impregnating resin based on unsaturated polyesterimides, Eur. Phys. J. Appl. Phys. 80, 10901, 2017.

[98] Wang J., Wang P., Wang W., Zhou K., Zhou Q., Lei Y., Cavallini A.: Novel Repetitive Square Wave Voltage Generator Used for the Insulation Evaluation of Rotating Machines Driven by Power Electronics, IEEE Transactions on Dielectrics and Electrical Insulation Vol. 24, No. 4, pp. 2041-2049, August 2017.

[99] Kimura K., Ushirone S., Koyanagi T., Iiyama Y., Ohtsuka S., Hikita M.: Study of PD behaviors on a crossed sample of magnet-wire with repetitive bipolar impulses for inverter-fed motor coil insulation, CEIDP '05. Annual Report Conference on Electrical Insulation and Dielectric Phenomena, 2005.

[100] IEC 60851-5:2008 Winding wires – Test methods – Part 5: Electrical properties, 2008.

[101] IEC 60034-18-21:2012 Rotating electrical machines - Part 18-21: Functional evaluation of insulation systems - Test procedures for wire-wound windings - Thermal evaluation and classification, 2012.

[102] IEEE Std 117-2015 (Revision of IEEE Std 117-1974): IEEE Standard Test Procedure for Thermal Evaluation of Systems of Insulating Materials for

Random-Wound AC Electric Machinery, 2015.

[103] Stranges M. K. W., Ul Haq S., Dunn D. G.: Black-out test vs. UV camera for corona inspection of HV motor stator endwindings, Industry Applications Society 60th Annual Petroleum and Chemical Industry Conference, 2013.

[104] Kokko V.I.: Ageing due to thermal cycling by power regulation cycles in lifetime estimation of hydroelectric generator stator windings, XXth International Conference on Electrical Machines (ICEM), pp. 1559-1564, 2012.

[105] Schemmel F., Bauer K., Kaufhold M.: Reliability and Statistical Lifetime - Prognosis of Motor Winding Insulation in Low-Voltage Power Drive Systems, IEEE Electrical Insulation Magazine, vol. 25 (4), pp. 6-13, 2009.

[106] Endicott H. S., Hatch B. D., Sohmen R. G.: Application of the Erying Model to Capacitor Aging Data, IEEE Trans. CP-12, pp. 34-40, March 1965.

[107] Montanari G. C., Simoni L.: Aging Phenomenology and Modeling, IEEE Transactions on Electrical Insulation, vol. 28 no. 5, pp. 755-776, October 1993.

[108] Guastavine F., Rossi F., Gianoglio C., Torello E., Cordano D.: PDIV and RPDIV on Different Temperatures on Different Kind of Type I Insulating System, 2017 IEEE Conference on Electrical Insulation and Dielectric Phenomenon (CEIDP, 2017).

[109] Simoni L., Mazzanti G., Montanari G. C. Lefebre L.: A general multi-stress life model for insulating materials with or without evidence for thresholds, IEEE Transactions on Electrical Insulation, vol. 28 no.3, pp. 349-364, June 1993.

[110] Wichmann A.: Accelerated Voltage Endurance Testing of Micaceous Insulation Systems for Large Turbogenerators Under Combined Stresses, IEEE Transactions on Power Apparatus and Systems, vol. 96 (1), pp. 255-260, Jan. 1977.

[111] Johnston D. R., LaForte J. T., Podhorez P. E., Galpern H. N.: Frequency Acceleration of Voltage Endurance, IEEE International Conference on Electrical Insulation, June 1978.

[112] Lahoud N., Faucher J., Malec D., Maussion P.: Electrical aging of the insulation of low-voltage machines: model definition and test with the design of experiments, IEEE Transactions on Industrial Electronics, vol. 60, no.9, September 2013.

[113] Salameh F., Picot A., Chabert M., Leconte E., Ruiz-Gazen A., Maussion P.: Variable importance assessment in lifespan models of insulation materials: a comparative study, IEEE 10th International Symposium on Diagnostics for Electrical Machines, 2015.

[114] Stone G. C., Sedding H.: Detection of stator winding stress relief coating deterioration in conventional and inverter fed motors and generators, 2016

International Conference on Condition Monitoring and Diagnosis (CMD), September 2016.

[115] Toriyama Y., Okamoto H., Kanazshi M., Horii K.: Degradation of polyethylene by partial discharge, IEEE Transactions on Electrical Insulation, vol. EI-2, no. 2, p. 83-92, August 1967.

[116] Riekerink M. B.: Structural and Chemical Modification of Polymer Surfaces by Gas Plasma Etching, PhD Thesis, University of Twente, 2001.

[117] Millet C., Nguyen D. N., Lépine L., Bélec M., Lessard-Déziel D., Guddemi C.: Case study – high ozone concentration in hydro generators, IEEE Electrical Insulation Conference, Montreal, QC, Canada, 2009.

[118] Commercial materials from Oldham (now 3M group).

[119] Commercial materials from Drägerwerk AG & Co. KGaA, 2018.

[120] Szczepanski M., Malec D., Maussion P., Petitgas B., Manfé P.: Ozone concentration impact on the lifespan of enameled wires (conventional and corona-resistant) for low voltage rotating machines fed by inverters, IEEE 35th Electrical Insulation Conference, Baltimore, 2017.

[121] Kikuchi Y., Murata T., Uozumi Y., Fukumoto N., Nagata M., Wakimoto Y., Yoshimitsu T.: Effects of Ambient Humidity and Temperature on Partial Discharge Characteristics of Conventional and Nanocomposite Enameled Magnet Wires,, IEEE Transactions on Dielectrics and Electrical Insulation, vol. 15 no. 6, pp. 1617 - 1625, December 2008.

[122] Jones T. B., Gunji M., Washizu M.: Dielectrophoretic Liquid Actuation and Nanodroplet formation, J. Appl. Phys., Vol. 89, pp. 1441-1448, 2001.

[123] Daisuke M., Makoto O., Tsuneo A., Takahiro U.: A Study on Partial Discharge Phenomena of Winding Wires, Polymer Materials Technology Special Issue, Furukawa Review No.45, 2014.

[124] IEC 60216-1:2013 Electrical insulating materials - Thermal endurance properties - Part 1: Ageing procedures and evaluation of test results, 2013.

[125] IEC 60216-2:2005 Electrical insulating materials - Thermal endurance properties - Part 2: Determination of thermal endurance properties of electrical insulating materials - Choice of test criteria, 2005.

[126] IEC 60216-3:2006 Electrical insulating materials - Thermal endurance properties - Part 3: Instructions for calculating thermal endurance characteristics, 2006.

[127] IEC 61251:2015 Electrical insulating materials and systems - AC voltage endurance evaluation, 2015.

[128] IEC 62068:2013 Electrical insulating materials and systems - General method of evaluation of electrical endurance under repetitive voltage impulses, 2013.

[129] IEC 60034-18-32:2010 Rotating electrical machines - Part 18-32: Functional evaluation of insulation systems - Test procedures for form-wound windings - Evaluation by electrical endurance, 2010.

[130] NF C20-540 Essais d'environnement - Méthodes d'essais - Essai de vieillissement climatique des matériels et des matériaux synthétiques à usage extérieur, 1990.

[131] NF T51-034 Plastiques. Détermination des caractéristiques en traction, 1981.

[132] ISO 604:2002 Plastics - Determination of compressive properties, 2002.

[133] Gjerde A. C.: Multifactor ageing models-origin and similarities, IEEE Electrical Insulation Magazine, vol. 13, no 1, p. 6-13. 1997.

[134] J. P. Crine, A model of solid dielectrics aging, IEEE International Symposium on Electrical Insulation, pp. 25-26, 1990.

[135] Montanari G. C., Mazzanti G., Fabiani D., Albertini M., Perego G.: Investigation of DC threshold of polyetylenes as a tool insulation characterization, Conference on Electrical Insulation and Dielectric Phenomena, vol. 2, pp. 559-563, 1999.

[136] Fallou B., Burguiere C., Morel J.F.: First Approach on Multiple Accelerated Life Testing on Electrical Insulation, IEEE Conference on Electrical Insulation and Dielectric Phenomena, pp. 621-628, 1979.

[137] Fisher R.: The design of experiments, Oliver and Boyd, 1935.

[138] Fisher R., Statistical methods for research workers, Oliver and Boyd, 1925.

[139] Zhu X., Yan B., Chen L., Zhang R., Quan L., Mo L.: Multi-Objective Optimization Design of a Magnetic Planetary Geared Permanent Magnet Brushless Machine by Combined Design of Experiments and Response Surface Methods, IEEE Transactions on Magnetics, vol. 50 no. 11, seq. no. 8204004, 2014.

[140] Fragomeni J. M.: An Organizational Design of Experiments. Statistical Approach to Investigate the Effect of Extrusion Process Manufacturing on the Mechanical Behavior of an Aluminum Alloy, International Conference on Engineering and Technology Management, IEMC '98, pp. 11-14, 1998.

[141] Silva Nunes Jr. M. A., Clé de Oliveira T., Carvalho Filho J. M., Gonçalves de Abreu J. P.: Design of Experiments for Sensitivity Analysis of Voltage Sags Variables, IEEE 15th International Conference on Harmonics and Quality of Power, pp. 398-402, 2012.

[142] Zernig A., Bluder O., Spöck G.: Optimal design of experiments for semiconductor lifetime data, 9th Conference on Ph.D. Research in Microelectronics and Electronics (PRIME), pp. 285-288, 2013.

[143] Lahoud N., Faucher J., Malec D., Maussion P.: Electrical aging of the insulation of low-voltage machines: model definition and test with the design of experiments, IEEE Transactions on Industrial Electronics, vol. 60, no.9, September 2013.

[144] Salameh F., Picot A., Chabert M., Leconte E., Ruiz-Gazen A., Maussion P.: Variable importance assessment in lifespan models of insulation materials: a comparative study, IEEE 10th International Symposium on Diagnostics for Electrical Machines, 2015.

[145] Khelil Y., Maussion P., Lebey T.: Experimental design for tracking the influent operating parameters on insulation reliability, IEEE International Symposium on Diagnostics for Electric Machines, Power Electronics and Drives, 2009.

[146] ReliaSoft Corporation: Experiment Design & Analysis Reference, Tucson, 2018.

[147] Khuri A. I., Cornell J. A.: Response surfaces: designs and analyses, CRC press, 1996.

[148] Starr W. T., Steffen H.G.: Searching for threshold in voltage endurance, ICPADM, pp. 285-294, Xian, 1985.

[149] Szczepanski M., Malec D., Maussion P., Petitgas B., Manfé P.: Prediction of the lifespan of enameled wires used in low voltage inverter-fed motors by using the Design of Experiments (DoE), IEEE Industry Applications Society Annual Meeting, 2017.

[150] Szczepanski M., Malec D., Maussion P., Petitgas B., Manfé P.: Use of Design of Experiments (DoE) predictive models as a method of comparison of enameled wires used in low voltage inverter-fed motors, IEEE Industry Applications Society Annual Meeting, 2018.

[151] Bernot F.: Modulations MLI et MPI, Techniques de l'Ingénieur, 2003.

[152] Kececioglu D. B.: Reliability Engineering Handbook, Volume 1 and 2, DEStech Publications Inc., Lancaster, 2002.

[153] Nelson W.: Applied Life Data Analysis, Wiley, 1982.

[154] IEC 60034-15:2009 Rotating electrical machines - Part 15: Impulse voltage withstand levels of form-wound stator coils for rotating a.c. machines, 2009.

[155] White J.S.: The Moments of Log-Weibull Order Statistics, Technometrics, 11(2), pp. 373-386, 1969.

_____

[156] IEC 60851-5:2008 Winding wires – Test methods – Part 5: Electrical properties, 2008.

[157] Belec M., Li S., Nguyen D.N., Lepine L., C. Guddemi C., Lessard-Deziel D., Schwartz T., Lamarre L.: Investigation and diagnosis of a 184-MVA air-cooled generator heavily affected by slot partial discharge activity, Electrical Insulation Conference and Electrical Manufacturing Expo, pp. 85-90, 2007.

LIST OF FIGURES

_____

_____

LIST OF TABLES